

MICROCOPY RESOLUTION TEST CHART
NATIONAL BUREAU OF STANDARDS-1963-A

12

NSWC TR-83-380 ✓

AN ELEMENTARY ANALYSIS OF OCEAN WAVE STATISTICS

BY DONNA LEE ROBERT H. BARAN

UNDERWATER SYSTEMS DEPARTMENT

AUGUST 1983

AD-A148 706

Approved for public release, distribution unlimited

DTIC
ELECTE
DEC 26 1984
S D
E



NAVAL SURFACE WEAPONS CENTER

Dahlgren, Virginia 22448 • Silver Spring, Maryland 20910

84 12 12 008

UNCLASSIFIED

SECURITY CLASSIFICATION OF THIS PAGE (When Data Entered)

REPORT DOCUMENTATION PAGE		READ INSTRUCTIONS BEFORE COMPLETING FORM
1. REPORT NUMBER NSWC TR 83-350	2. GOVT ACCESSION NO. AD-A148706	3. RECIPIENT'S CATALOG NUMBER
4. TITLE (and Subtitle) AN ELEMENTARY ANALYSIS OF OCEAN WAVE STATISTICS		5. TYPE OF REPORT & PERIOD COVERED
7. AUTHOR(s) Donna M. Lee Robert H. Baran		6. PERFORMING ORG. REPORT NUMBER
9. PERFORMING ORGANIZATION NAME AND ADDRESS Naval Surface Weapons Center (Code U12) White Oak Silver Spring, Maryland 20910		8. CONTRACT OR GRANT NUMBER(s)
11. CONTROLLING OFFICE NAME AND ADDRESS		10. PROGRAM ELEMENT, PROJECT, TASK AREA & WORK UNIT NUMBERS 61152N, ZR00001, U01AA
14. MONITORING AGENCY NAME & ADDRESS (if different from Controlling Office)		12. REPORT DATE August 1983
		13. NUMBER OF PAGES
		15. SECURITY CLASS. (of this report) UNCLASSIFIED
		15a. DECLASSIFICATION/DOWNGRADING SCHEDULE
16. DISTRIBUTION STATEMENT (of this Report) Approved for public release; distribution unlimited.		
17. DISTRIBUTION STATEMENT (of the abstract entered in Block 20, if different from Report)		
18. SUPPLEMENTARY NOTES		
19. KEY WORDS (Continue on reverse side if necessary and identify by block number) Ocean Waves Statistics		
20. ABSTRACT (Continue on reverse side if necessary and identify by block number) Ocean wave statistics were obtained from twenty recordings of fifteen minutes each. Spectral densities are presented together with amplitude distributions and the results are discussed in light of relevant theories. In particular, it is shown that the sea surface fluctuation is a Gaussian statistic in the majority of cases; but that non-Gaussian fluctuations are observed from time to time. ^		

DD FORM 1 JAN 73 1473

EDITION OF 1 NOV 68 IS OBSOLETE
S/N 0102-LF-014-6601

UNCLASSIFIED

SECURITY CLASSIFICATION OF THIS PAGE (When Data Entered)

CONTENTS

	<u>Page</u>
INTRODUCTION	1
OCEAN WAVE STATISTICS	2
DATA ANALYSIS	11
NON-GAUSSIAN FLUCTUATIONS	75
CONCLUSION	83
REFERENCES	91
DISTRIBUTION	(1)

ILLUSTRATIONS

<u>Figure</u>		<u>Page</u>
1	ENVELOPE (dotted line) OF A NARROWBAND PROCESS (solid line) FOR $\epsilon \sim 0$	8
2	ENVELOPE (dotted line) OF A NARROWBAND PROCESS (solid line) FOR $\epsilon \sim 1$	12
3A	TIME SERIES $X(t)$ FOR DATA FILE P577R6	13
3B	SPECTRAL DENSITY $S(f)$ FOR DATA FILE P577R6	14
3C	NORMALIZED HISTOGRAM $h(x)$ FOR DATA FILE P577R6	15
4A	TIME SERIES $X(t)$ FOR DATA FILE P345R4	16
4B	SPECTRAL DENSITY $S(f)$ FOR DATA FILE P345R4	17
4C	NORMALIZED HISTOGRAM $h(x)$ FOR DATA FILE P345R4	18
5A	TIME SERIES $X(t)$ FOR DATA FILE P340R3	19
5B	SPECTRAL DENSITY $S(f)$ FOR DATA FILE P340R3	20
5C	NORMALIZED HISTOGRAM $h(x)$ FOR DATA FILE P340R3	21
6A	TIME SERIES $X(t)$ FOR DATA FILE P584R6	22
6B	SPECTRAL DENSITY $S(f)$ FOR DATA FILE P584R6	23
6C	NORMALIZED HISTOGRAM $h(x)$ FOR DATA FILE P584R6	24
7A	TIME SERIES $X(t)$ FOR DATA FILE P584R4	25
7B	SPECTRAL DENSITY $S(f)$ FOR DATA FILE P584R4	26
7C	NORMALIZED HISTOGRAM $h(x)$ FOR DATA FILE P584R4	27
8A	TIME SERIES $X(t)$ FOR DATA FILE C506T4	28
8B	SPECTRAL DENSITY $S(f)$ FOR DATA FILE C506T4	29
8C	NORMALIZED HISTOGRAM $h(x)$ FOR DATA FILE C506T4	30
9A	TIME SERIES $X(t)$ FOR DATA FILE C231T4	31
9B	SPECTRAL DENSITY $S(f)$ FOR DATA FILE C231T4	32
9C	NORMALIZED HISTOGRAM $h(x)$ FOR DATA FILE C231T4	33
10A	TIME SERIES $X(t)$ FOR DATA FILE C540T4	34
10B	SPECTRAL DENSITY $S(f)$ FOR DATA FILE C540T4	35
10C	NORMALIZED HISTOGRAM $h(x)$ FOR DATA FILE C540T4	36

ILLUSTRATIONS (Cont.)

<u>Figure</u>		<u>Page</u>
11A	TIME SERIES $X(t)$ FOR DATA FILE C516T4	37
11B	SPECTRAL DENSITY $S(f)$ FOR DATA FILE C516T4	38
11C	NORMALIZED HISTOGRAM $h(x)$ FOR DATA FILE C516T4	39
12A	TIME SERIES $X(t)$ FOR DATA FILE C514T4	40
12B	SPECTRAL DENSITY $S(f)$ FOR DATA FILE C514T4	41
12C	NORMALIZED HISTOGRAM $h(x)$ FOR DATA FILE C514T4	42
13A	TIME SERIES $X(t)$ FOR DATA FILE C237T4	43
13B	SPECTRAL DENSITY $S(f)$ FOR DATA FILE C237T4	44
13C	NORMALIZED HISTOGRAM $h(x)$ FOR DATA FILE C237T4	45
14A	TIME SERIES $X(t)$ FOR DATA FILE C211T4	46
14B	SPECTRAL DENSITY $S(f)$ FOR DATA FILE C211T4	47
14C	NORMALIZED HISTOGRAM $h(x)$ FOR DATA FILE C211T4	48
15A	TIME SERIES $X(t)$ FOR DATA FILE C183T4	49
15B	SPECTRAL DENSITY $S(f)$ FOR DATA FILE C183T4	50
15C	NORMALIZED HISTOGRAM $h(x)$ FOR DATA FILE C183T4	51
16A	TIME SERIES $X(t)$ FOR DATA FILE C558T4	52
16B	SPECTRAL DENSITY $S(f)$ FOR DATA FILE C558T4	53
16C	NORMALIZED HISTOGRAM $h(x)$ FOR DATA FILE C558T4	54
17A	TIME SERIES $X(t)$ FOR DATA FILE C518T4	55
17B	SPECTRAL DENSITY $S(f)$ FOR DATA FILE C518T4	56
17C	NORMALIZED HISTOGRAM $h(x)$ FOR DATA FILE C518T4	57
18A	TIME SERIES $X(t)$ FOR DATA FILE A633T4	58
18B	SPECTRAL DENSITY $S(f)$ FOR DATA FILE A633T4	59
18C	NORMALIZED HISTOGRAM $h(x)$ FOR DATA FILE A633T4	60
19A	TIME SERIES $X(t)$ FOR DATA FILE A455T4	61
19B	SPECTRAL DENSITY $S(f)$ FOR DATA FILE A455T4	62
19C	NORMALIZED HISTOGRAM $h(x)$ FOR DATA FILE A455T4	63
20A	TIME SERIES $X(t)$ FOR DATA FILE A515T2	64
20B	SPECTRAL DENSITY $S(f)$ FOR DATA FILE A515T2	65
20C	NORMALIZED HISTOGRAM $h(x)$ FOR DATA FILE A515T2	66

ILLUSTRATIONS (Cont.)

<u>Figure</u>		<u>Page</u>
21A	TIME SERIES $X(t)$ FOR DATA FILE A508T2	67
21B	SPECTRAL DENSITY $S(f)$ FOR DATA FILE A508T2	68
21C	NORMALIZED HISTOGRAM $h(x)$ FOR DATA FILE A508T2	69
22A	TIME SERIES $X(t)$ FOR DATA FILE A380T2	70
22B	SPECTRAL DENSITY $S(f)$ FOR DATA FILE A380T2	71
22C	NORMALIZED HISTOGRAM $h(x)$ FOR DATA FILE A380T2	72
23	SMOOTH SAMPLE PDF FOR DATA FILE A515T2	77
24	SMOOTH SAMPLE PDF FOR DATA FILE A508T2	78
25	SMOOTH SAMPLE PDF FOR DATA FILE A380T2	79
26	SMOOTH SAMPLE PDF FOR DATA FILE A455T4	80
27	SMOOTH SAMPLE PDF FOR DATA FILE C514T4	81
28	SMOOTH SAMPLE PDF FOR DATA FILE P345R4	82
29	$Q(x)$ FOR DATA FILE A515T2	84
30	$Q(x)$ FOR DATA FILE A508T2	85
31	$Q(x)$ FOR DATA FILE A380T2	86
32	$Q(x)$ FOR DATA FILE A455T4	87
33	$Q(x)$ FOR DATA FILE C514T4	88
34	$Q(x)$ FOR DATA FILE P345R4	89

TABLES

<u>Table</u>		<u>Page</u>
1	OCEAN WAVE DATA	74

INTRODUCTION

Waves on the ocean surface exemplify a number of important lessons in the mathematical study of random processes. The casual observer sees a series of irregular moving crests and troughs that gradually grow and shrink in the course of time. Mathematically, the ocean surface within certain boundaries is a single-valued function of the planar coordinates (y,z) and time (t) . Let it be $X(y,z,t)$. The air motions above this surface and the water motions below it must satisfy the nonlinear boundary conditions at the surface. These equations have never been solved exactly.¹ The reasonable approximations that yield solutions corresponding to experiences have been determined.² Yet even under the simplifying assumptions that yield provisional solutions, the behavior of $X(y,z,t)$ indicates a complex structure involving distances ranging from centimeters to many kilometers.

A one-dimensional wave study begins with a continuous recording of the sea surface elevation at a particular point (y_0, z_0) , the recording instrument being functionally equivalent to a "blind staff" which ignores the directions from which the waves approach. If an electro-mechanical pressure transducer were placed on the bottom at (x_0, y_0, z_0) , one can define $x_0=0$, and the instantaneous pressure would be linearly related to the varying depth, which is $X(y_0, z_0, t)$. Let $V(t)$ be the voltage out of the transducer. Then

$$V(t) = \int_{-\infty}^t X(y_0, z_0, t') h(t-t'; \mu) dt' \quad (1)$$

expresses $V(t)$ as the convolution of X with h , the impulse response of a low-pass filter that models the interaction of the surface with the device at average depth μ . Very long term observation of $V(t)$ shows that it has an average value, proportional to the mean depth, to which periodic and quasi-periodic fluctuations are added. In practice, the duration (T_r) of the recorded waveform will be insufficient to define the true mean. For example, a 15 minute record will yield a value

$$\bar{v} = (1/T_r) \int_0^{T_r} V(t) dt \quad (2)$$

which reflects the short-term average depth for a given phase in the tidal cycle. It makes sense then for the analyst, who is interested in the activity of the waves, to take

$$X(t) = [V(t) - \bar{v}]/c \quad (3)$$

as the history of sea surface fluctuation at the point in question, where c is a constant that accounts for the midband behavior of the low-pass filter model. In other words, $X(t)$ is the one-dimensional fluctuation as a function of time.

OCEAN WAVE STATISTICS

The two most salient features of any wave-like phenomenon are its amplitude and period. For a pure (sinusoidal) wave,

$$A \sin(2\pi t/T + \phi),$$

the amplitude (A), period (T), and phase (ϕ) can be determined by inspection of a single wavelet, as the behavior of X on (t_1, t_1+T) is repeated during (t_1+T, t_1+2T) , and so on. Ocean waves, however,

are only quasi-periodic; and the peak fluctuation at successive crests is likewise subject to variation.

Based on physical insight into the generation and propagation of ocean waves, or on an understanding of abstract harmonic analysis, the scientific observer knows that $X(t)$ can be represented very precisely over any observation interval (of T_r seconds) as a sum of sinusoidal components:

$$X(t) = \sum_{n=1}^{\infty} A_n \sin(2\pi n t / T_r + \phi_n) \quad (4)$$

Since the flow of energy that the component wave embodies is proportional to the squared amplitude, the sequence $\{A_n^2, n=1,2,\dots\}$ shows the allocation of total power among the components. The mathematical tools which extract the component amplitudes from the recordings of $X(t)$ fall into the domain of spectral analysis. Fast Fourier Transform (FFT) algorithms are commonly used today.

Most of the significant studies of ocean wave statistics were written prior to the widespread availability of the digital electronic technology that makes FFT the standard analytic tool that it has become. These pre-1965 studies often assume a tautological model in which $X(t)$ is represented as a sequence of individual wavelets. Let t_k be the time of the k -th up-crossing of the axis ($X=0$) by $X(t)$. Then if the recording begins with an up-crossing at $t=0$, the sequence

$$t_2, t_3 - t_2, t_4 - t_3, \dots, t_K - t_{K-1}$$

gives the respective periods of the successive wavelets. Defining $T_k = t_k - t_{k-1}$, the tautological model is

$$X(t) = \sum_{k=1}^K B_k \sin(2\pi t / T_k) I(t_{k-1} \leq t < t_k) \quad (5)$$

where the indicator function $I(\cdot)$ is one when its argument condition is satisfied, and zero otherwise. To determine B_k , one could take $\sqrt{2}$ times the root-mean-square (r.m.s.) fluctuation over the corresponding interval, or just the peak positive fluctuations, or some other measure. Indeed, there is no way to choose the B_k 's that will make equation (5) exact, since the sine function is just an approximation of the behavior of the ocean wave over each period. While equation (4), on the other hand, may be precise in principle, the number of terms in the summation will in practice be truncated at some value N :

$$X(t) \doteq \sum_{n=1}^N A_n \sin(2\pi n t / T_r + \beta_n) \quad (4')$$

The analyst may, for example, include only the N most significant components, with

$$\sum_{n=1}^N A_n^2 = S_N$$

adding up to 90 percent of the total energy in the record. Thus, whether the analyst uses the tautological model of equation (5) or the spectral linear model of equation (4'), the model is just an approximation to the true behavior of $X(t)$.

Bretschneider observes that, for application to the design of coastal engineering structures, there is a greater need for knowledge of the joint probability distribution of wave heights and periods than for the actual wave spectrum.³ In this and similar applications, the effects of waves are nonlinear functions of size and duration. Hence the tautological model is preferred. It is usually assumed (and generally borne out by analysis) that B_k and T_k are independent random variables. In other words, the (marginal) distribution of the random variable B_k is unaffected by knowledge of T_k , and conversely too.

Since $\{T_k, k=1, \dots, K\}$ is a sequence of independent, identically distributed random variables, it is important to know the probability density function (p.d.f.) of T , a randomly selected element of the sequence. To this end one defines

$$\tau = T/\bar{T} \quad (6)$$

where

$$\bar{T} = \sum_{k=1}^K T_k/K \quad (7)$$

is the mean period. The variance of τ will then reflect the deviation from pure sinusoidal behavior. Furthermore, it has long been known that the shape of the wave period distribution is somewhat more consistent from place-to-place and time-to-time than is its centroid. Therefore, the distribution or p.d.f. of the relative wave period, τ , has broader generality. Many experiments through the years have shown that the p.d.f. of the relative wave period is approximated by

$$p(\tau) = K_1 \tau^3 e^{-b_1 \tau^4} \quad (8)$$

where $K_1 = \pi/E\tau^2$, $b_1 = \pi/4E\tau^2$, and $E\tau^2 = 1.07871$. The first, second, and third quartile points of this distribution are 0.8, 1.0, and 1.2, respectively, so that half of all the periods are within ±20% of the median.

The definition $f = 1/T$ of the "frequency" of a wavelet leads to consideration of the relative frequency $v = f/\bar{f} = 1/\tau$, by analogy to equation (6). It follows from equation (8) that the p.d.f. of v is

$$p_v(s) = K_2 s^{-5} e^{-b_2/s^4} \quad (9)$$

This is the Bretschneider spectrum of ocean waves. When (9) applies, half the energy of the waves is concentrated at frequencies between $0.75\bar{f}$ and $1.1\bar{f}$. Yet the relationship of the Bretschneider spectrum to the Fourier spectrum of ocean waves is not a simple matter. The transformation which converts (8) to (9) is consistent with the tautological model, but not with the linear model. As an example, consider the case of white Gaussian noise for which the relative period has the p.d.f.

$$w(\tau) = e^{-\tau}.$$

The change of variable $\nu = 1/\tau$, $|\mathrm{d}\tau| = \nu^{-2}\mathrm{d}\nu$, gives the corresponding ν -spectrum

$$w_{\nu}(s) = s^{-2}e^{-1/s},$$

which implies that half the energy is distributed between relative frequencies of 0.7 and 3.5. But the Fourier spectrum of white Gaussian noise is flat, since a sufficiently long record of this process is delta-correlated and the Fourier transform of the delta function is a constant. On the other hand, inverse Fourier transformation of the last expression, taken as a spectral density with $s = 2\pi i f/\bar{f}$, would give an autocorrelation function of the form $(1/\bar{f}u)K_1(2u)$, where $u = \sqrt{2\pi i \bar{f}t}$ and K_1 is the modified Hankel function of first order.

The Bretschneider spectrum is only one of the theoretical ocean wave spectra that have been formulated over the years. Walden portrays a unanimous disagreement among the different theoretical wave spectra, remarking that "it is strange that the authors of the various hindcasting methods nearly always find that their data agree well with the properties of the sea in question even though the differences between the diagrams or spectra are immense."⁴

Better agreement can be found among the attempts to derive the amplitude distribution of ocean waves from first principles. None of the derivations is entirely convincing; but they all possess the unique feature of arriving at essentially the same result: a random, moving surface defined by a stationary Gaussian process.⁵ The fact that $X(t)$, for a randomly selected t , is Gaussian leads to the conclusion that the wave amplitude follows the Rayleigh distribution. In the terminology of communication signal processing, one is given a real-valued, narrowband Gaussian process $X(t)$ with midband frequency ω_0 ; and the problem is to find the p.d.f. of the envelope of the process. The notion of the envelope of a time series is usually an intuitive concept arising from elementary studies of signal modulation.⁶ In Figure 1, the dotted lines are recognized as the envelope of the modulated signal. In order to make this intuitive concept mathematically demonstrable, one appeals to the theory of Hilbert transforms, wherein

$$Y(t) = (1/\pi) \int_{-\infty}^{\infty} X(\alpha) (t-\alpha)^{-1} d\alpha$$

is the Hilbert transform of $X(t)$. The "analytic signal" is defined as

$$Z(t) = X(t) + iY(t)$$

for $i = +\sqrt{-1}$. The analytic signal is also known as the pre-envelope and its magnitude,

$$r(t) = |Z(t)| = \sqrt{X^2(t) + Y^2(t)} ,$$

is the envelope of $X(t)$. Since the Hilbert transform of a Gaussian process is itself Gaussian, the independence of X and Y yields that their joint density is⁷

$$P_X(x)P_Y(y) = (2\pi\sigma^2)^{-1} e^{-r^2/2\sigma^2} \quad (10)$$

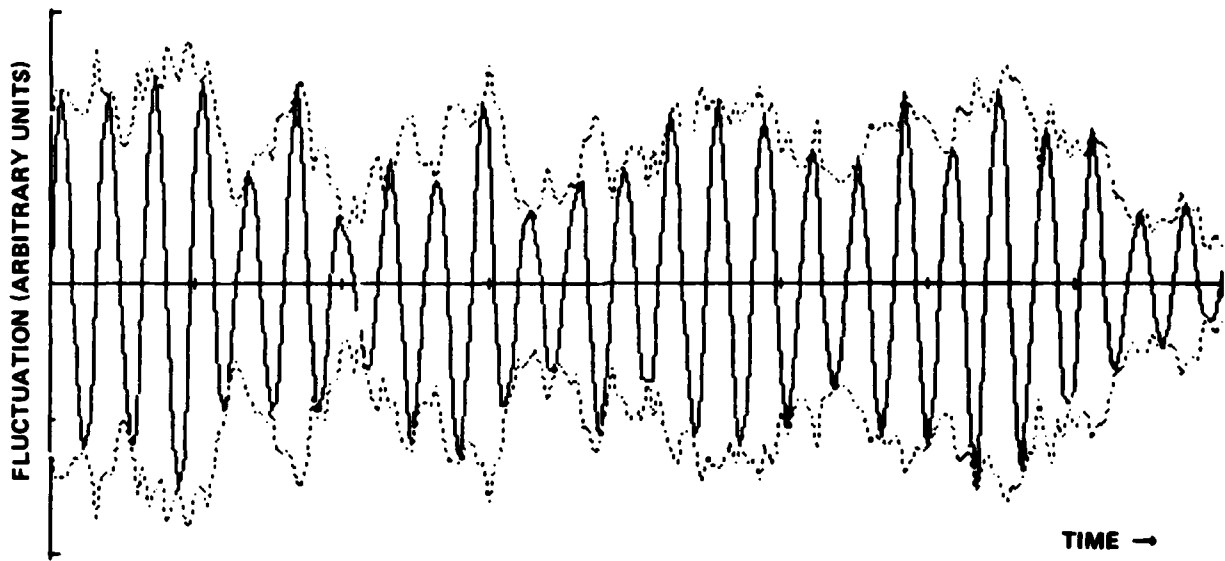


FIGURE 1. ENVELOPE (DOTTED LINE) OF A NARROWBAND PROCESS (SOLID LINE)
FOR $\epsilon \sim 0$

Then, on the X - Y plane, the joint density function can be written in terms of polar coordinates r and θ :

$$p_X(x)p_Y(y)dxdy = (2\pi\sigma^2)^{-1}e^{-r^2/2\sigma^2}rdrd\theta .$$

Integrating through θ on the right, one obtains

$$p_r(r) = (r/\sigma^2)e^{-r^2/2\sigma^2} , \quad (10)$$

the Rayleigh density.

The same result can be derived using the more familiar techniques of probability theory and real analysis. With reference to the tautological model of equation (5), one has

$$X = B \sin (wt)$$

for every wavelet, and

$$\Pr\{|X| \leq x | B=b\} = (2/\pi) \arcsin(x/b) \quad (11)$$

when t is uniform on the interval. Since $|X|$ is the symmetric and B is non-negative by convention,

$$\Pr\{|X| \leq x\} = \int_0^{\infty} \Pr\{|X| \leq x | B=b\} f(b) db ,$$

where $f(b)$ is the (unknown) p.d.f. of the amplitude (B). Breaking the integral in two about the point x , the last equation is the same as

$$\Pr\{|X| \leq x\} = \int_0^x \Pr\{|X| \leq x | B=b\} f(b) db + \int_x^{\infty} \Pr\{|X| \leq x | B=b\} f(b) db .$$

But $|X|$ is clearly less than x if b is less than x . Therefore, the probability measure in the first integral is unity. Hence,

$$\Pr\{|X| \leq x\} = \int_0^x f(b) db + \int_x^\infty \frac{2}{\pi} \arcsin\left(\frac{x}{b}\right) f(b) db \quad (12)$$

where equation (11) has been substituted in the second integral. The p.d.f. of $|X|$ is

$$g(x) = \frac{d}{dx} \Pr\{|X| \leq x\}$$

by definition. It follows from differentiation of equation (12) and an integration-by-parts that

$$g(x) = \int_x^\infty \frac{2f(b)}{\pi \sqrt{b^2 - x^2}} db \quad (13)$$

The question now becomes, "If

$$g(x) = \sqrt{\frac{2}{\pi}} \frac{1}{\sigma} e^{-x^2/2\sigma^2}, \quad x \geq 0, \quad (14)$$

then what p.d.f. $f(b)$ jointly satisfies (13) and (14)?" The answer is given in equation (10), i.e.,

$$f(b) = p_r(b) = (b/\sigma^2) e^{-b^2/2\sigma^2}. \quad (10')$$

The derivation follows from the change-of-variable

$$a^2 = b^2 - x^2, \quad db = da / \sqrt{a^2 + x^2};$$

but the details are omitted for the sake of brevity.

The equivalence of narrowband Gaussian fluctuations (on the one hand) to a Rayleigh-modulated sinusoid (on the other) is consistent with both the linear model and the tautological model. Yet it should be kept in mind that this equivalence is contingent in either case upon the spectral width being small as a fraction of center

frequency. This proviso is not always satisfied by ocean waves. Cartwright and Longuet-Higgins have derived a family of p.d.f.'s to describe the distribution of ocean wave amplitudes. The Cartwright-Longuet-Higgins density is parameterized by an ϵ which measures the relative spectral width of the fluctuations. In the case of $\epsilon=0$, corresponding to a very narrow spectrum, the C-L-H density coincides with the Rayleigh. As ϵ approaches one, the p.d.f. assumes the Gaussian shape with zero mean. In this latter case, the envelope of the fluctuations crosses zero from above and below in succession, as illustrated by Figure 2.

DATA ANALYSIS

Figures 3 through 22 show some ocean wave records together with spectra and normalized histograms. Each of these figures has three parts:

- (a) the time series, $X(t)$;
- (b) the spectral density, $S(f)$;
- (c) the normalized histogram, $h(X)$.

For example, Figure 8a shows the time series of a section of a data file having I.D. number C506T4. The sampling rate is one per second. Vertical scale calibration is not very relevant to the present study; so the vertical axis is omitted. Figure 8b shows the spectral density of the time series, which is arrived at by computing the FFT of the record and plotting its magnitude out to 0.5 Hz. The spectral density of record C506T4 is unimodal because, if one ignores the fine structure of narrow peaks and valleys, the graph shows a single "bump" spreading almost symmetrically about 0.16 Hz. Strictly speaking, the magnitude of the FFT should be squared to obtain the spectral density as that term is defined in most texts on random processes. Squaring would obviously tend to highlight both the midband and the fine structure. Figure 8c (solid line) is the

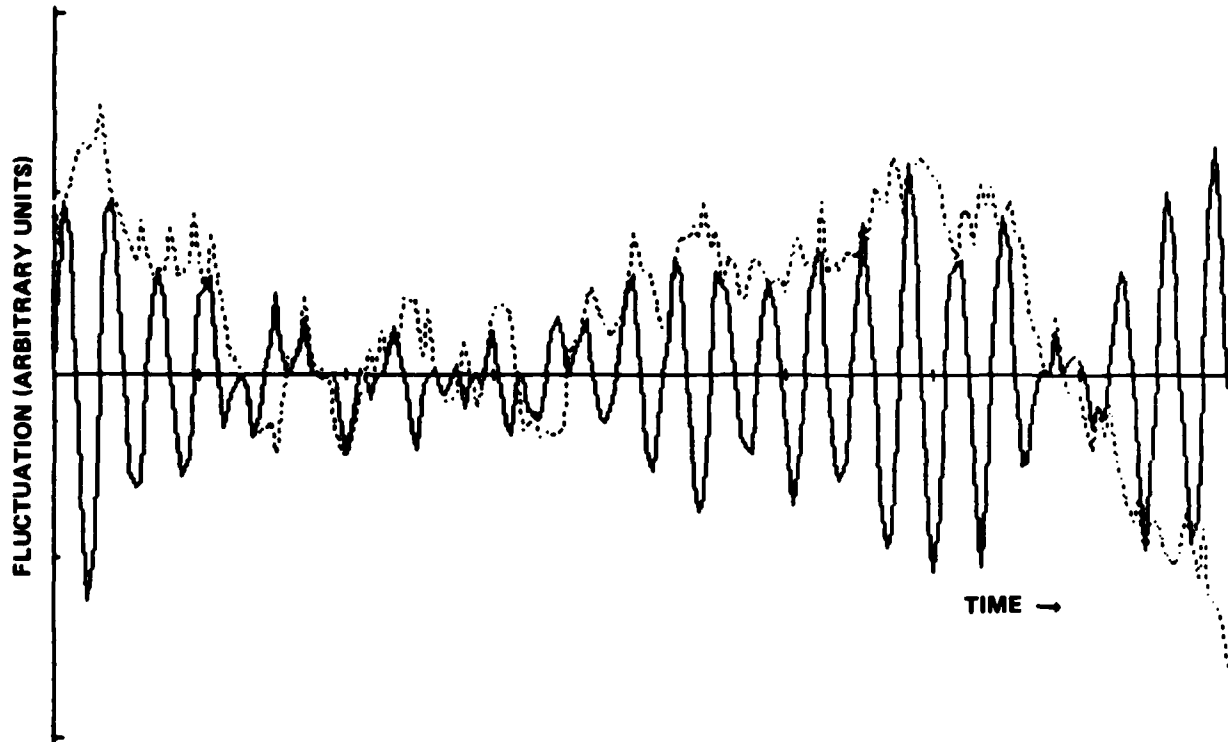


FIGURE 2. ENVELOPE (DOTTED LINE) OF A NARROWBAND PROCESS (SOLID LINE)
FOR $\epsilon \sim 1$

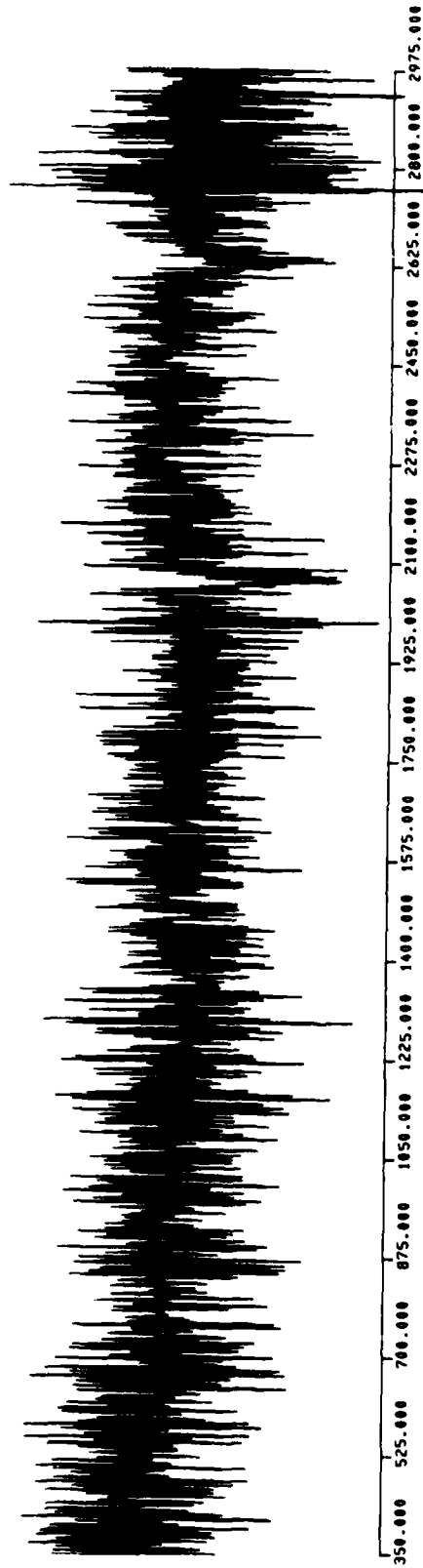


FIGURE 3A. TIME SERIES X(t) FOR DATA FILE P577R6

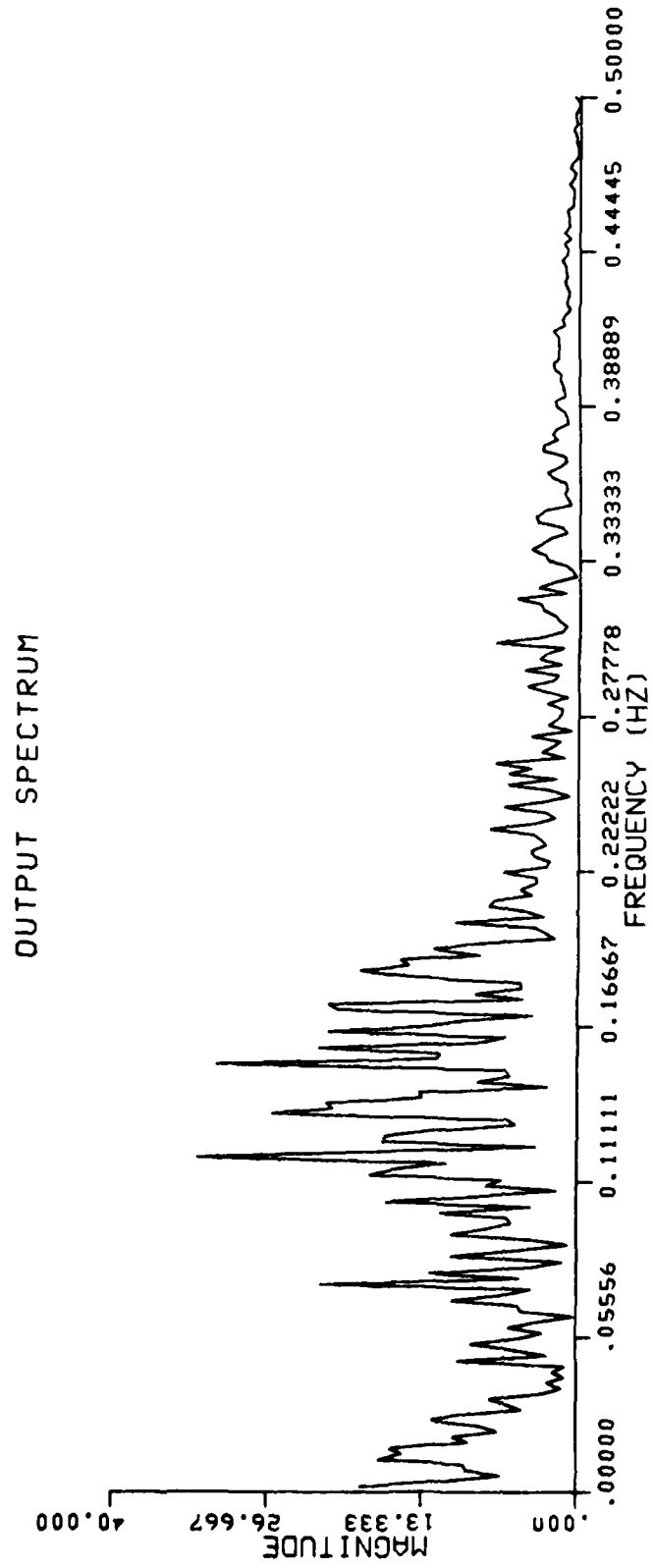


FIGURE 3B. SPECTRAL DENSITY S(f) FOR DATA FILE P577R6

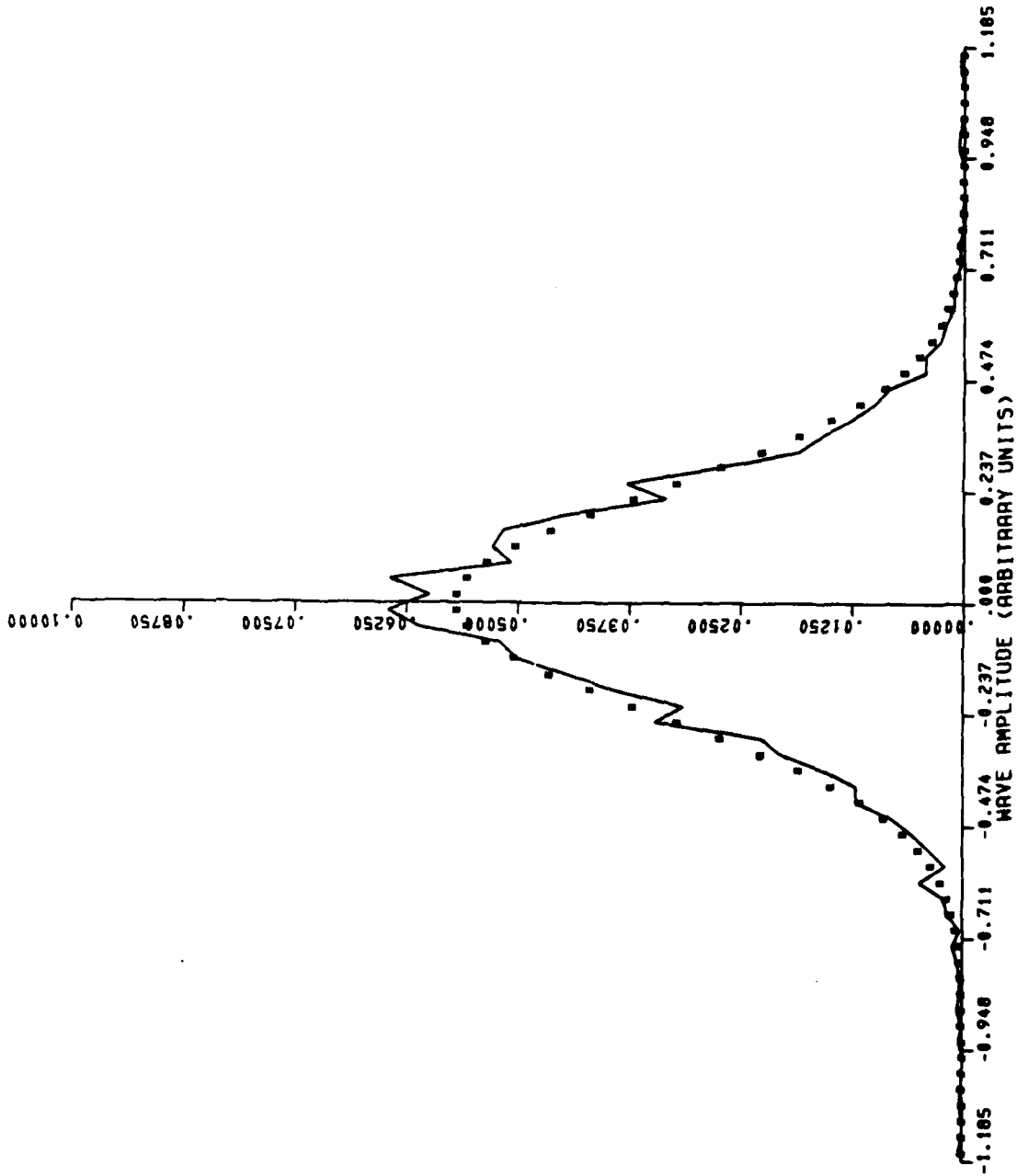


FIGURE 3C. NORMALIZED HISTOGRAM h(x) FOR DATA FILE P577R6

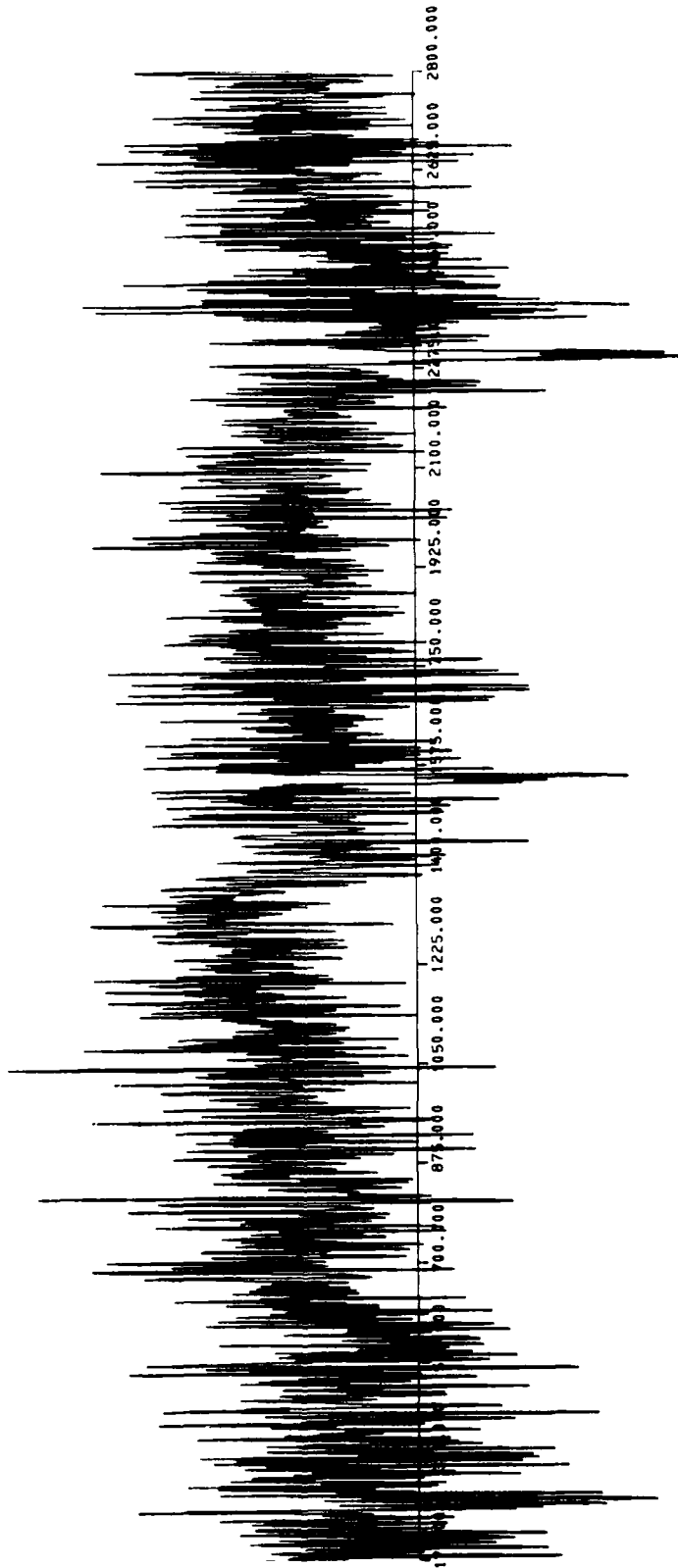


FIGURE 4A. TIME SERIES $X(t)$ FOR DATA FILE P345R4

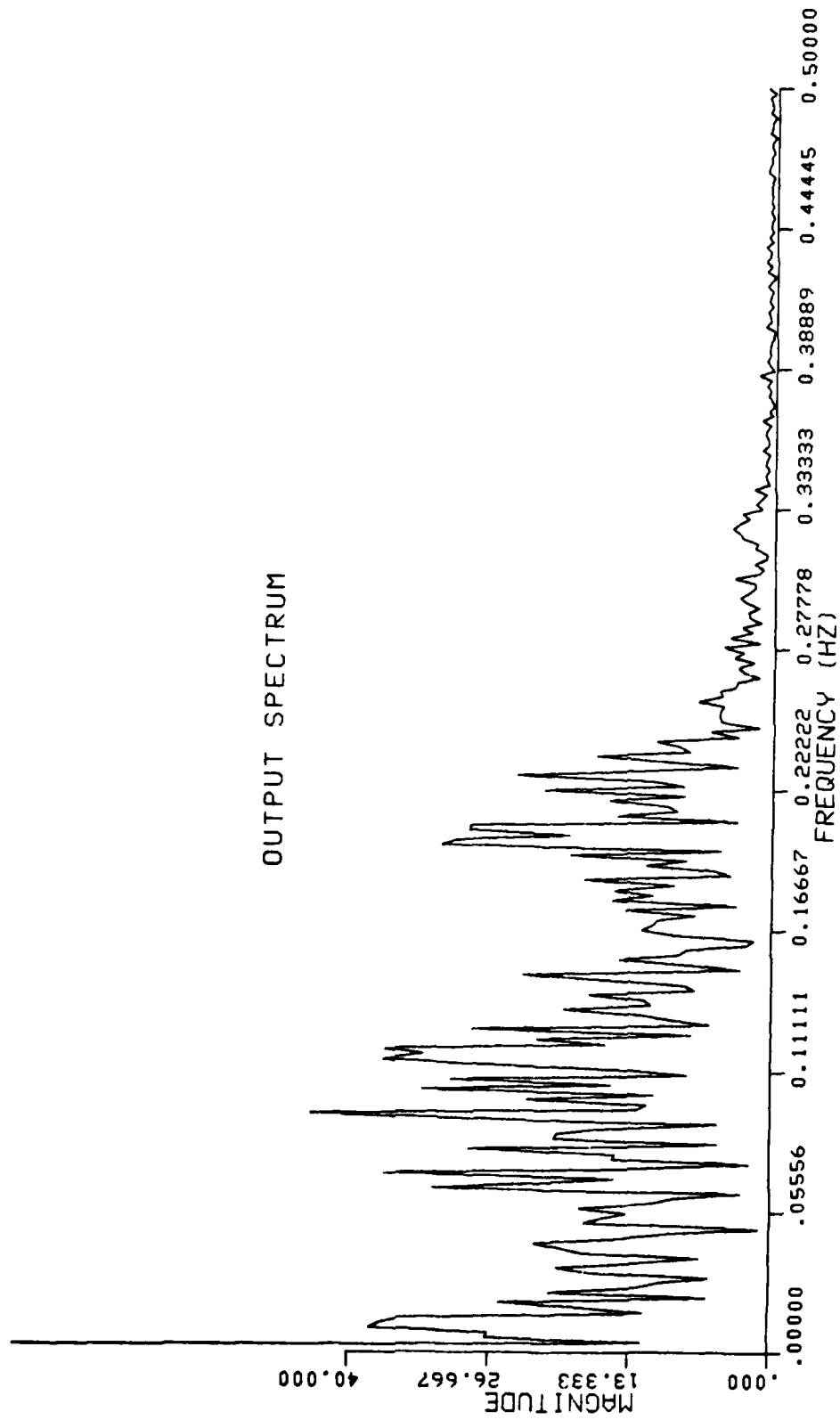


FIGURE 4B. SPECTRAL DENSITY S(f) FOR DATA FILE P345R4

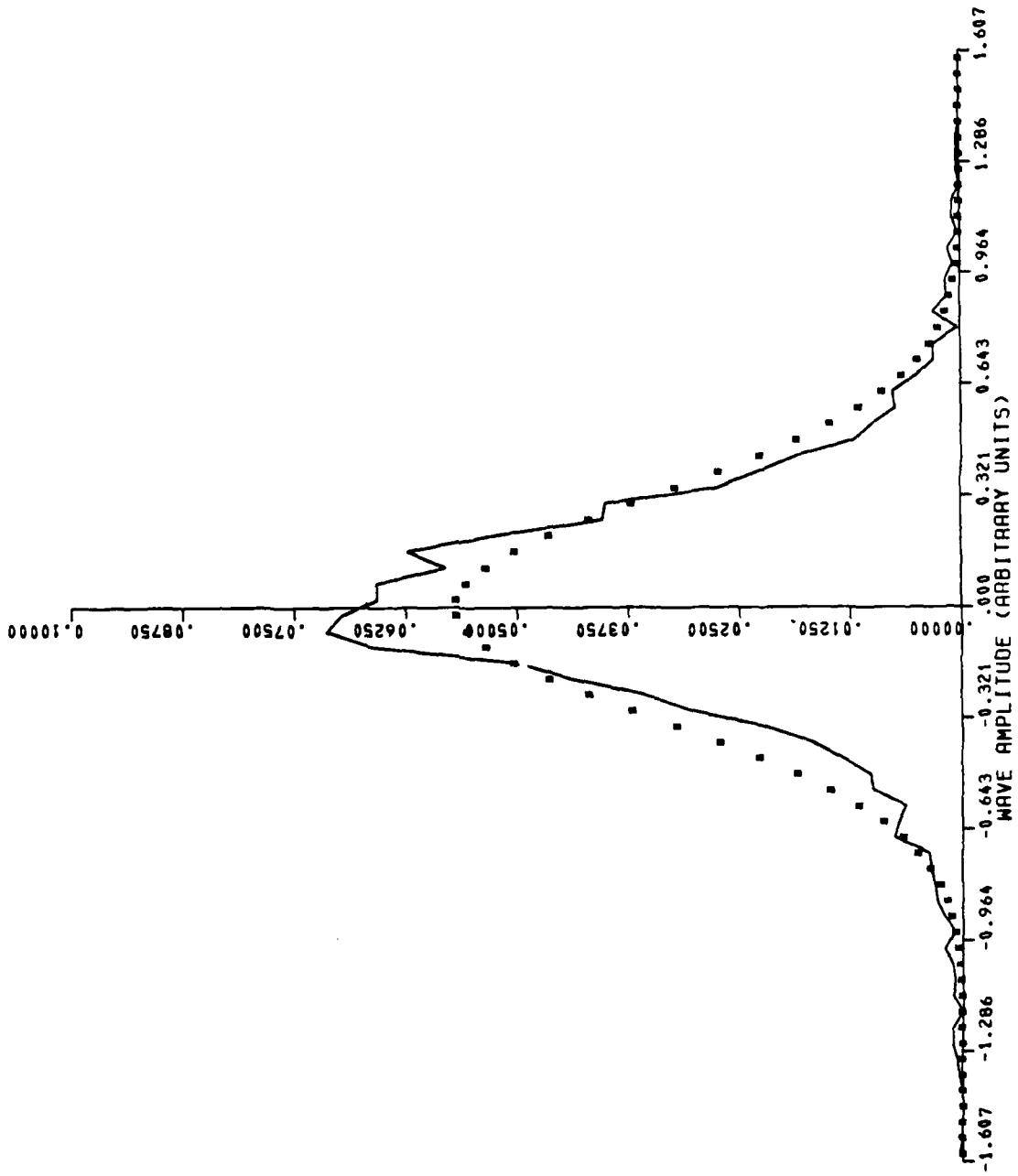


FIGURE 4C. NORMALIZED HISTOGRAM h(x) FOR DATA FILE P345R4

NORMALIZED HISTOGRAM

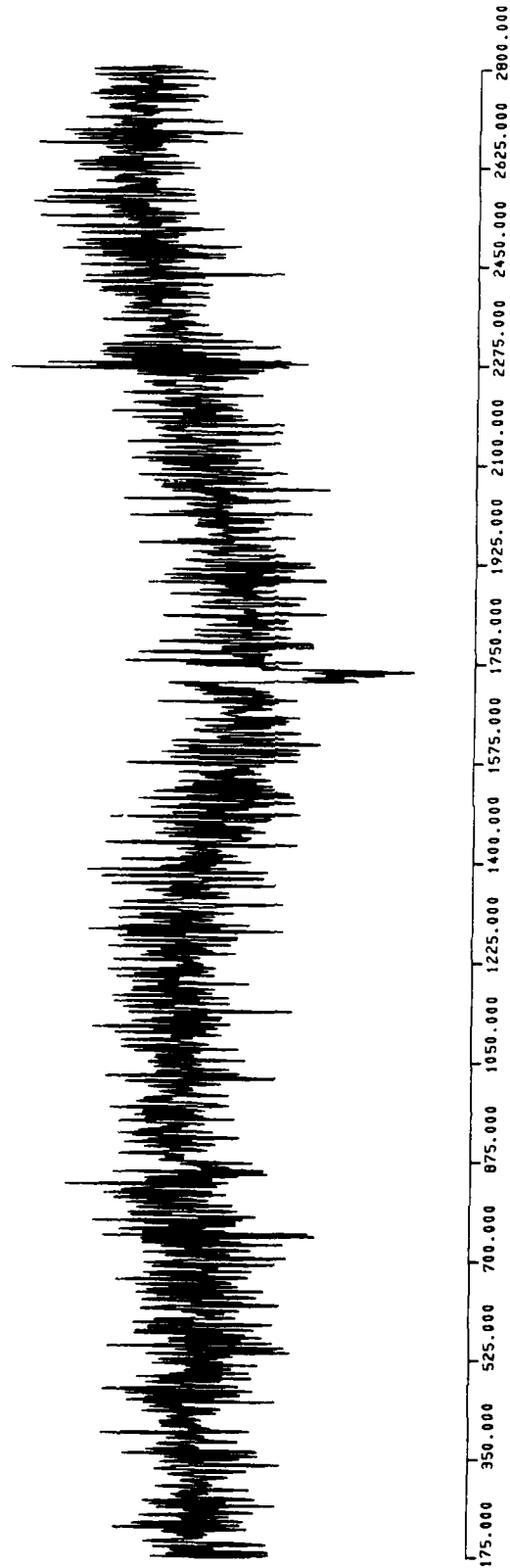


FIGURE 5A. TIME SERIES $X(t)$ FOR DATA FILE P340R3

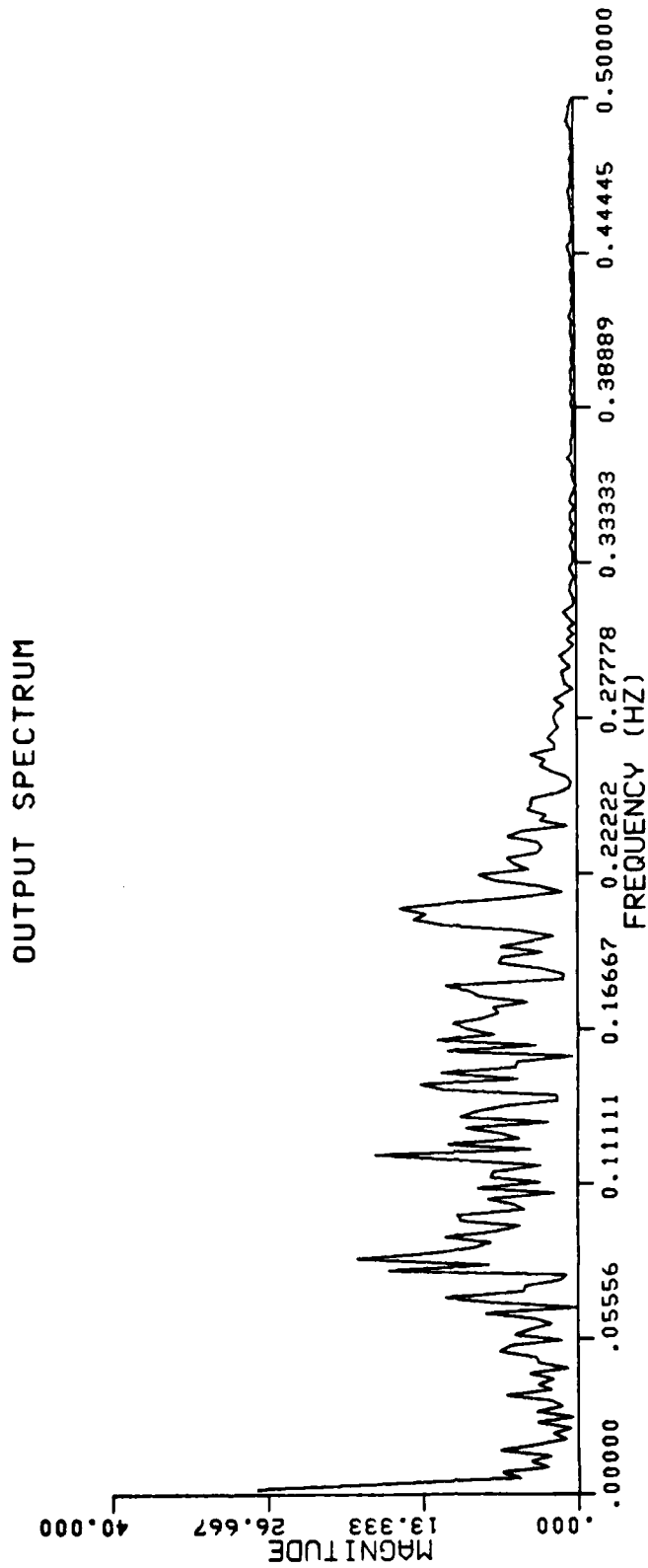


FIGURE 5B. SPECTRAL DENSITY S(f) FOR DATA FILE P340R3

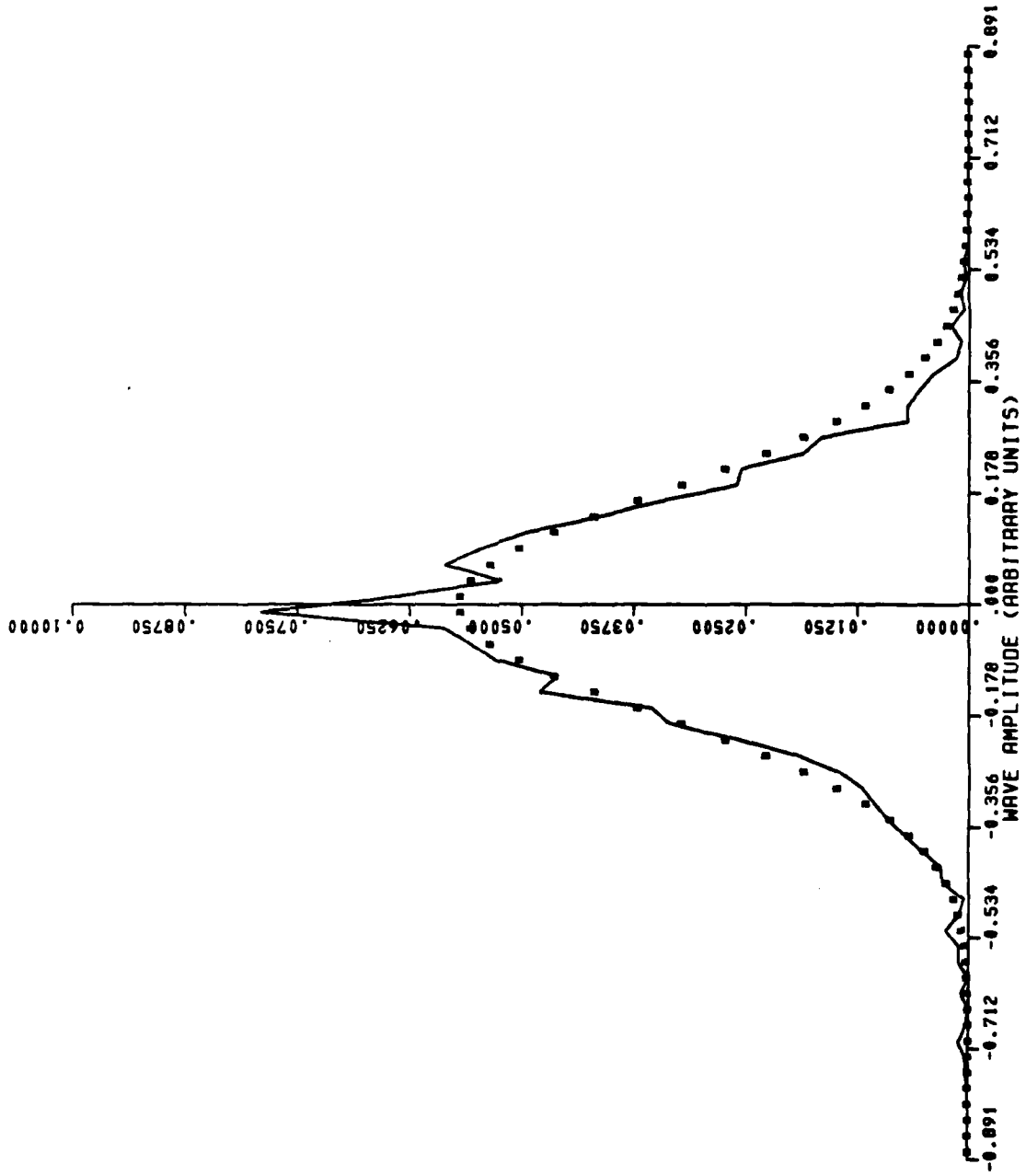


FIGURE 5C. NORMALIZED HISTOGRAM $h(x)$ FOR DATA FILE P340R3

NORMALIZED HISTOGRAM

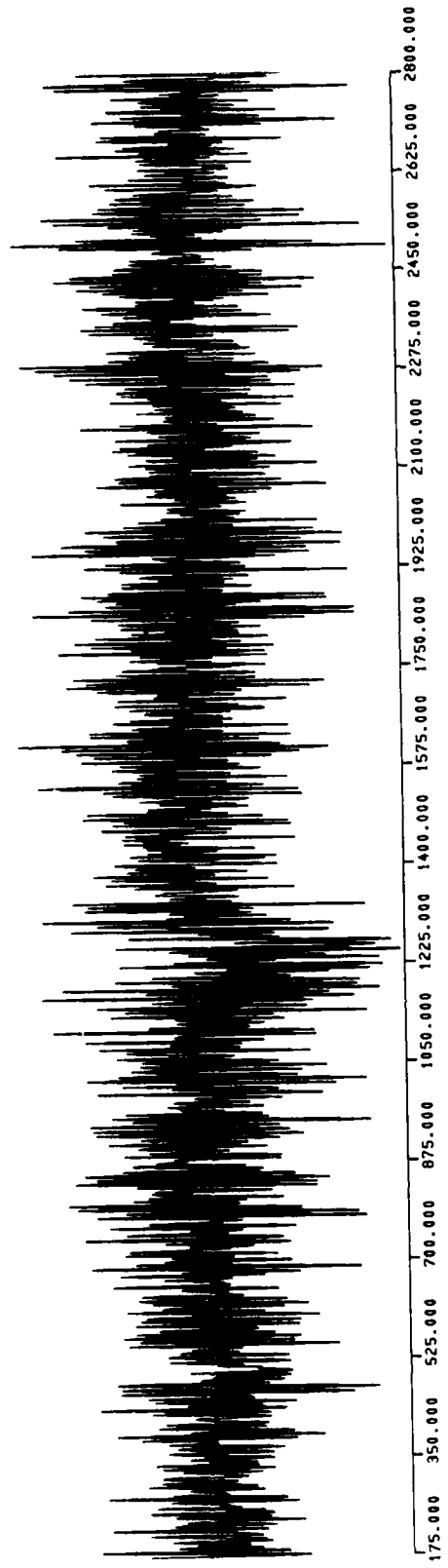


FIGURE 6A. TIME SERIES $X(t)$ FOR DATA FILE P584R6

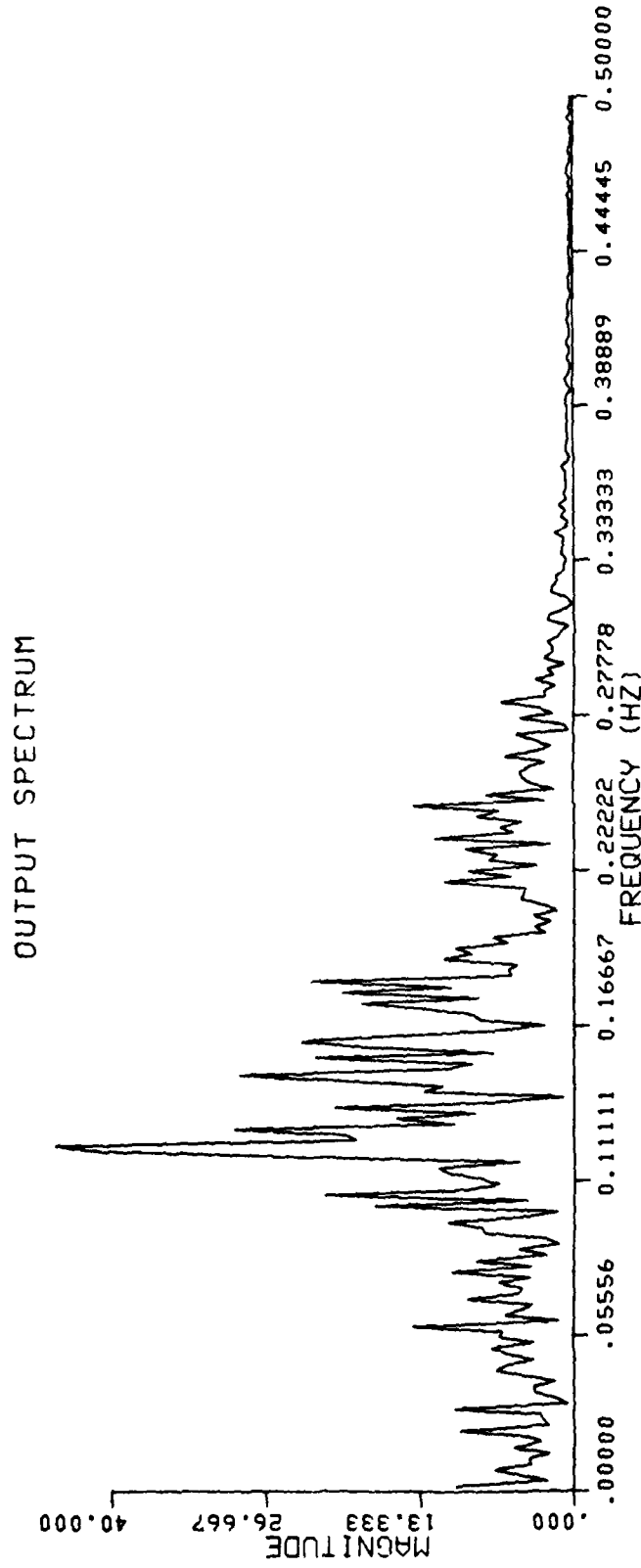


FIGURE 68. SPECTRAL DENSITY S(f) FOR DATA FILE P584R6

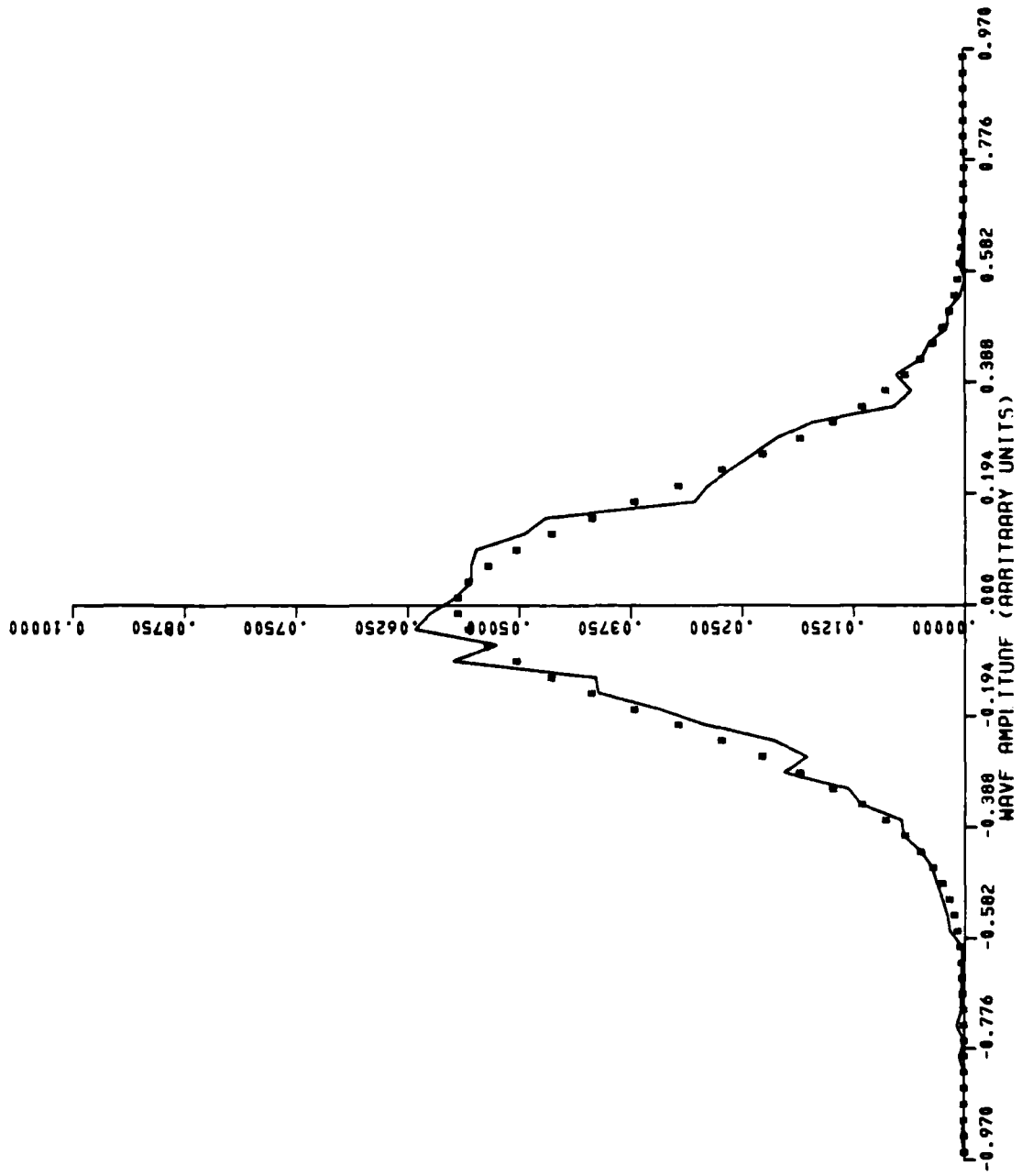


FIGURE 6C. NORMALIZED HISTOGRAM h(x) FOR DATA FILE P584R6

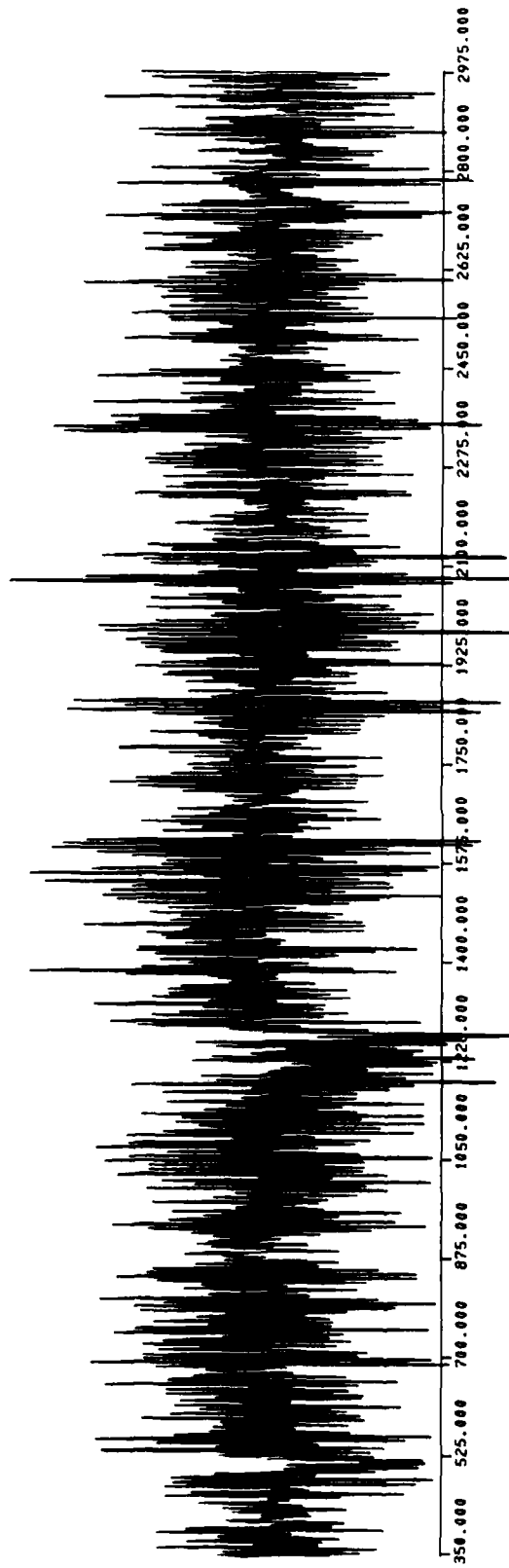


FIGURE 7A. TIME SERIES $X(t)$ FOR DATA FILE P584R4

OUTPUT SPECTRUM

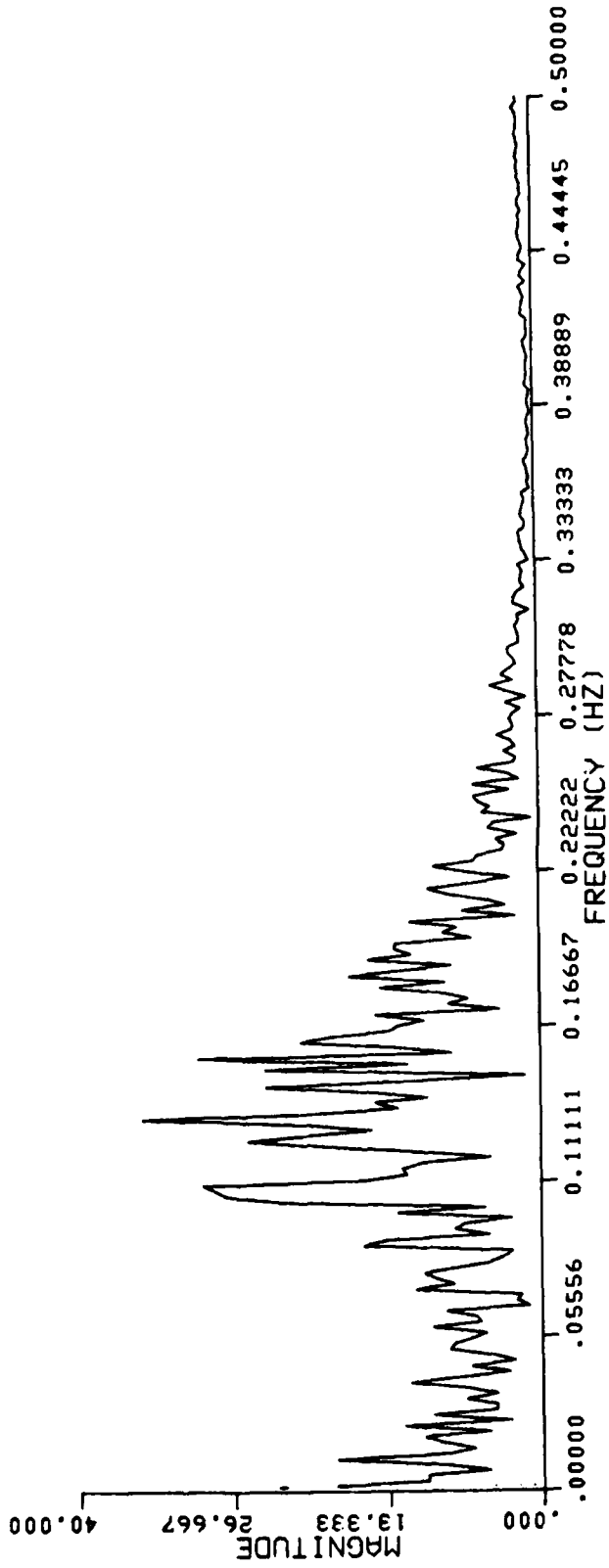


FIGURE 7B. SPECTRAL DENSITY S(f) FOR DATA FILE P584R4

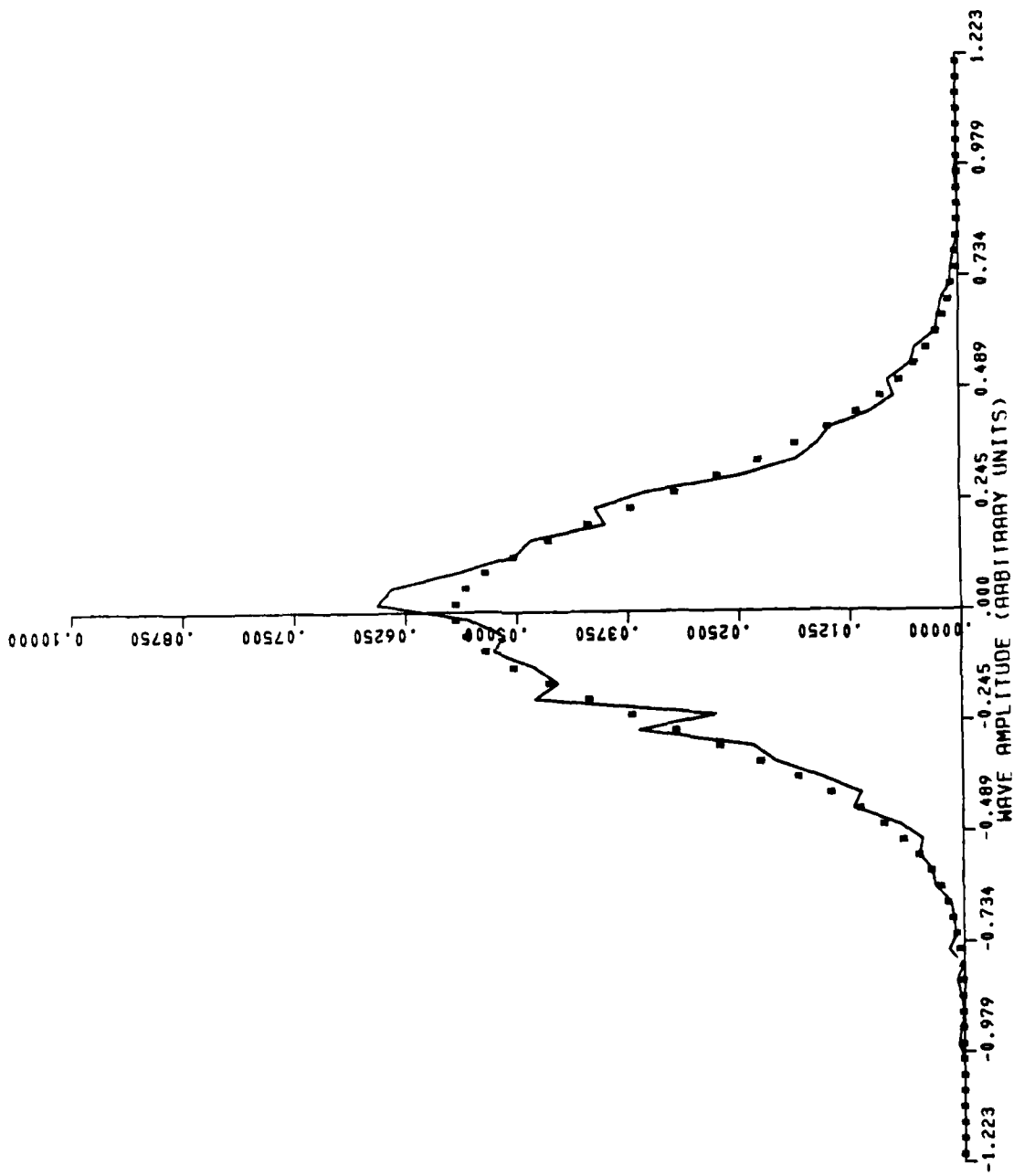


FIGURE 7C. NORMALIZED HISTOGRAM h(x) FOR DATA FILE P584R4

NORMALIZED HISTOGRAM

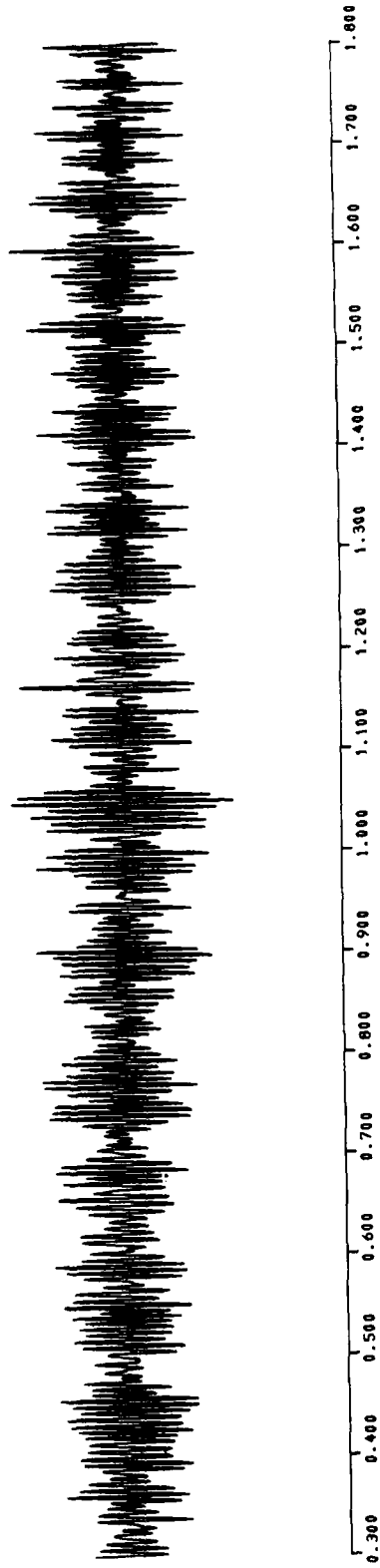


FIGURE 8A. TIME SERIES $X(t)$ FOR DATA FILE C506T4

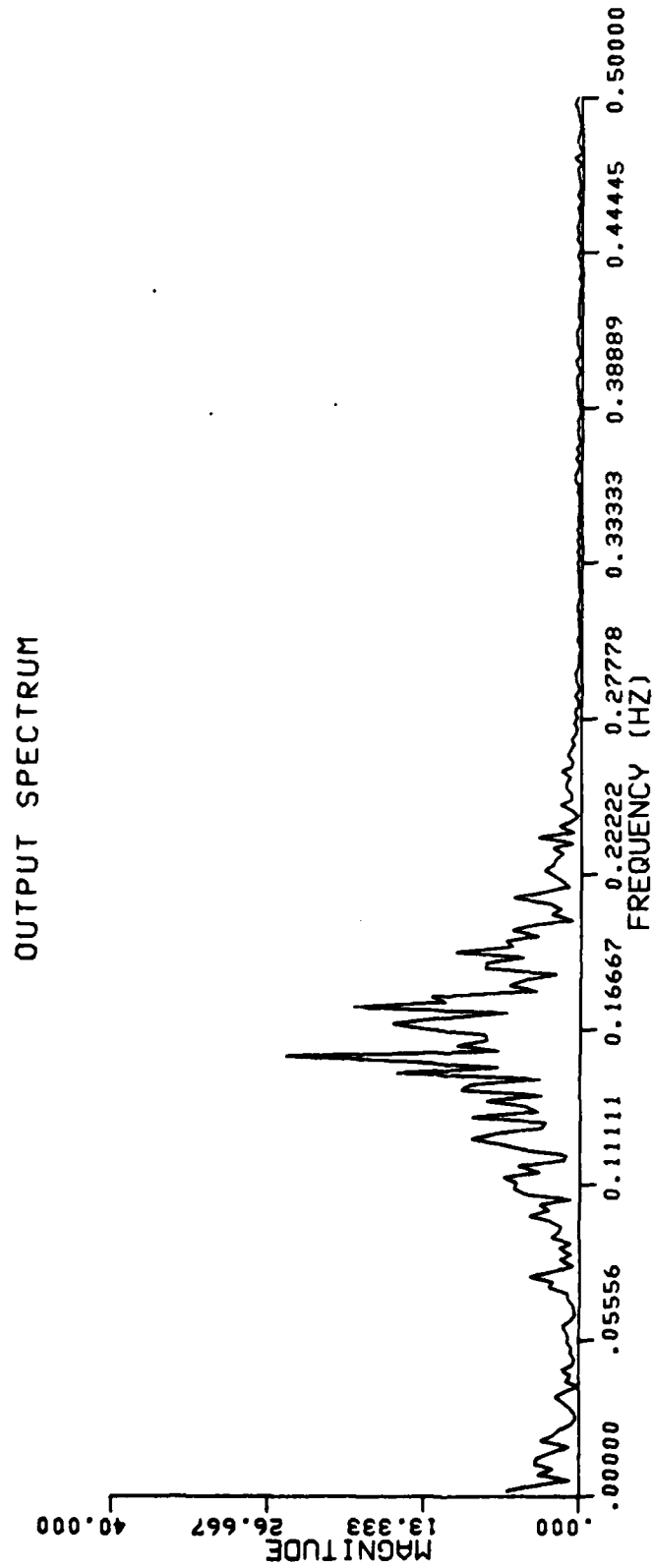


FIGURE 88. SPECTRAL DENSITY S(f) FOR DATA FILE C506T4

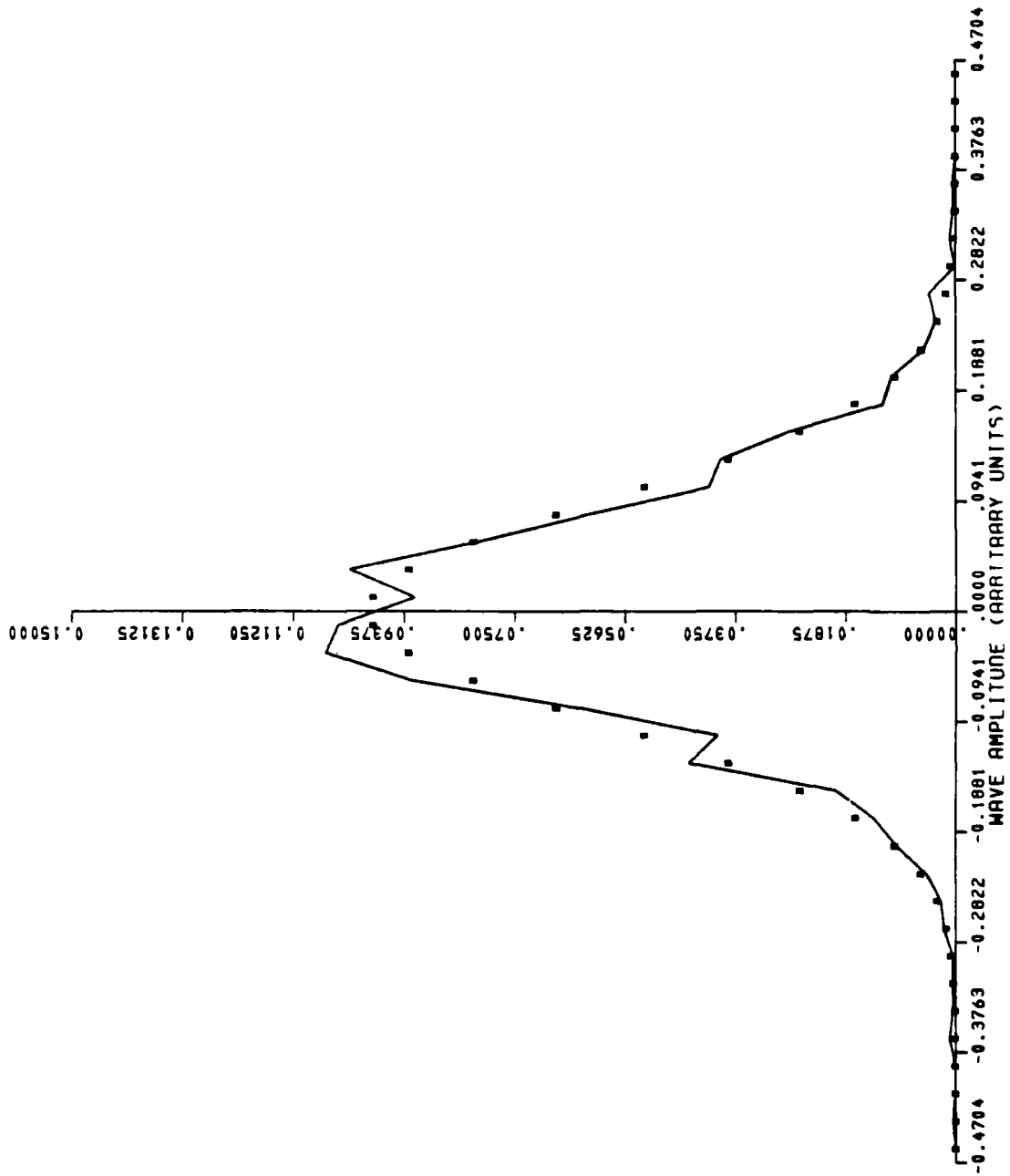


FIGURE 8C. NORMALIZED HISTOGRAM h(x) FOR DATA FILE C506T4

NORMALIZED HISTOGRAM

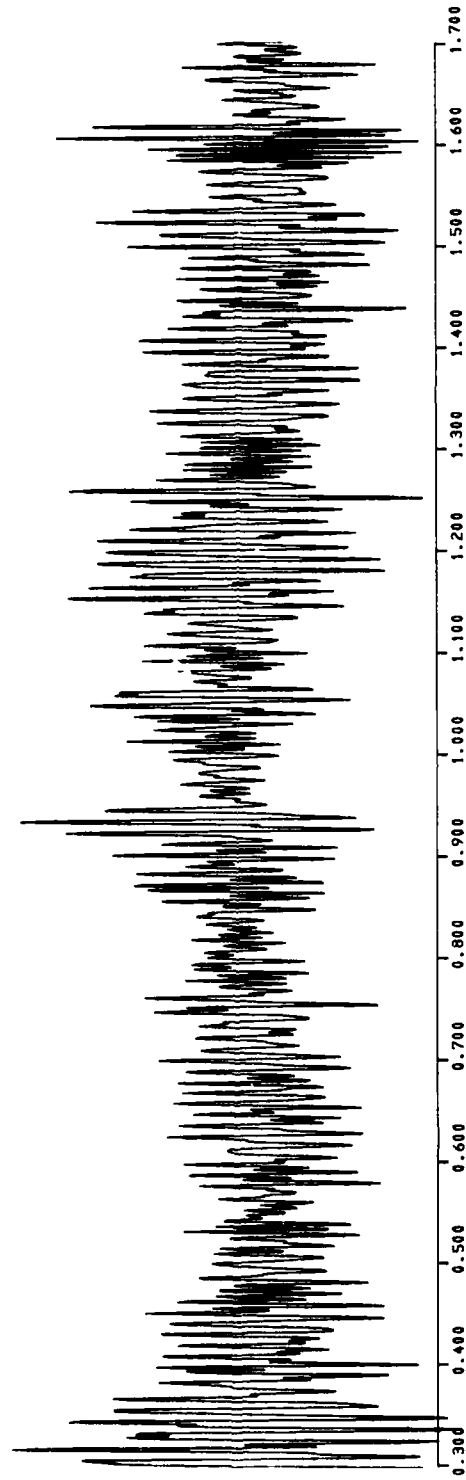


FIGURE 9A. TIME SERIES $X(t)$ FOR DATA FILE C231T4

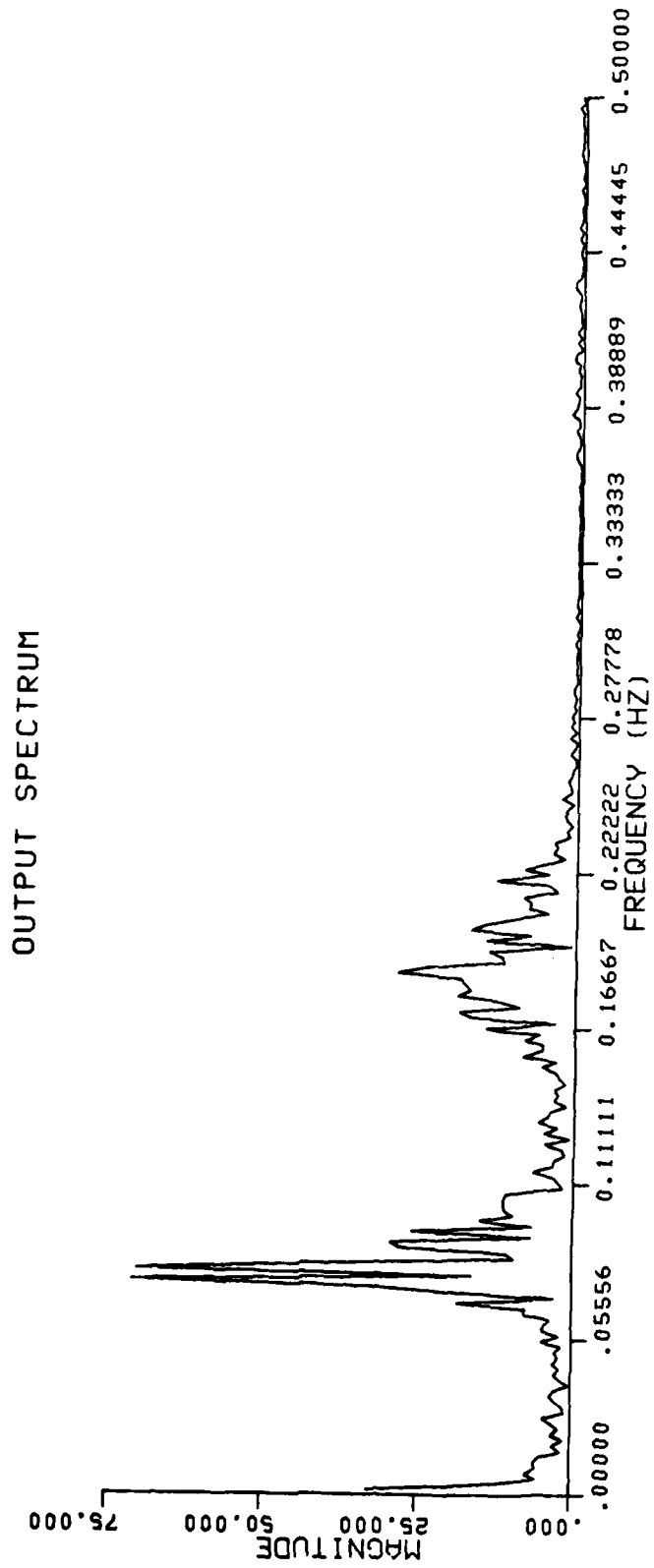


FIGURE 9B. SPECTRAL DENSITY S(f) FOR DATA FILE C231T4

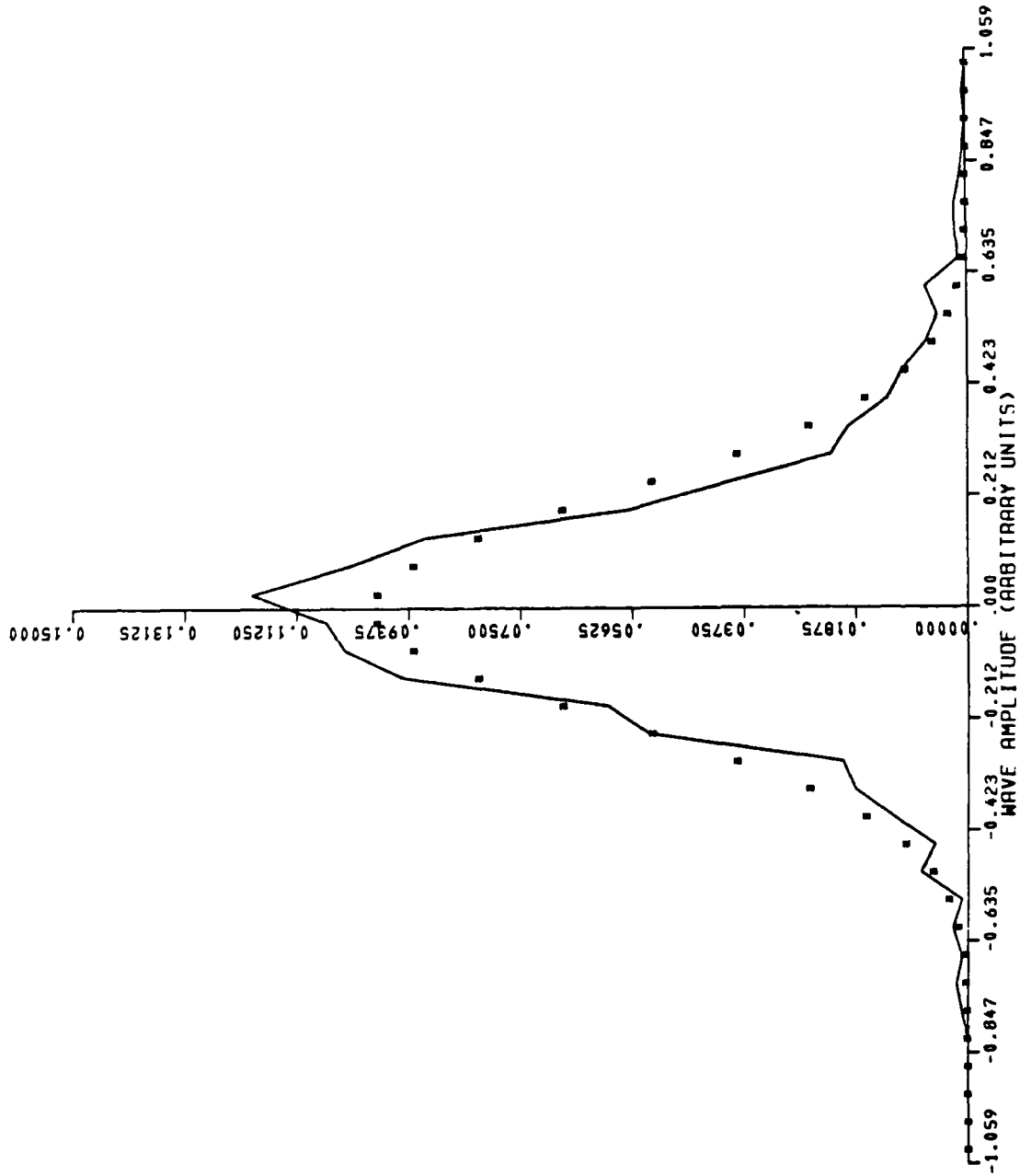


FIGURE 9C. NORMALIZED HISTOGRAM h(x) FOR DATA FILE C231T4

NORMALIZED HISTOGRAM

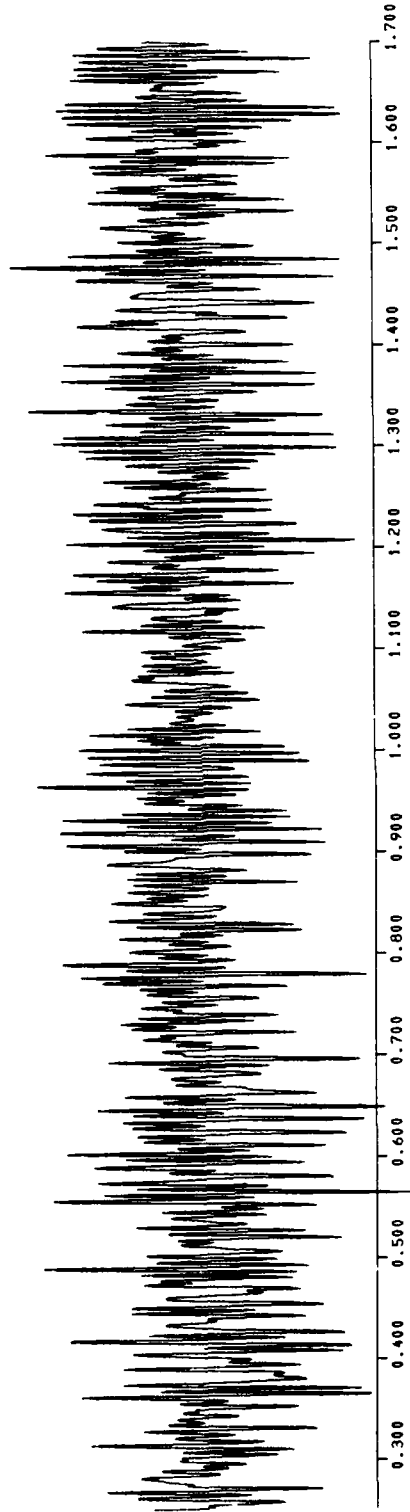


FIGURE 10A. TIME SERIES $X(t)$ FOR DATA FILE C540T4

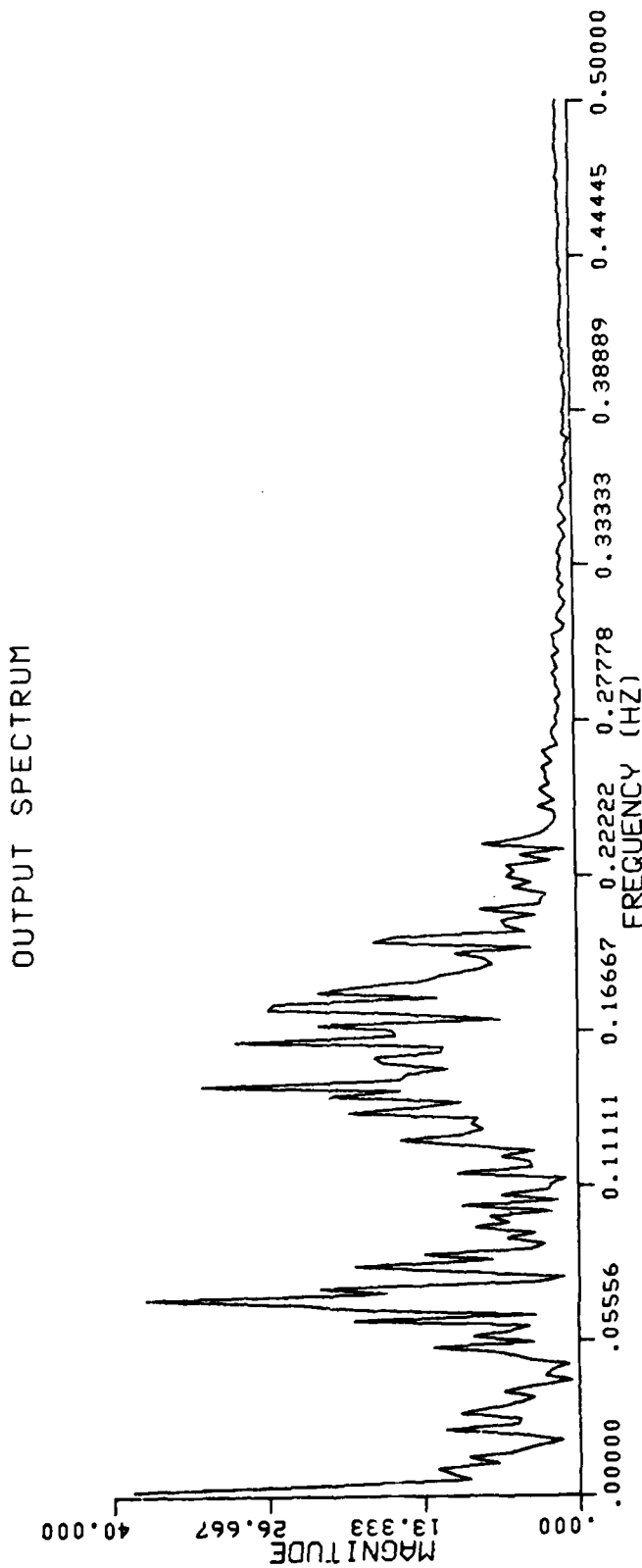


FIGURE 10B. SPECTRAL DENSITY S(f) FOR DATA FILE C540T4

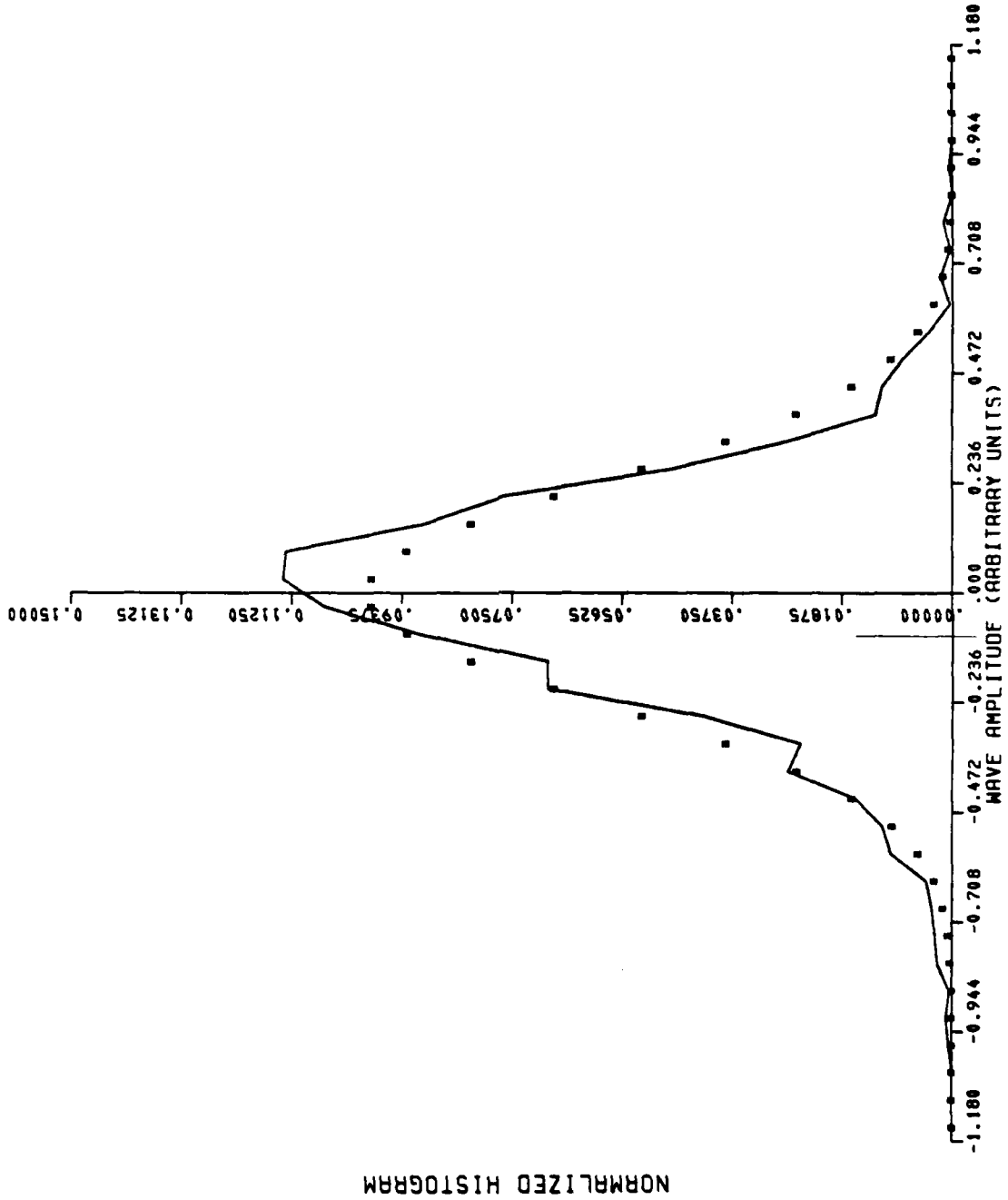


FIGURE 10C. NORMALIZED HISTOGRAM h(x) FOR DATA FILE C540T4

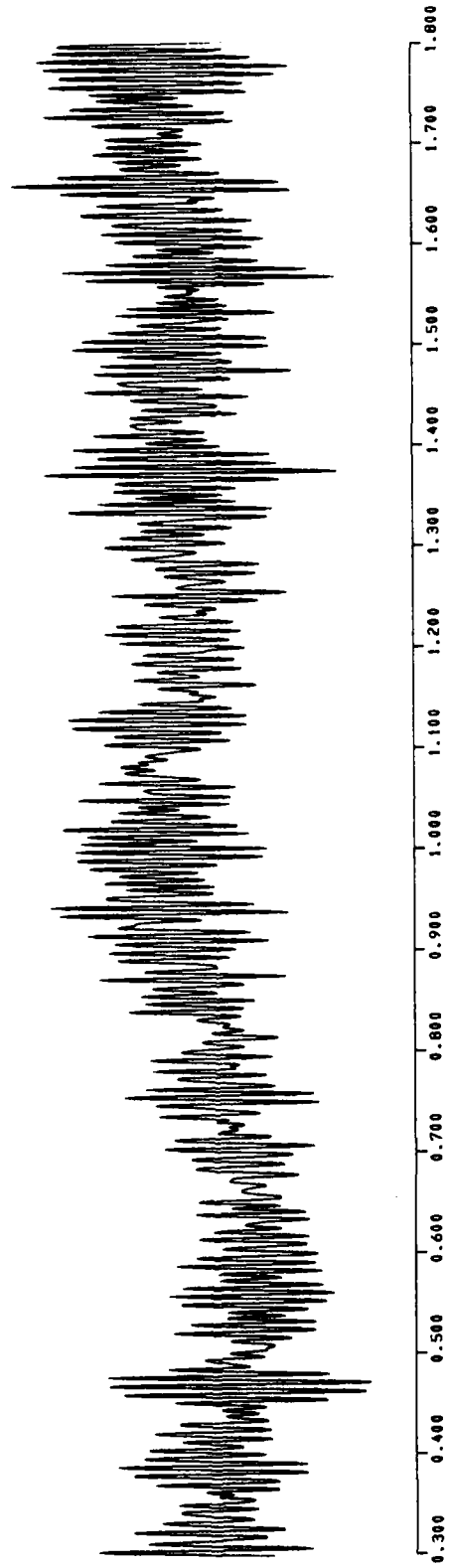


FIGURE 11A. TIME SERIES X(t) FOR DATA FILE C516T4

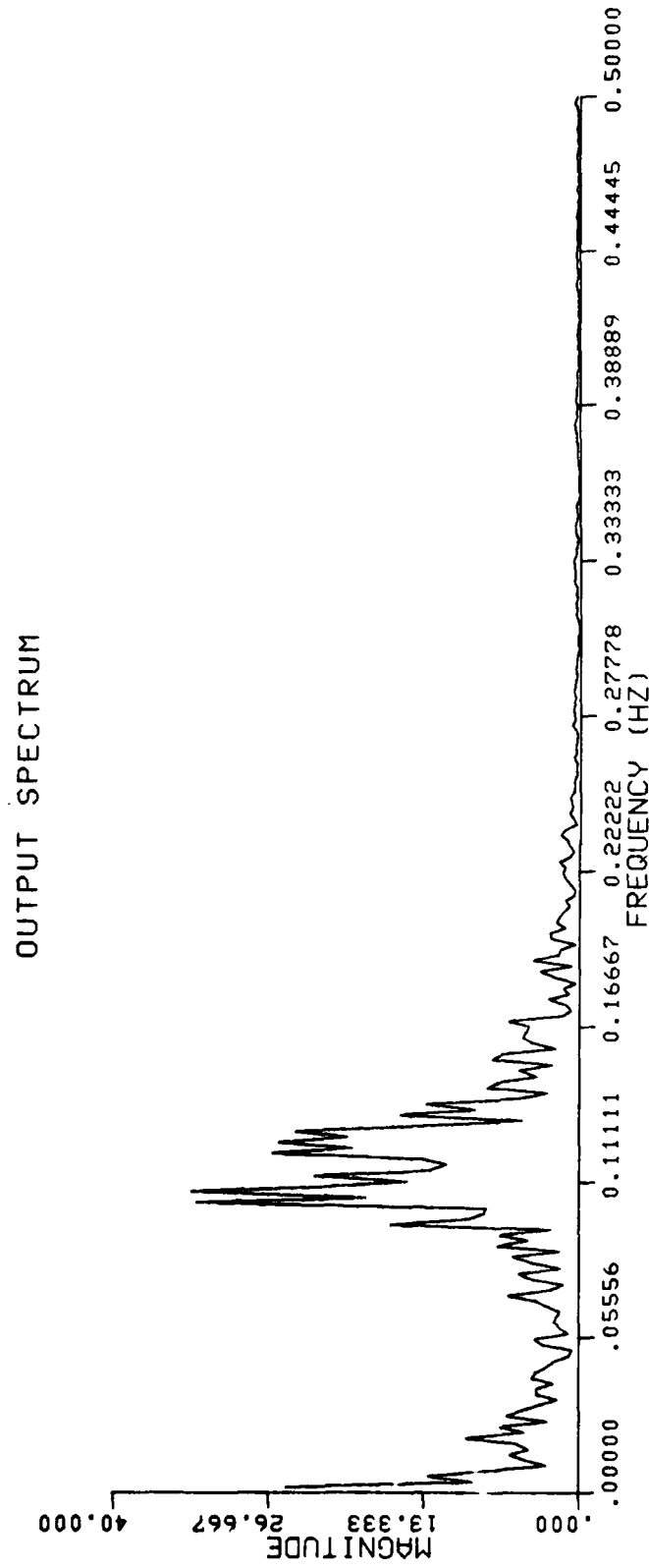


FIGURE 11B. SPECTRAL DENSITY S(f) FOR DATA FILE C516T4

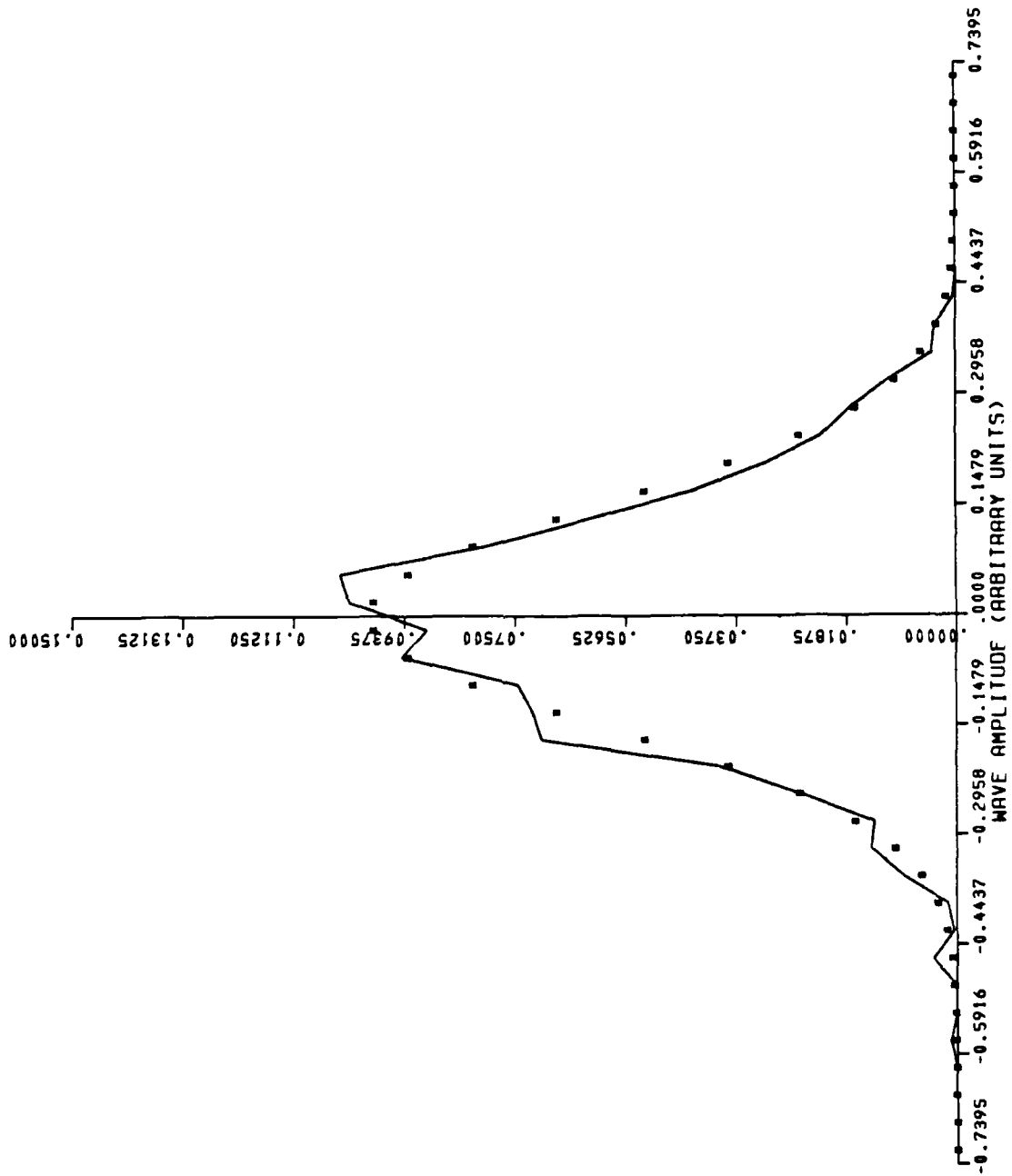


FIGURE 11C. NORMALIZED HISTOGRAM $h(x)$ FOR DATA FILE C516T4

NORMALIZED HISTOGRAM

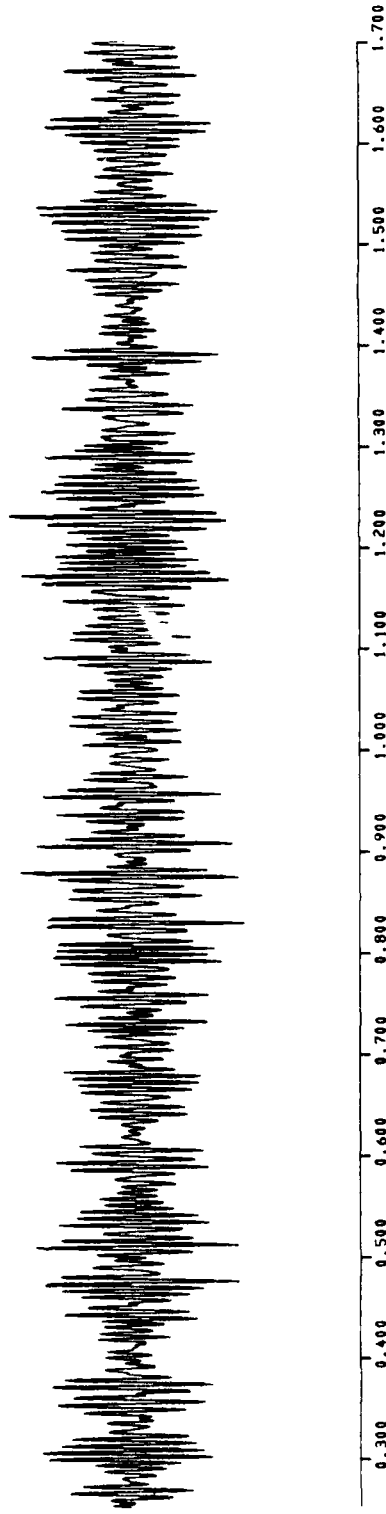


FIGURE 12A. TIME SERIES $X(t)$ FOR DATA FILE C514T4

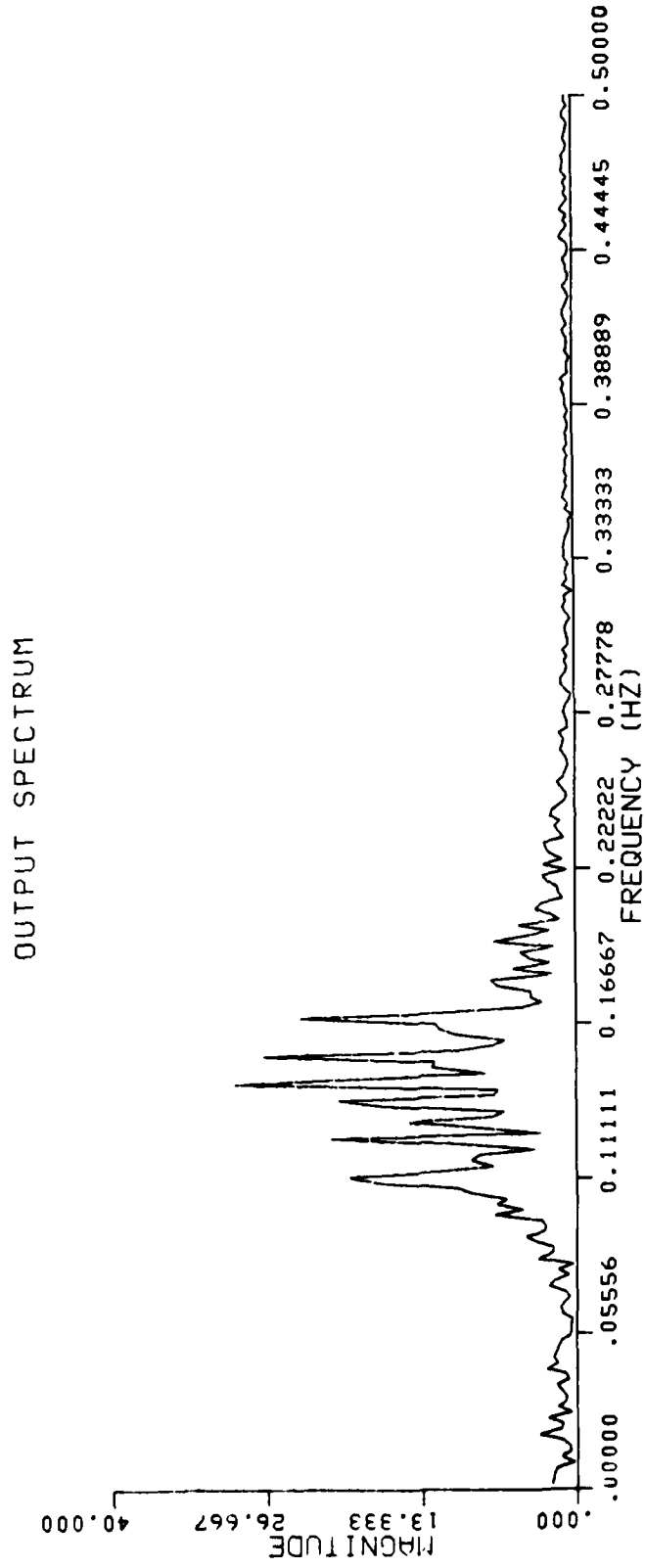


FIGURE 12B. SPECTRAL DENSITY S(f) FOR DATA FILE C514T4

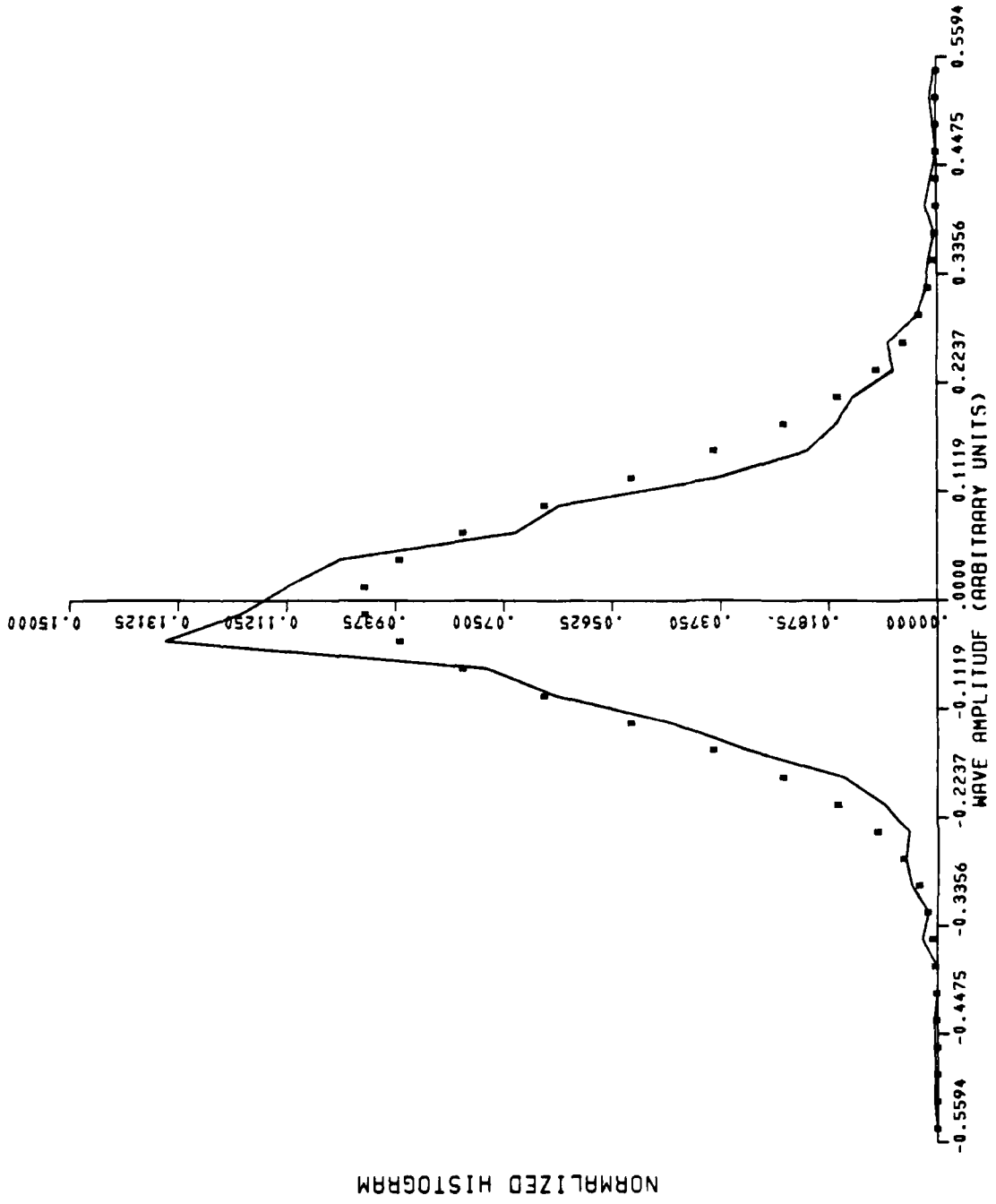


FIGURE 12C. NORMALIZED HISTOGRAM h(x) FOR DATA FILE C514T4

NORMALIZED HISTOGRAM

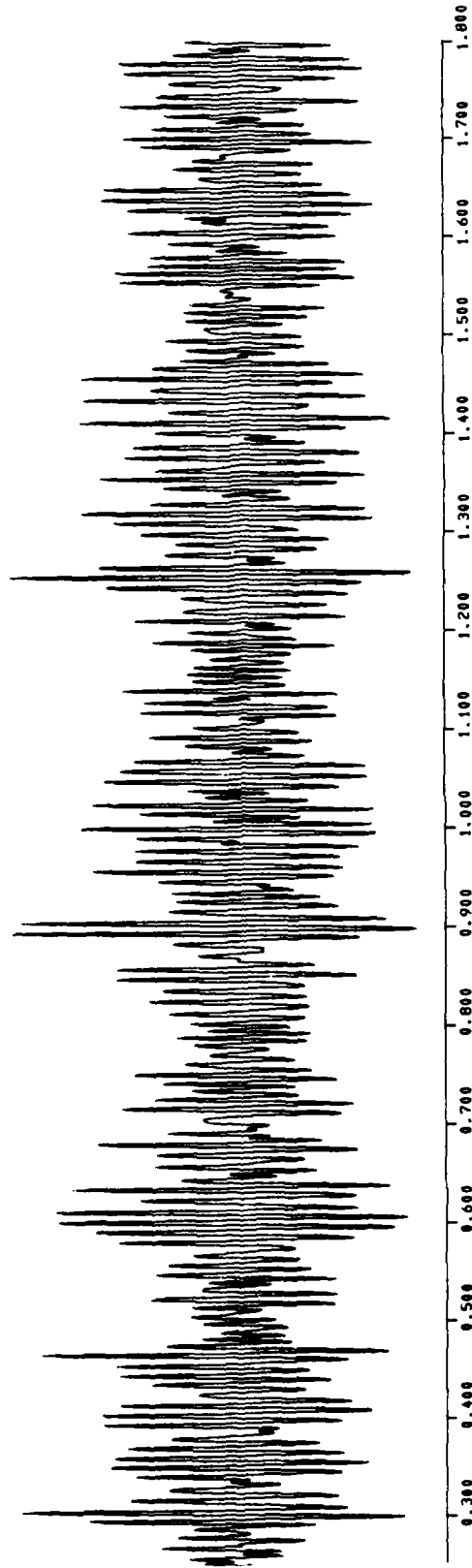


FIGURE 13A. TIME SERIES $X(t)$ FOR DATA FILE C237T4

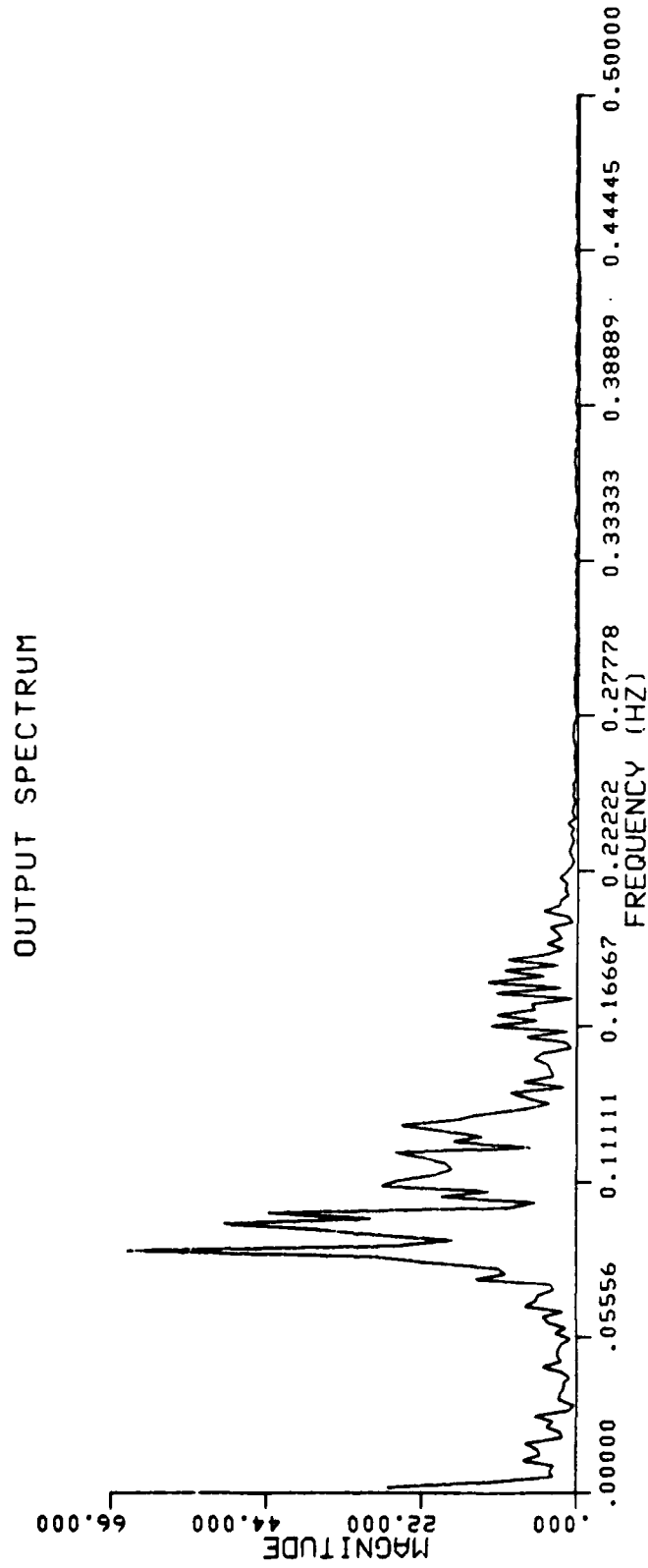


FIGURE 13B. SPECTRAL DENSITY S(f) FOR DATA FILE C237T4

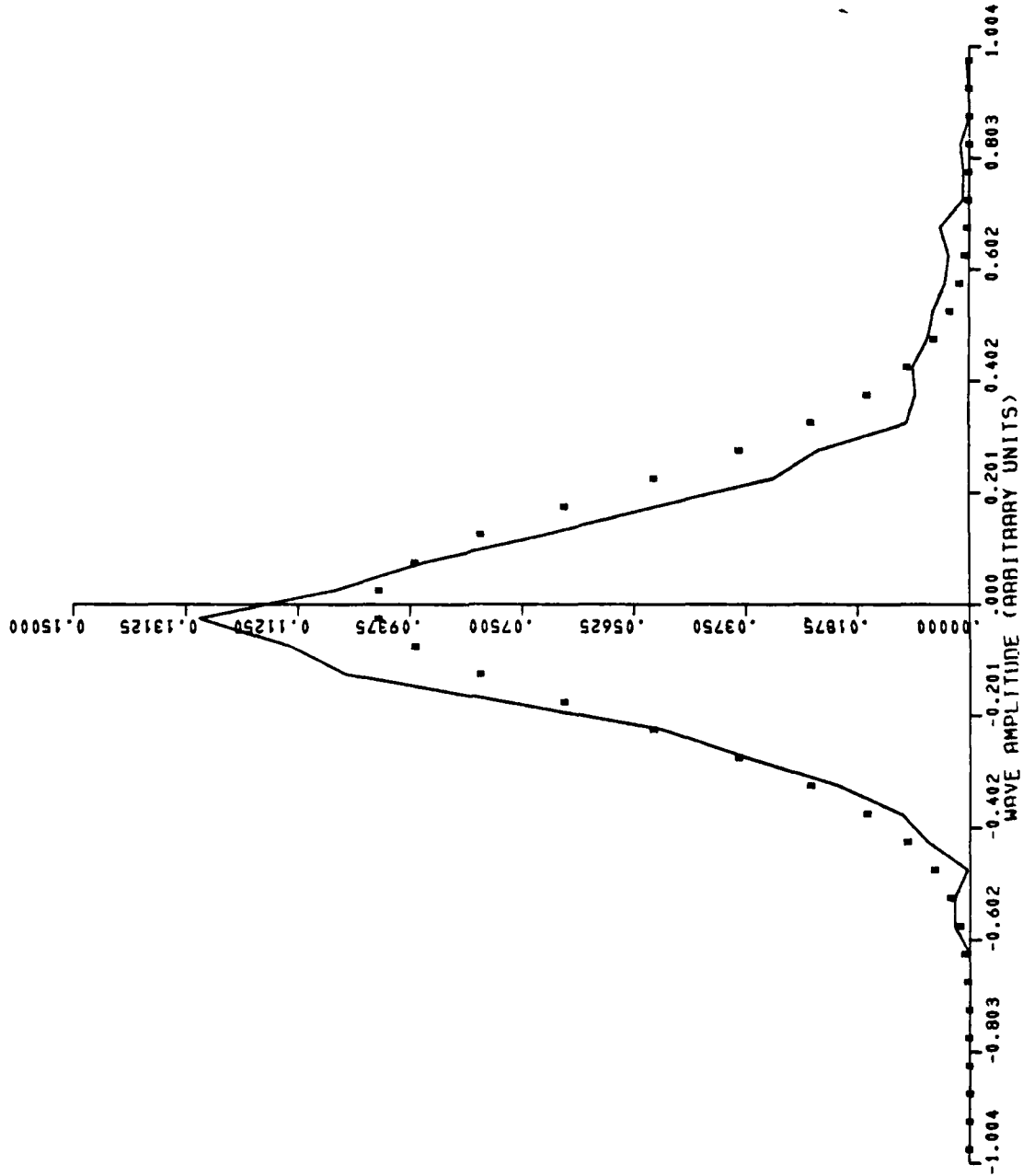


FIGURE 13C. NORMALIZED HISTOGRAM h(x) FOR DATA FILE C237T4

NORMALIZED HISTOGRAM

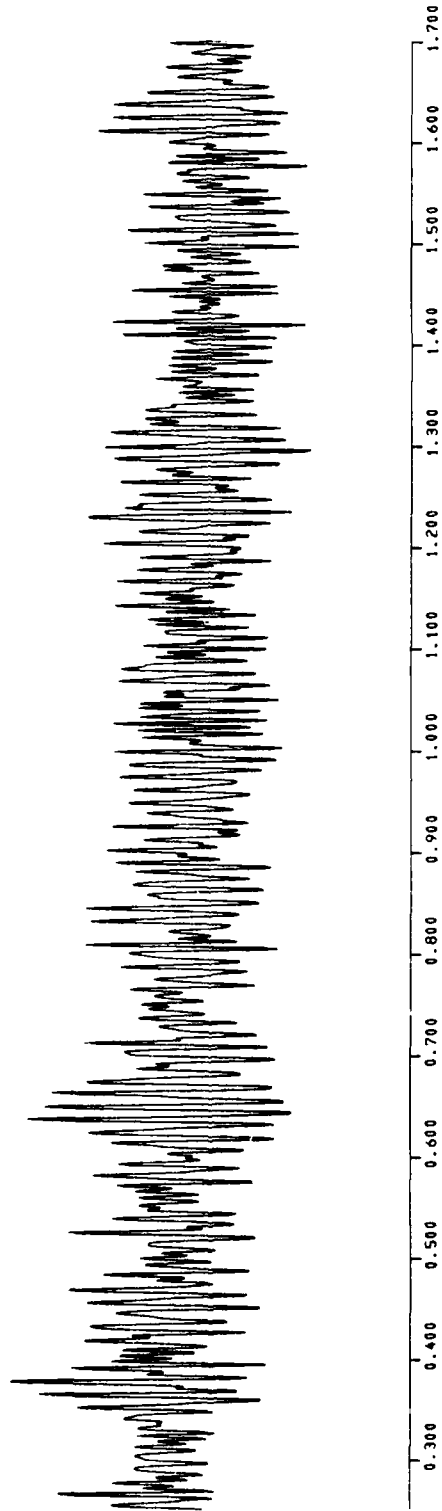


FIGURE 14A. TIME SERIES X(t) FOR DATA FILE C211T4

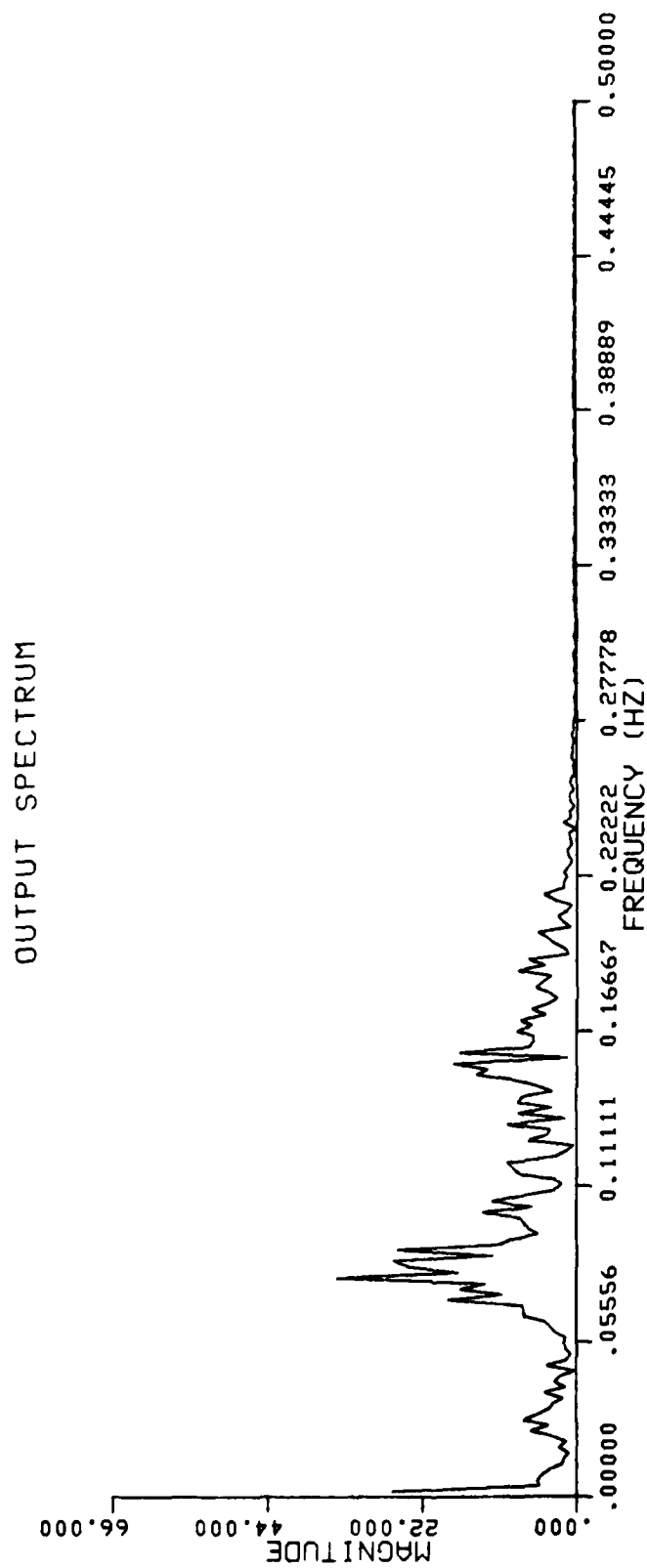


FIGURE 14B. SPECTRAL DENSITY S(f) FOR DATA FILE C211T4

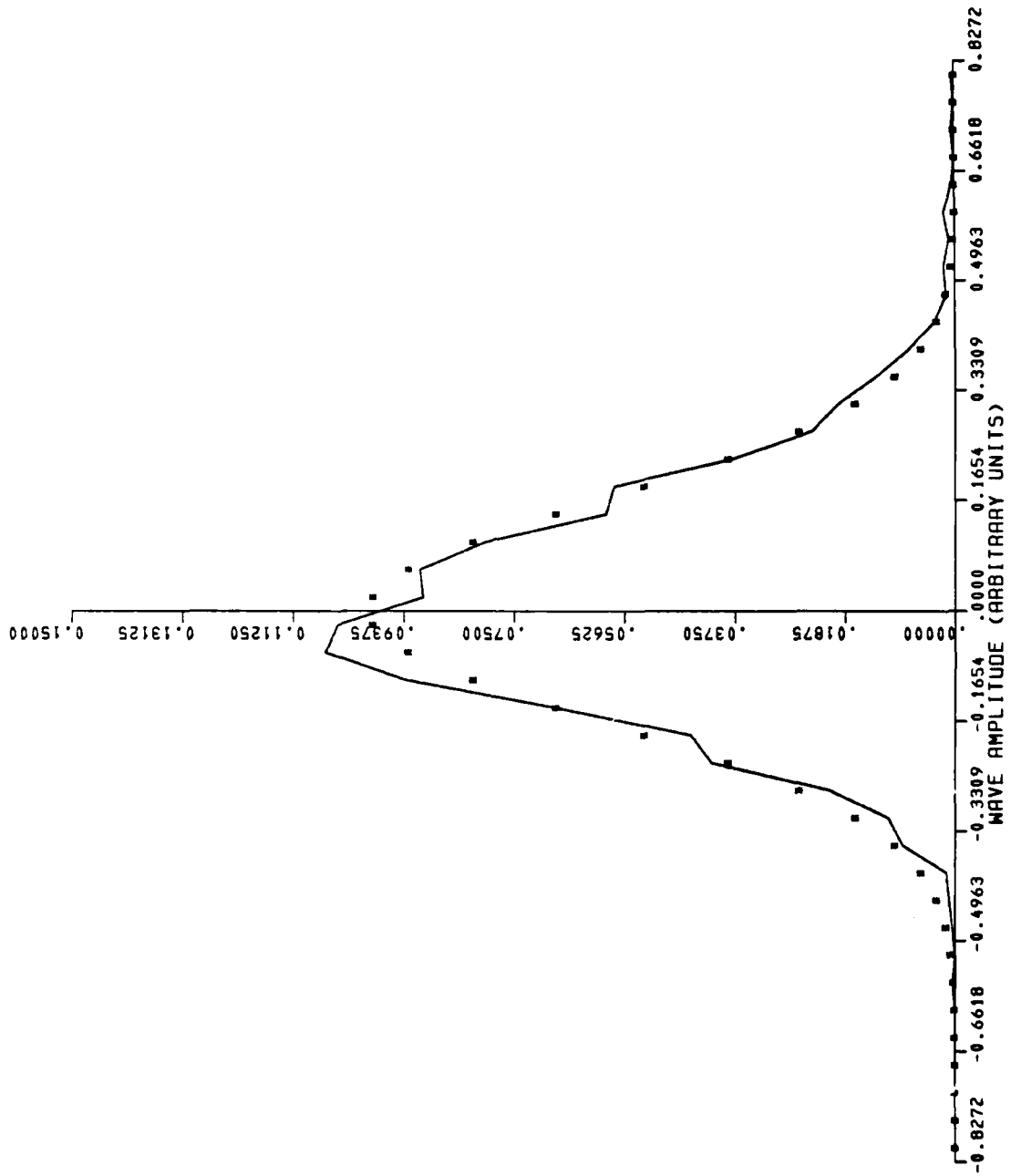


FIGURE 14C. NORMALIZED HISTOGRAM h(x) FOR DATA FILE C211T4

NORMALIZED HISTOGRAM

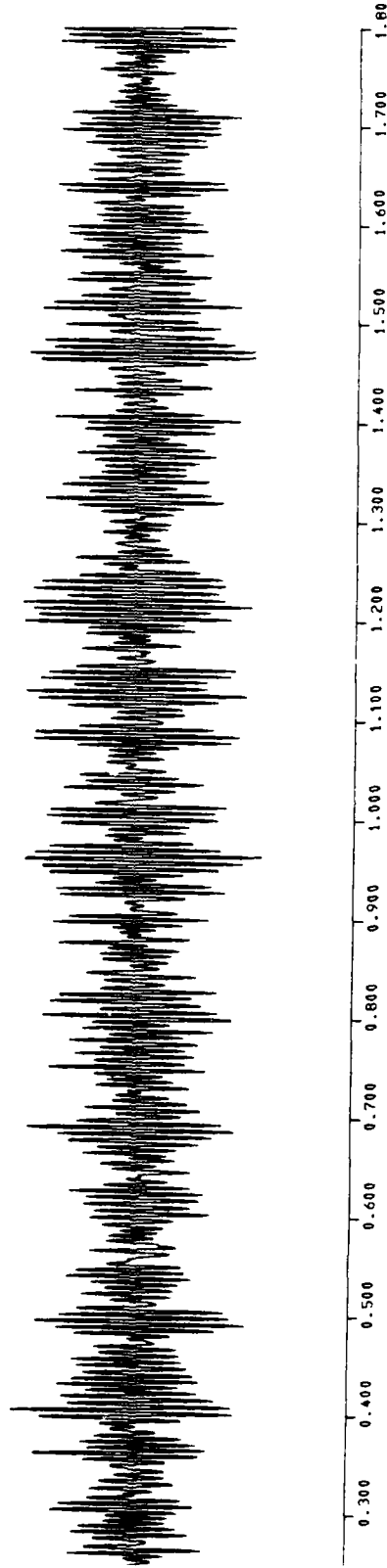


FIGURE 15A. TIME SERIES X(t) FOR DATA FILE C183T4

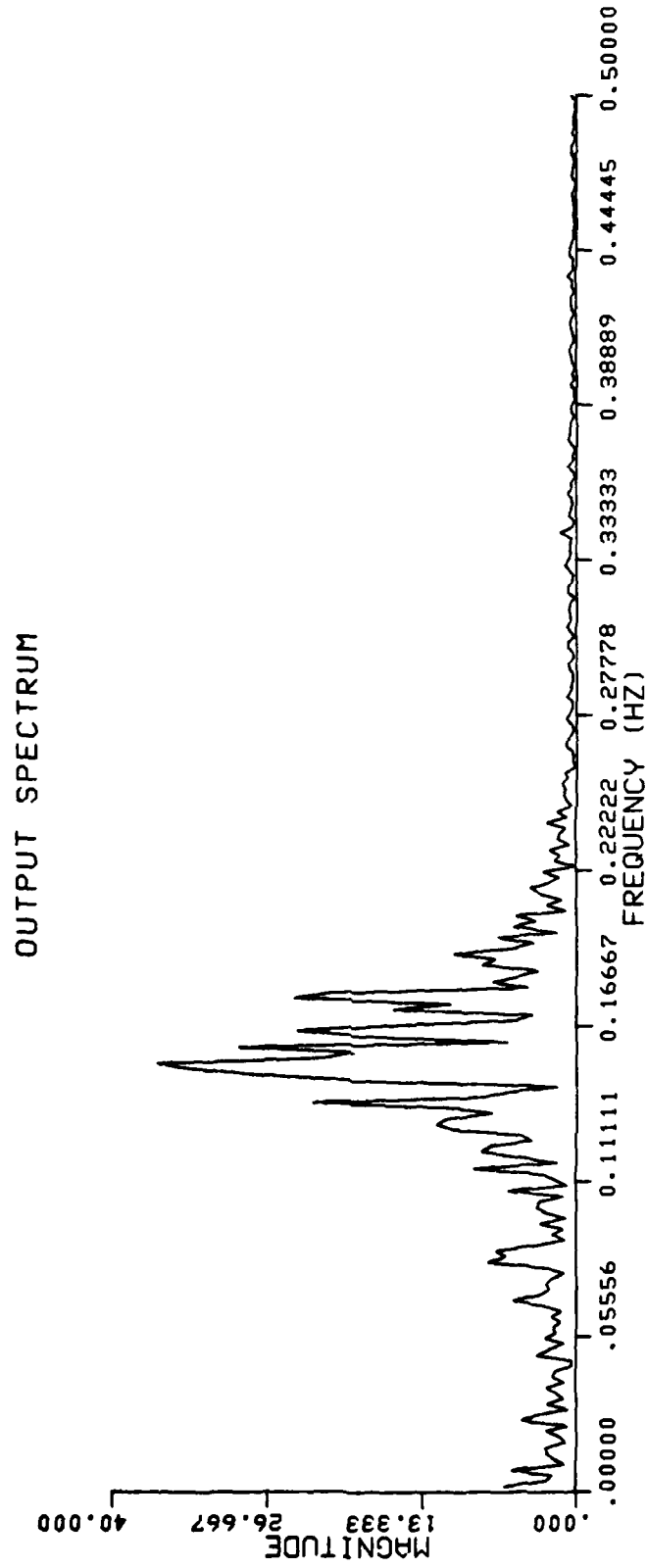
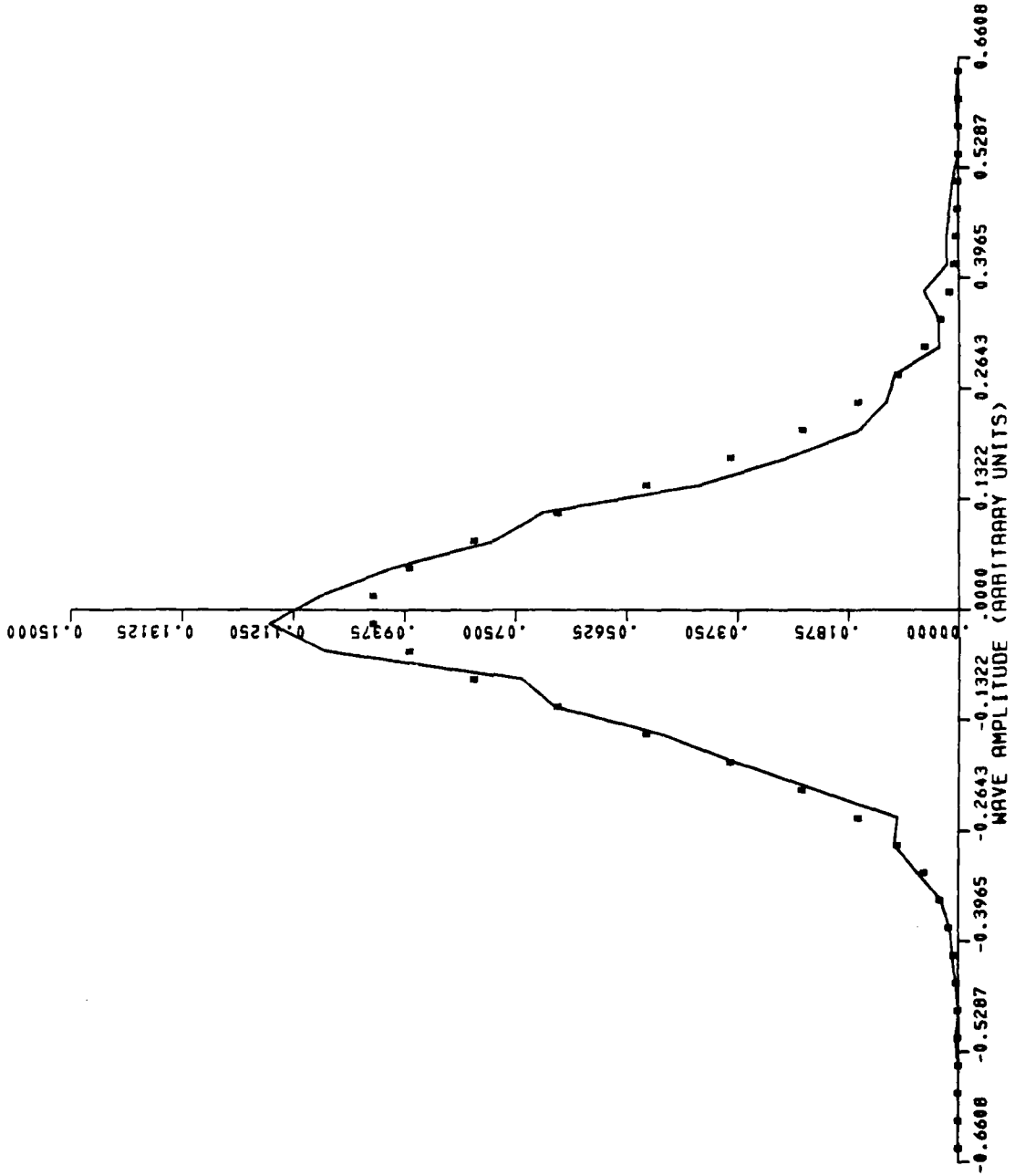


FIGURE 15B. SPECTRAL DENSITY S(f) FOR DATA FILE C183T4



NORMALIZED HISTOGRAM

FIGURE 15C. NORMALIZED HISTOGRAM h(x) FOR DATA FILE C183T4

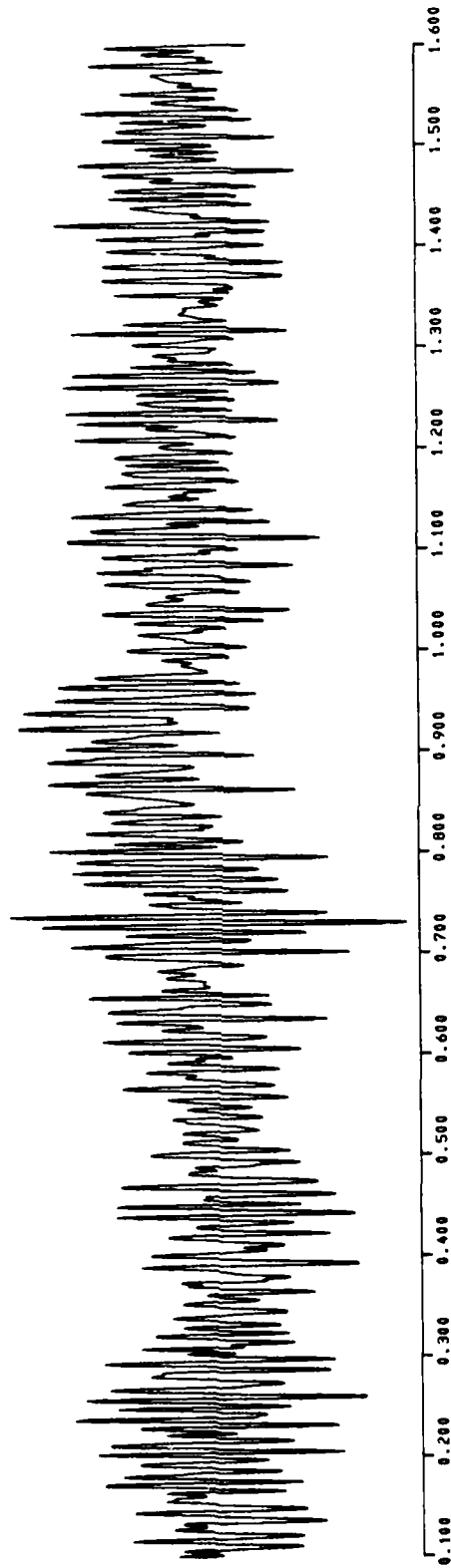


FIGURE 16A. TIME SERIES $X(t)$ FOR DATA FILE C558T4

OUTPUT SPECTRUM

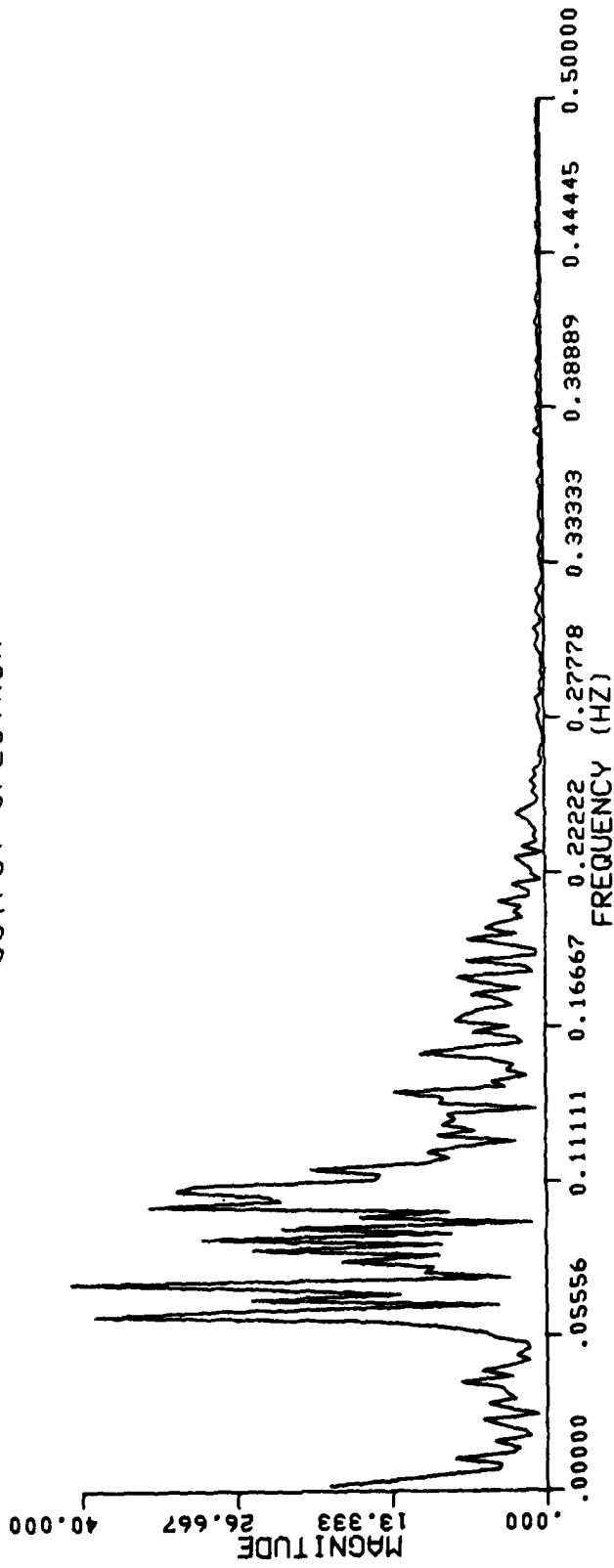


FIGURE 168. SPECTRAL DENSITY S(f) FOR DATA FILE C558T4

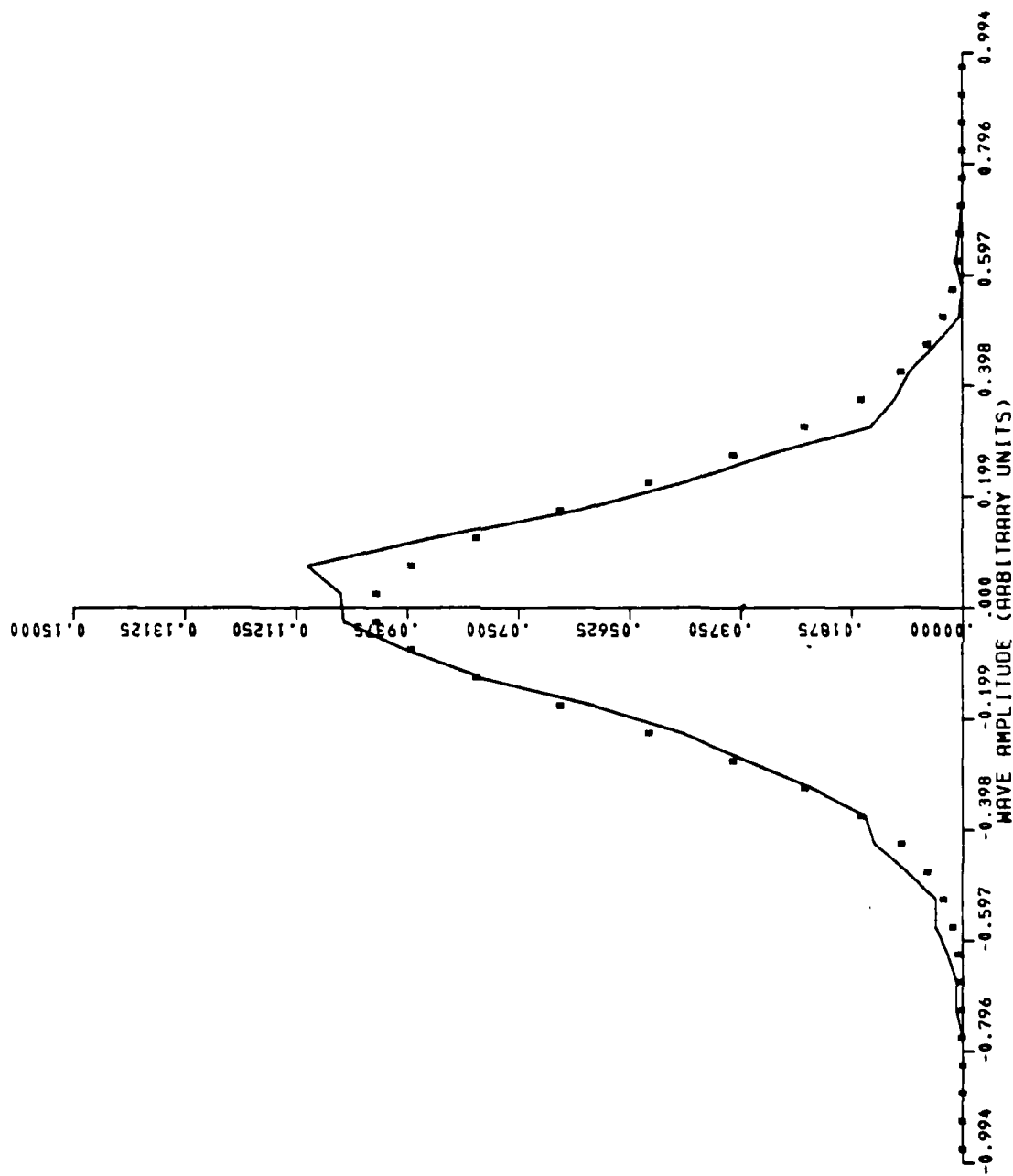


FIGURE 16C. NORMALIZED HISTOGRAM $h(x)$ FOR DATA FILE C558T4

NORMALIZED HISTOGRAM

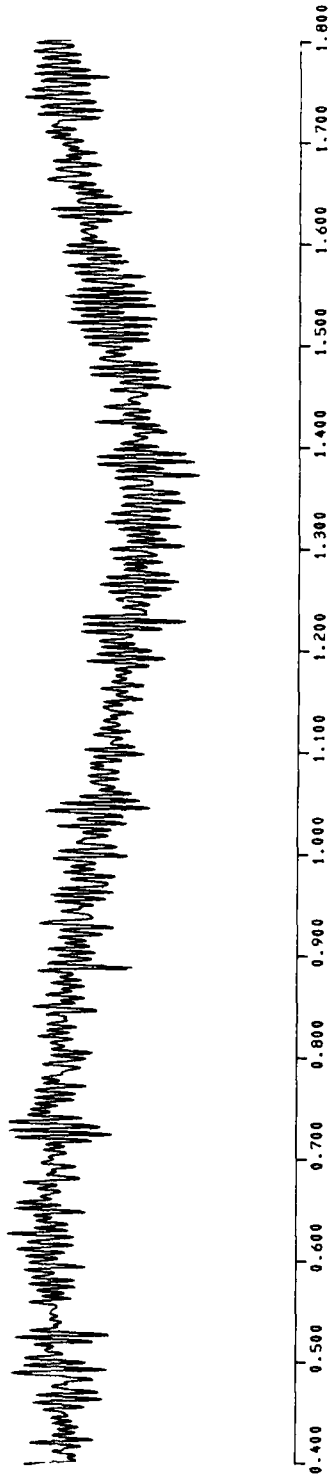


FIGURE 17A. TIME SERIES $X(t)$ FOR DATA FILE C518T4

OUTPUT SPECTRUM

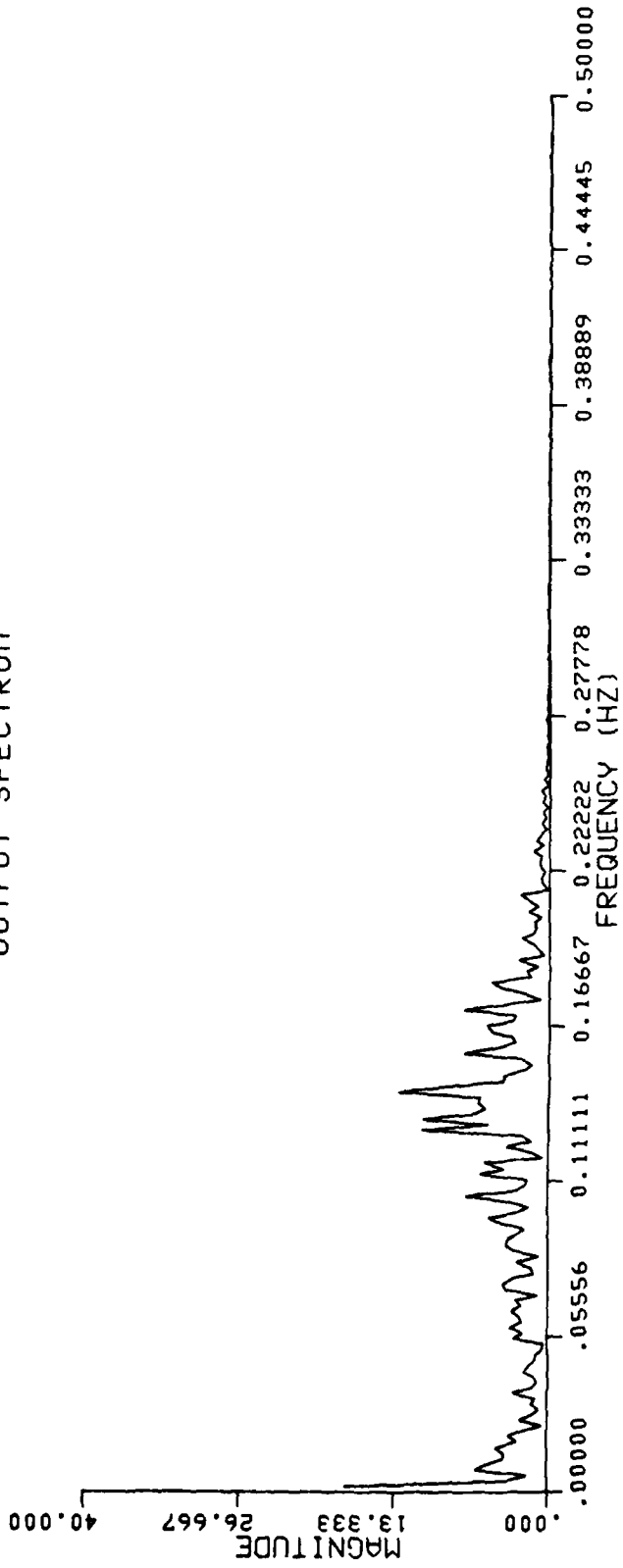


FIGURE 17B. SPECTRAL DENSITY S(f) FOR DATA FILE C518T4

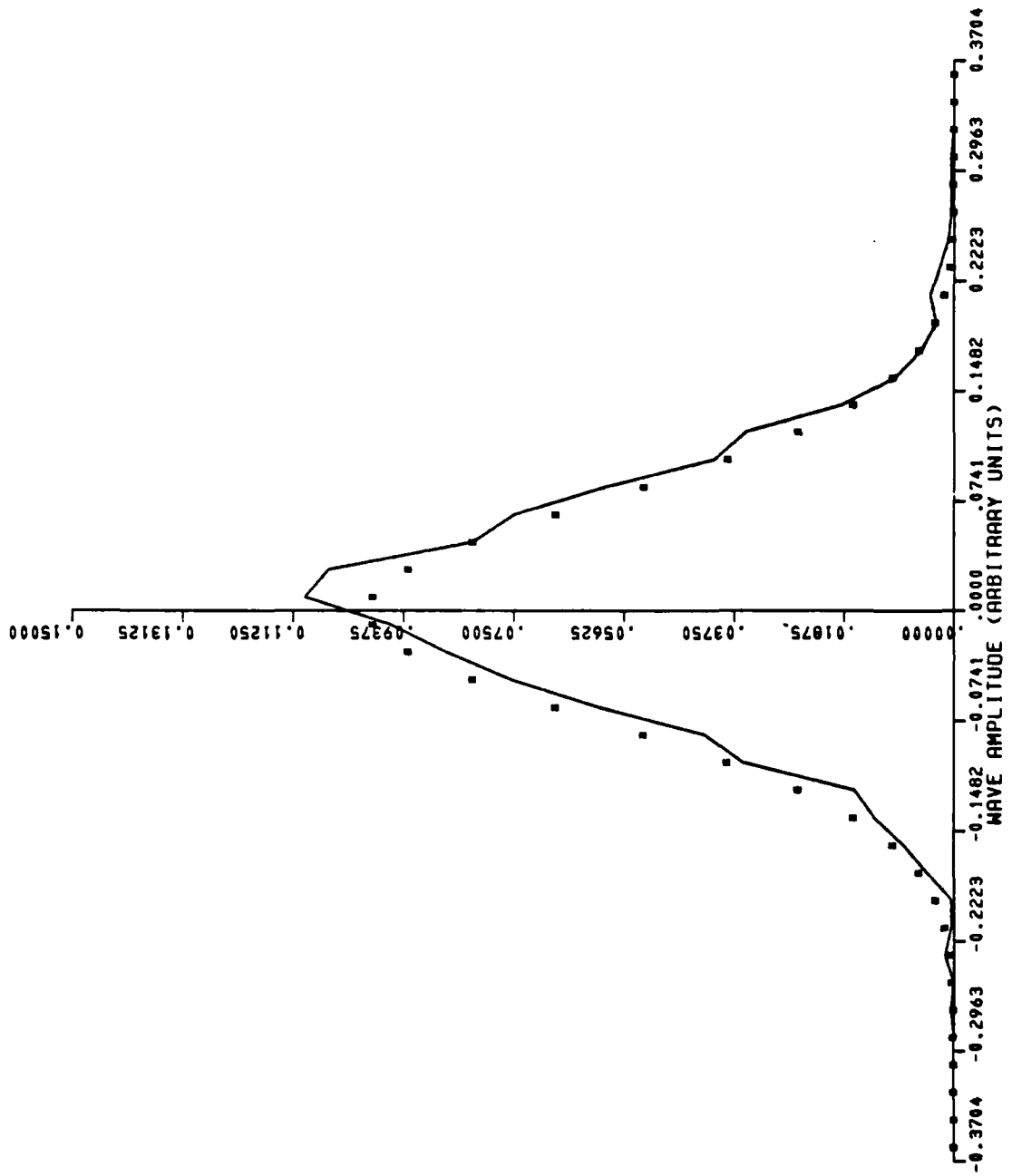


FIGURE 17C. NORMALIZED HISTOGRAM h(x) FOR DATA FILE C518T4

NORMALIZED HISTOGRAM

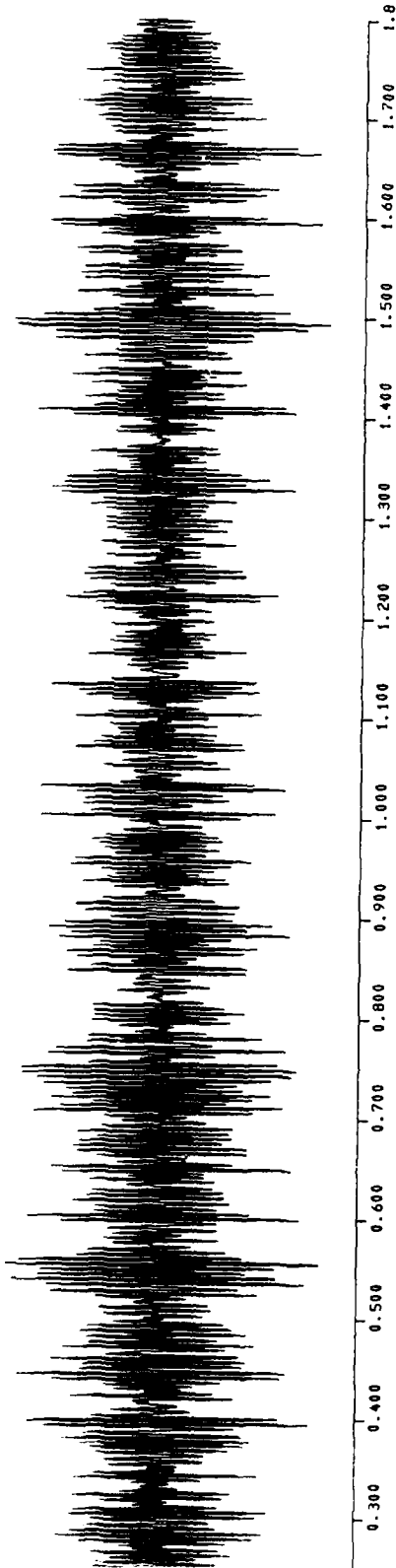


FIGURE 18A. TIME SERIES X(t) FOR DATA FILE A633T4

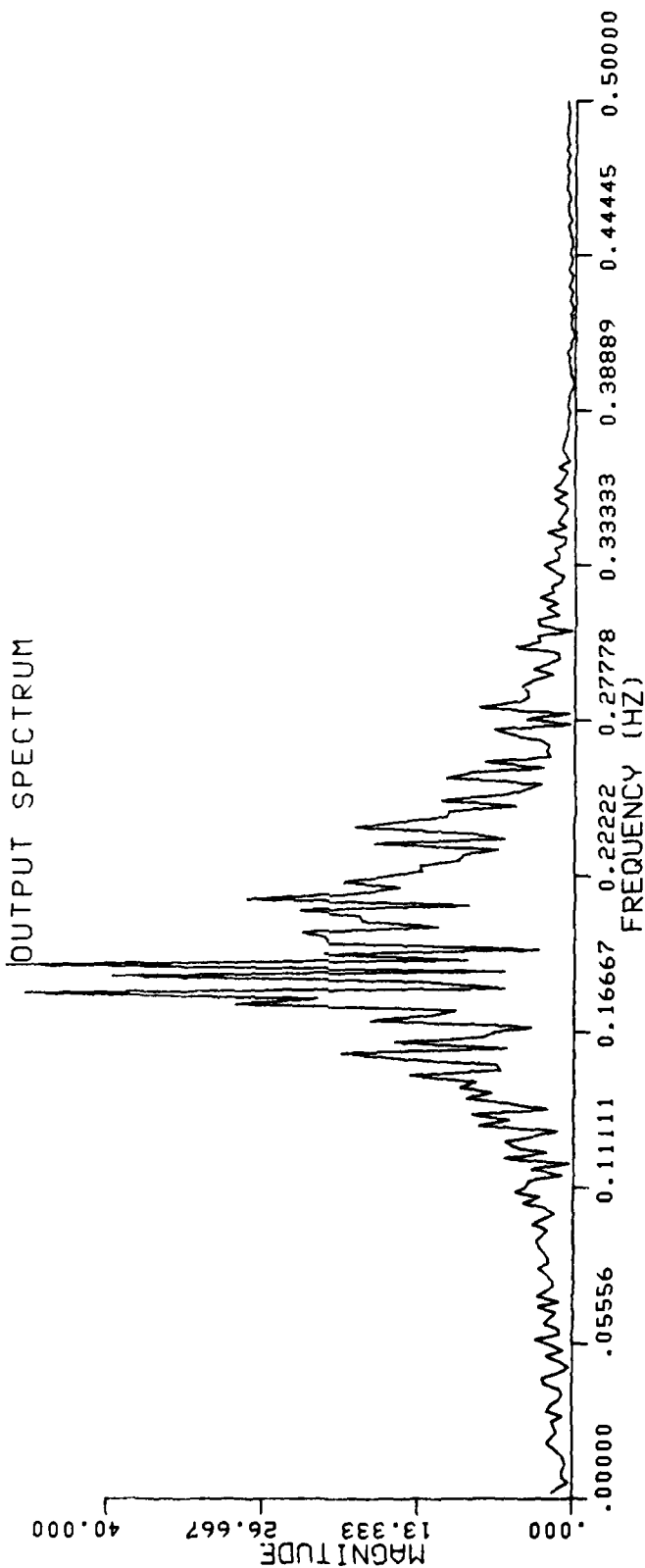


FIGURE 18B. SPECTRAL DENSITY S(f) FOR DATA FILE A633T4

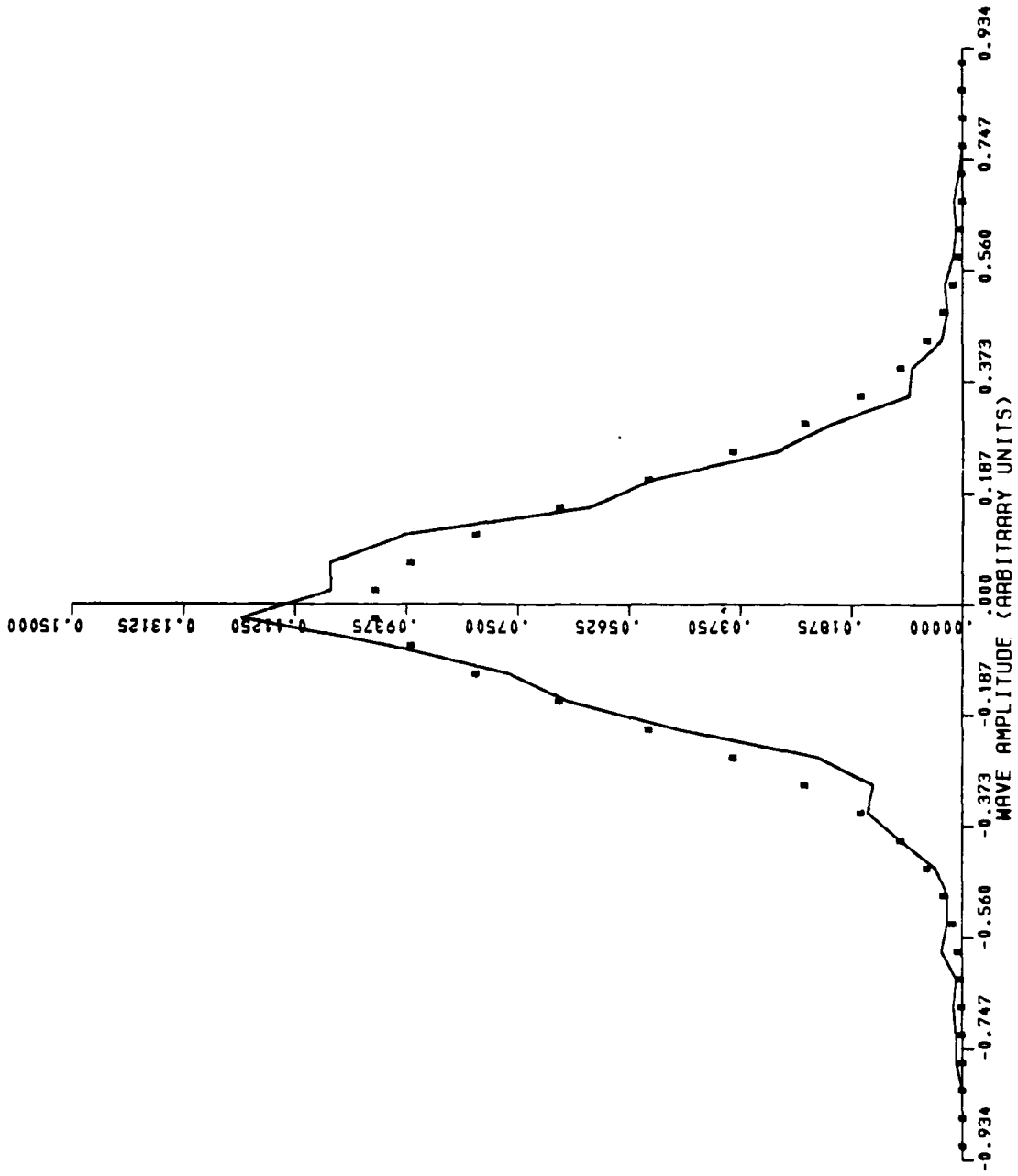


FIGURE 18C. NORMALIZED HISTOGRAM h(x) FOR DATA FILE A633T4

NORMALIZED HISTOGRAM

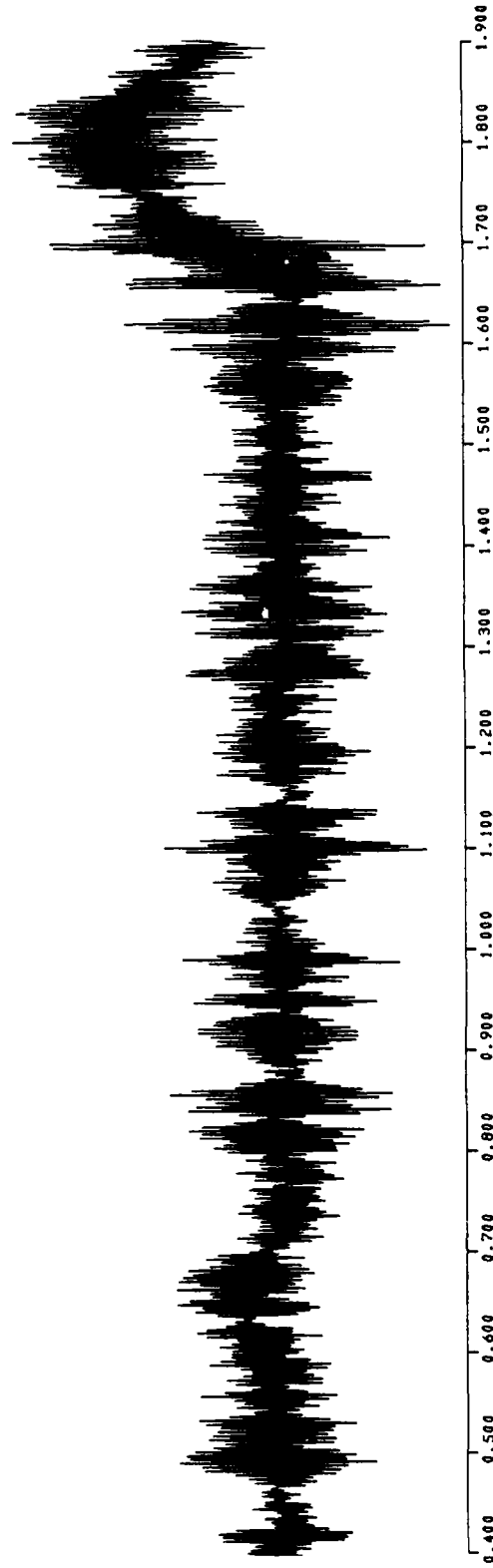


FIGURE 19A. TIME SERIES X(t) FOR DATA FILE A455T4

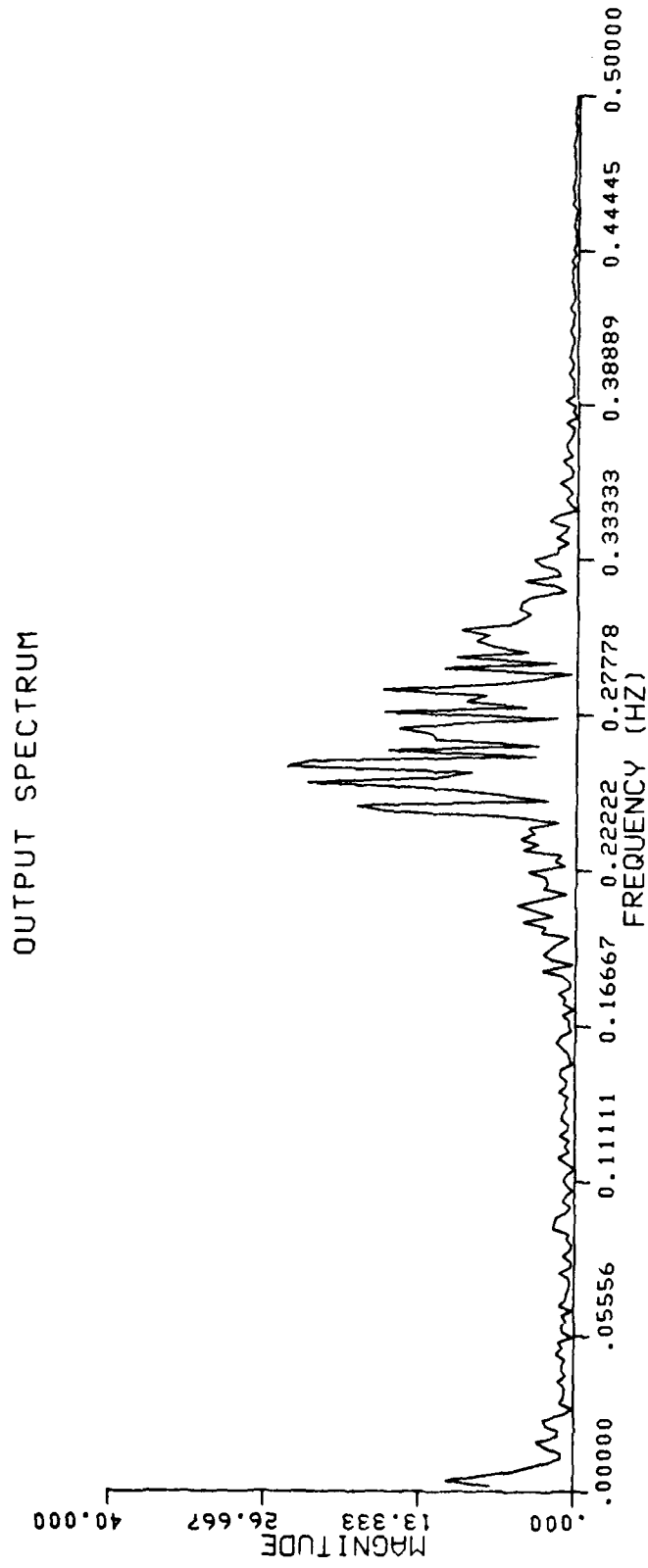


FIGURE 19B. SPECTRAL DENSITY S(f) FOR DATA FILE A455T4

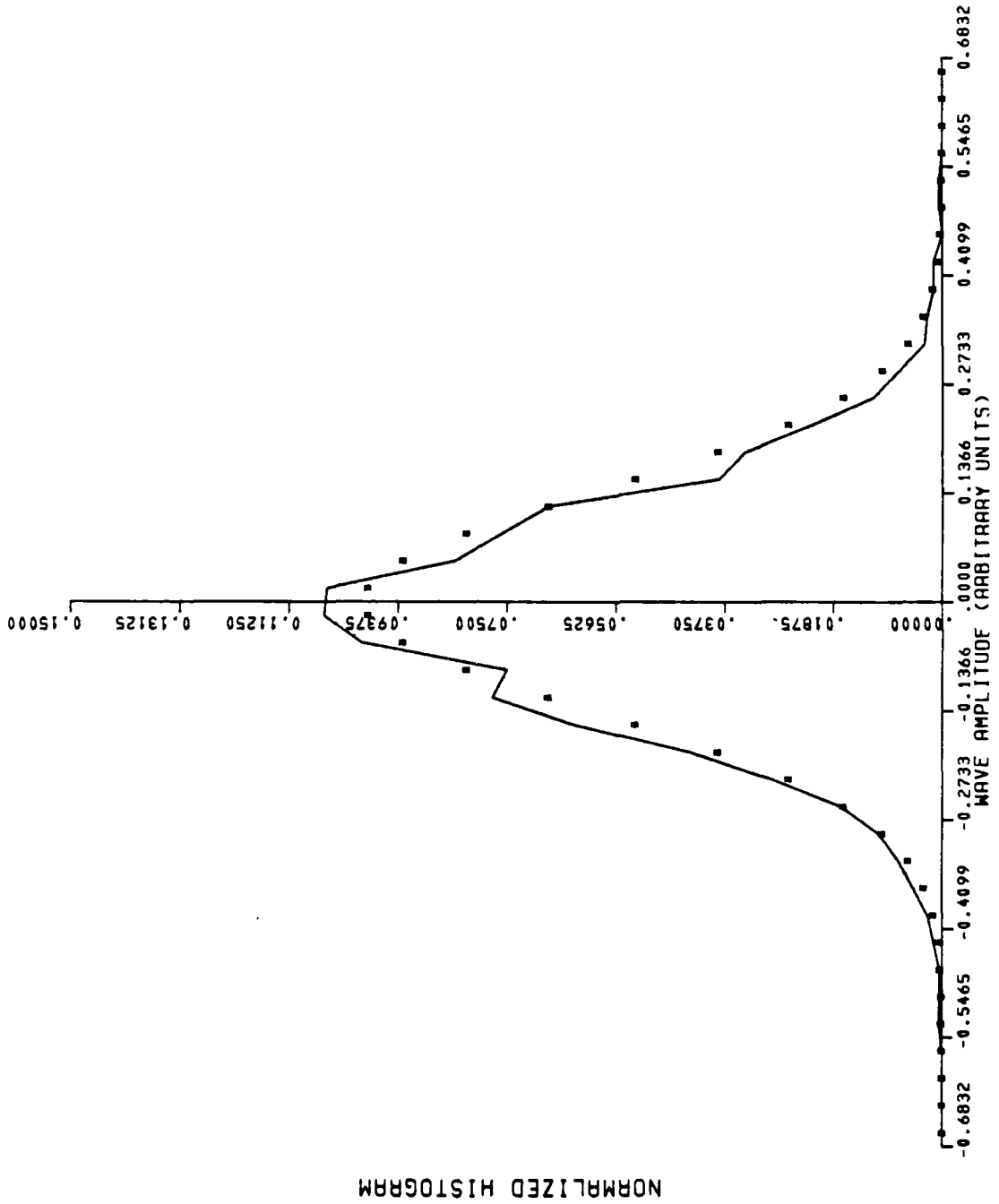


FIGURE 19C. NORMALIZED HISTOGRAM h(x) FOR DATA FILE A455T4

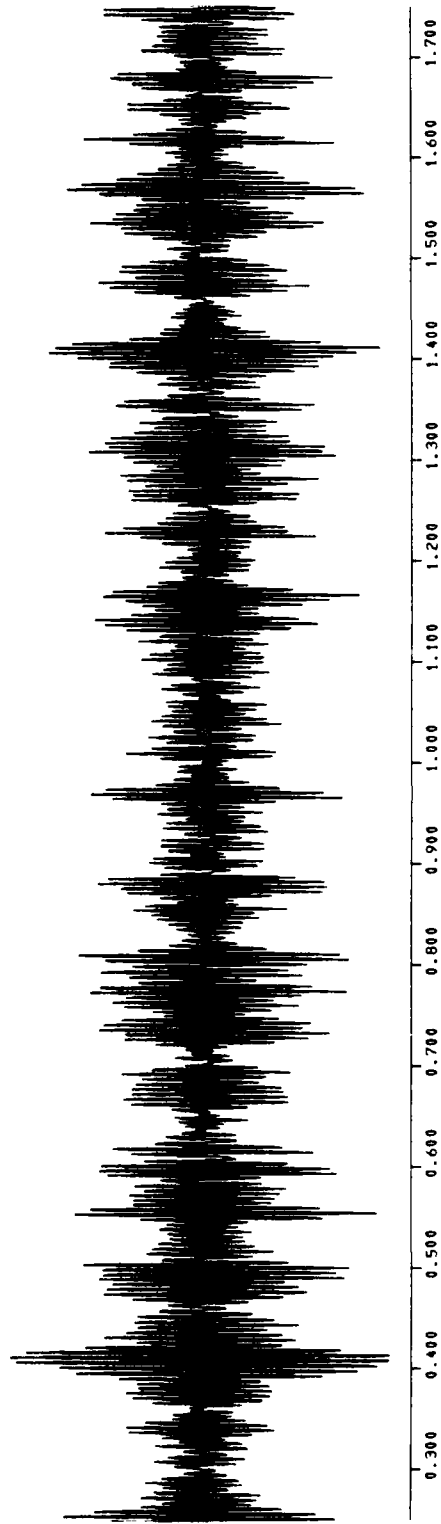


FIGURE 20A. TIME SERIES $X(t)$ FOR DATA FILE A515T2

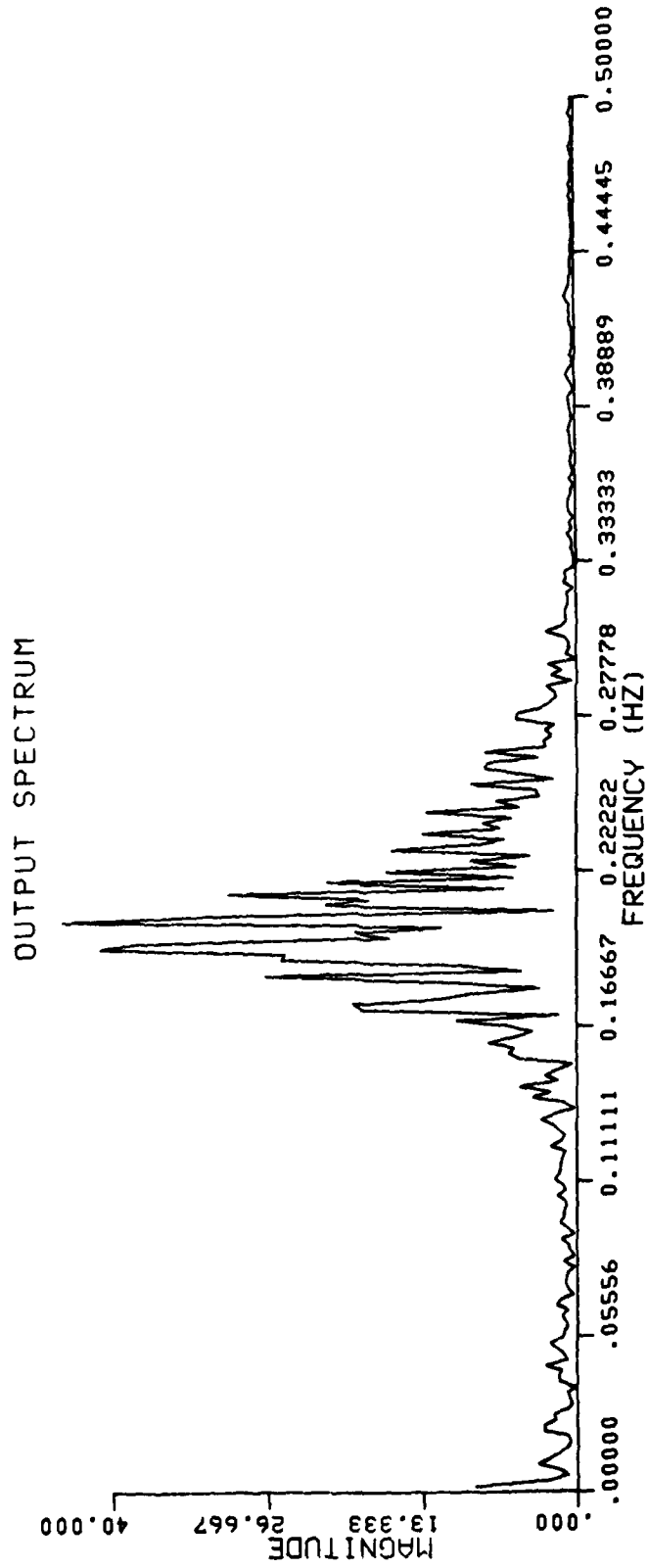


FIGURE 20B. SPECTRAL DENSITY S(f) FOR DATA FILE A515T2

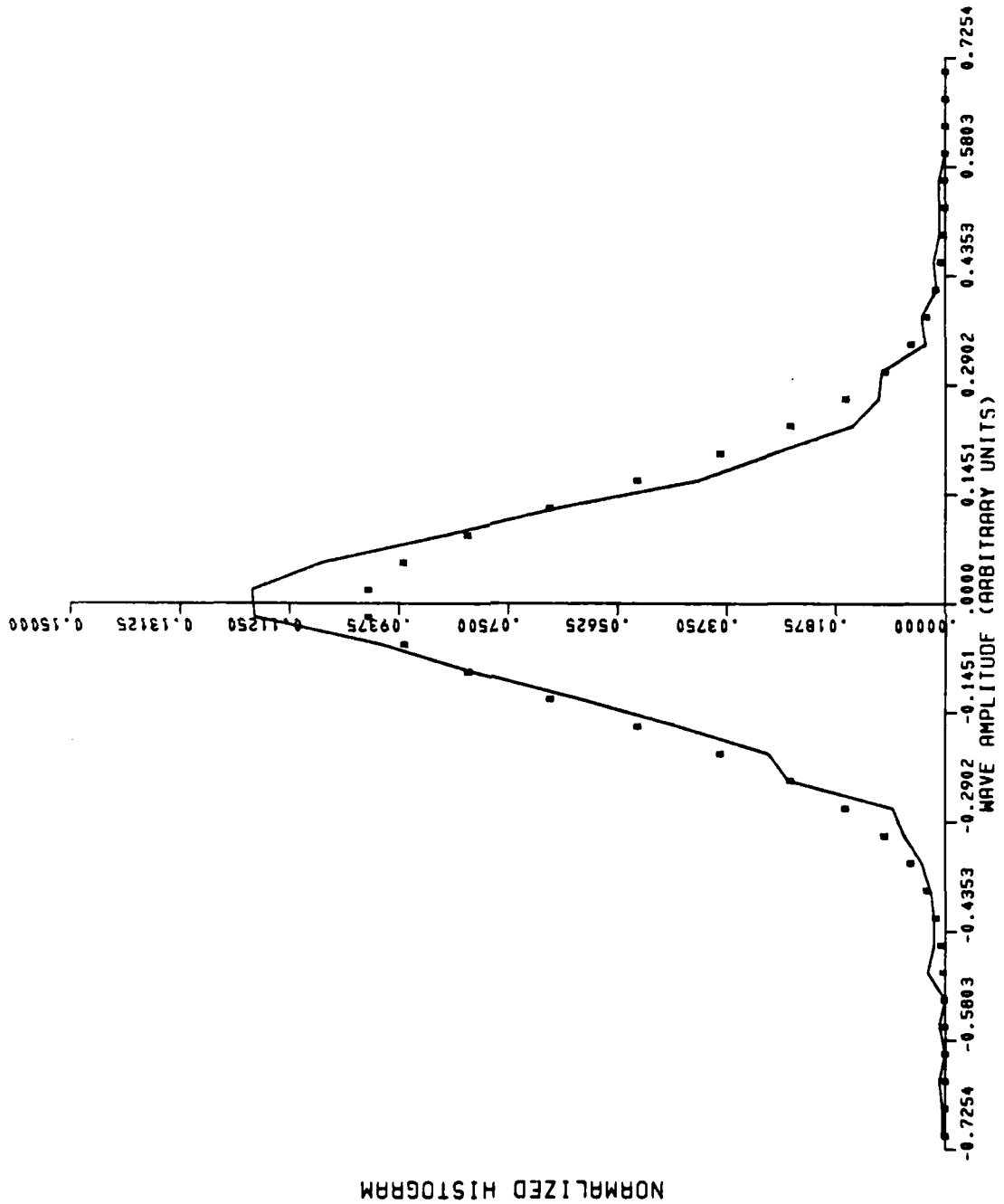


FIGURE 20C. NORMALIZED HISTOGRAM h(x) FOR DATA FILE A515T2

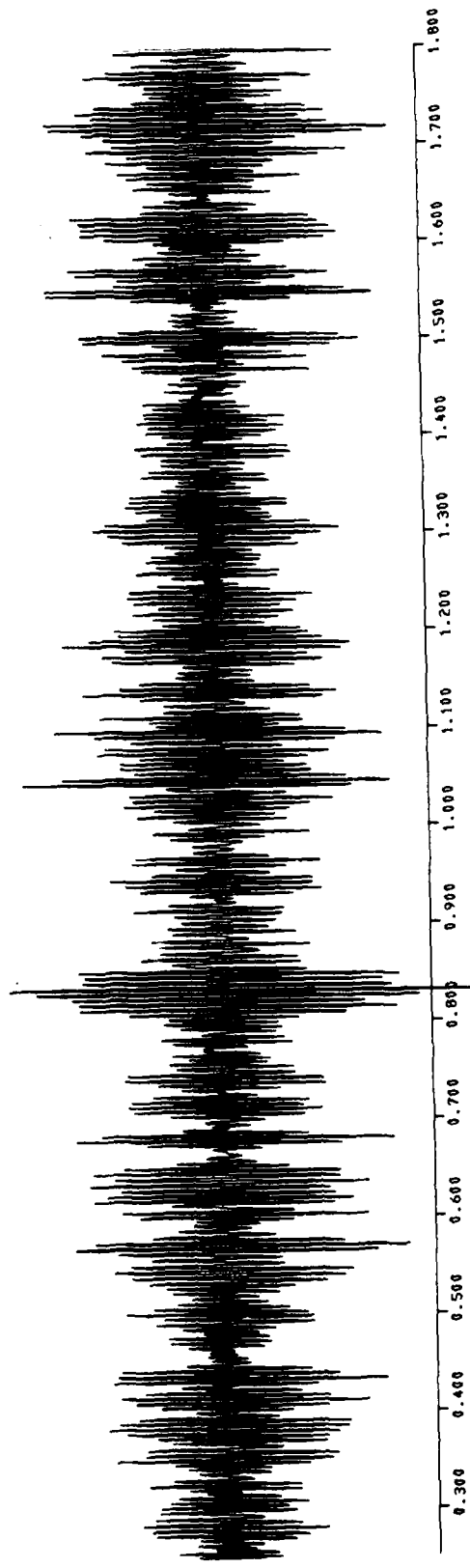


FIGURE 21A. TIME SERIES $X(t)$ FOR DATA FILE A508T2

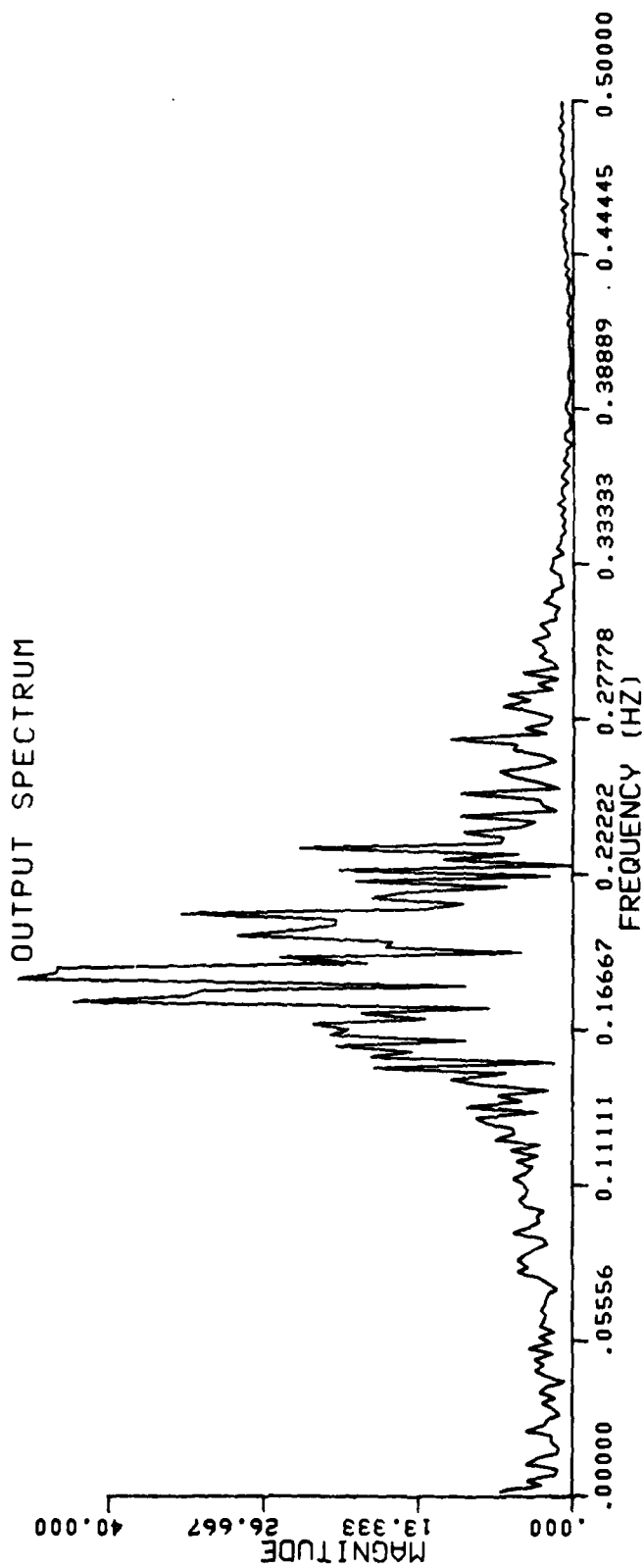


FIGURE 21B. SPECTRAL DENSITY S(f) FOR DATA FILE A508T2

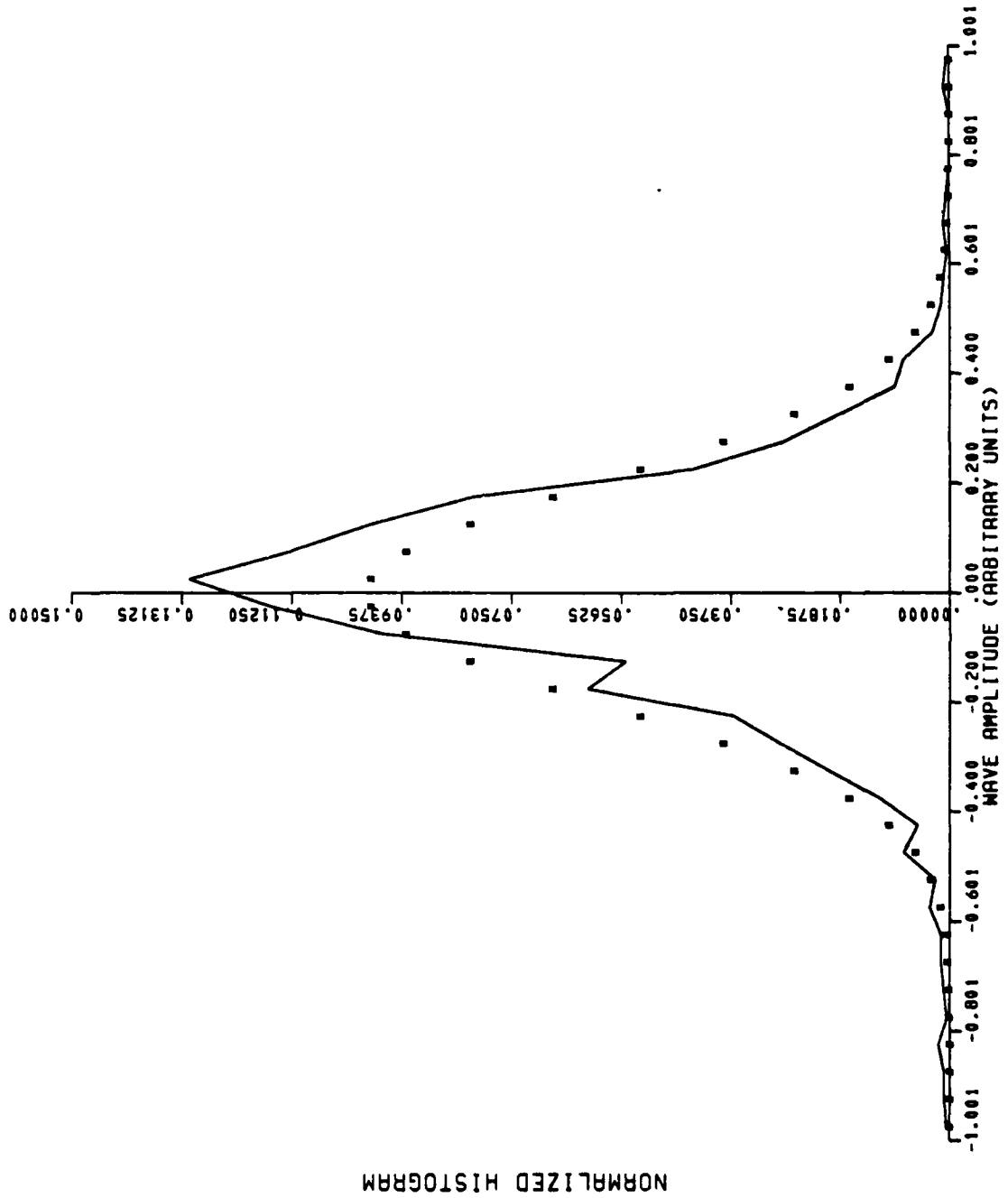


FIGURE 21C. NORMALIZED HISTOGRAM $h(x)$ FOR DATA FILE A508T2

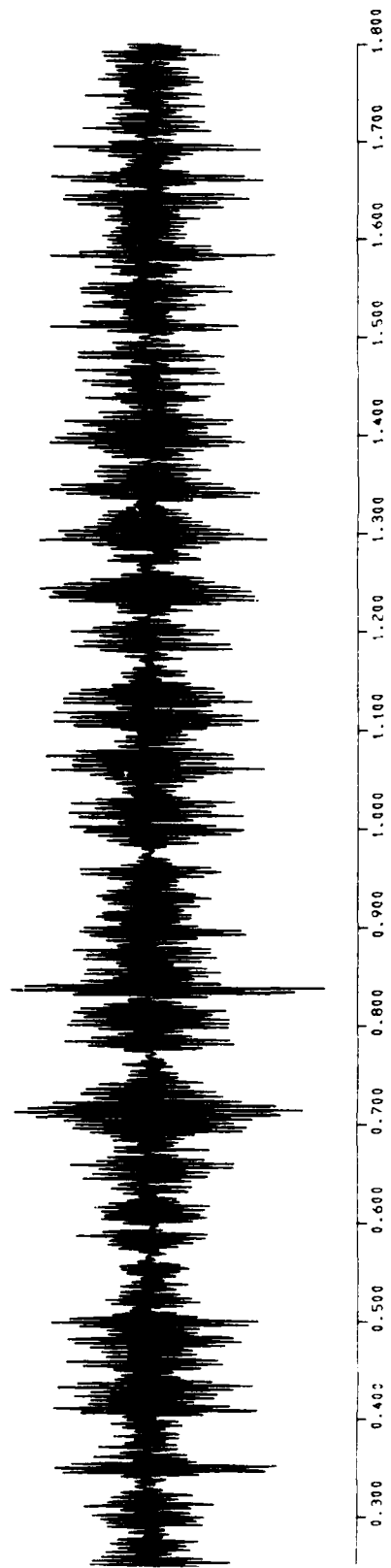


FIGURE 22A. TIME SERIES X(t) FOR DATA FILE A380T2

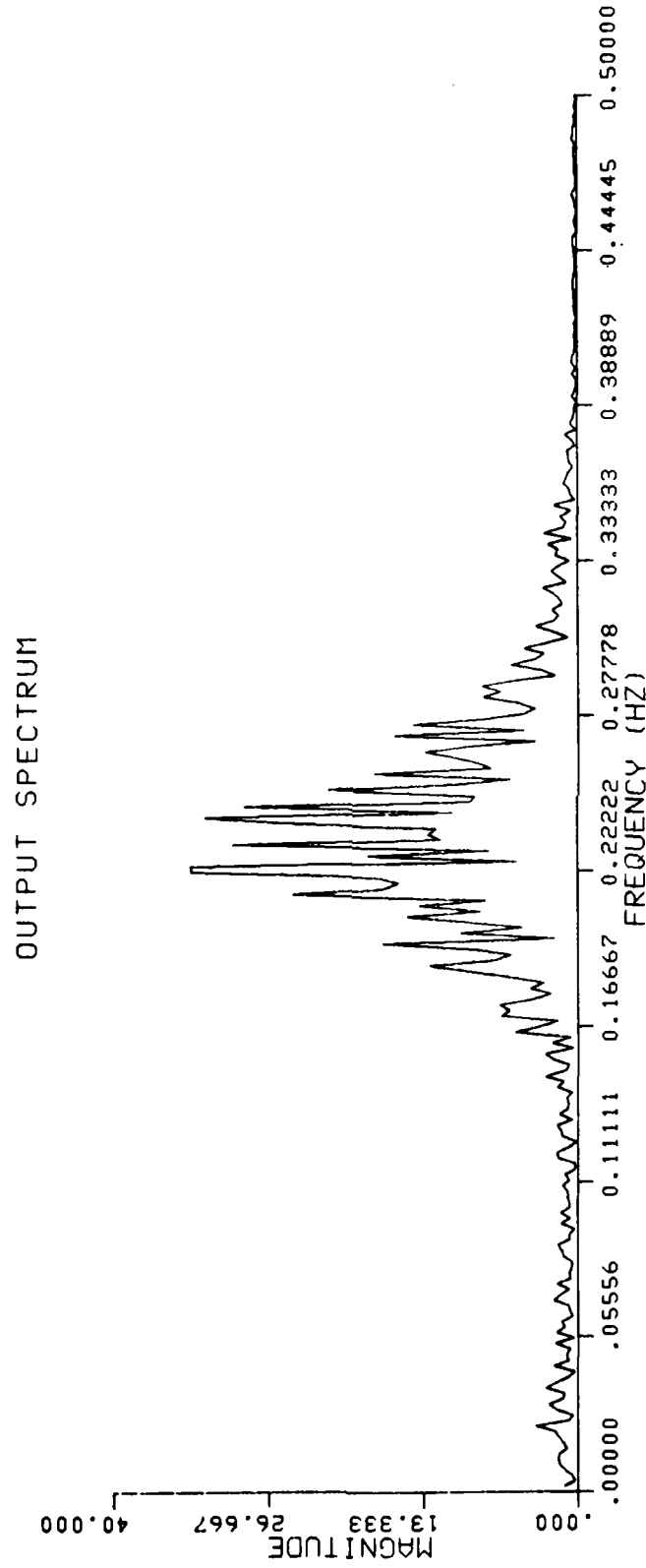


FIGURE 22B. SPECTRAL DENSITY S(f) FOR DATA FILE A380T2

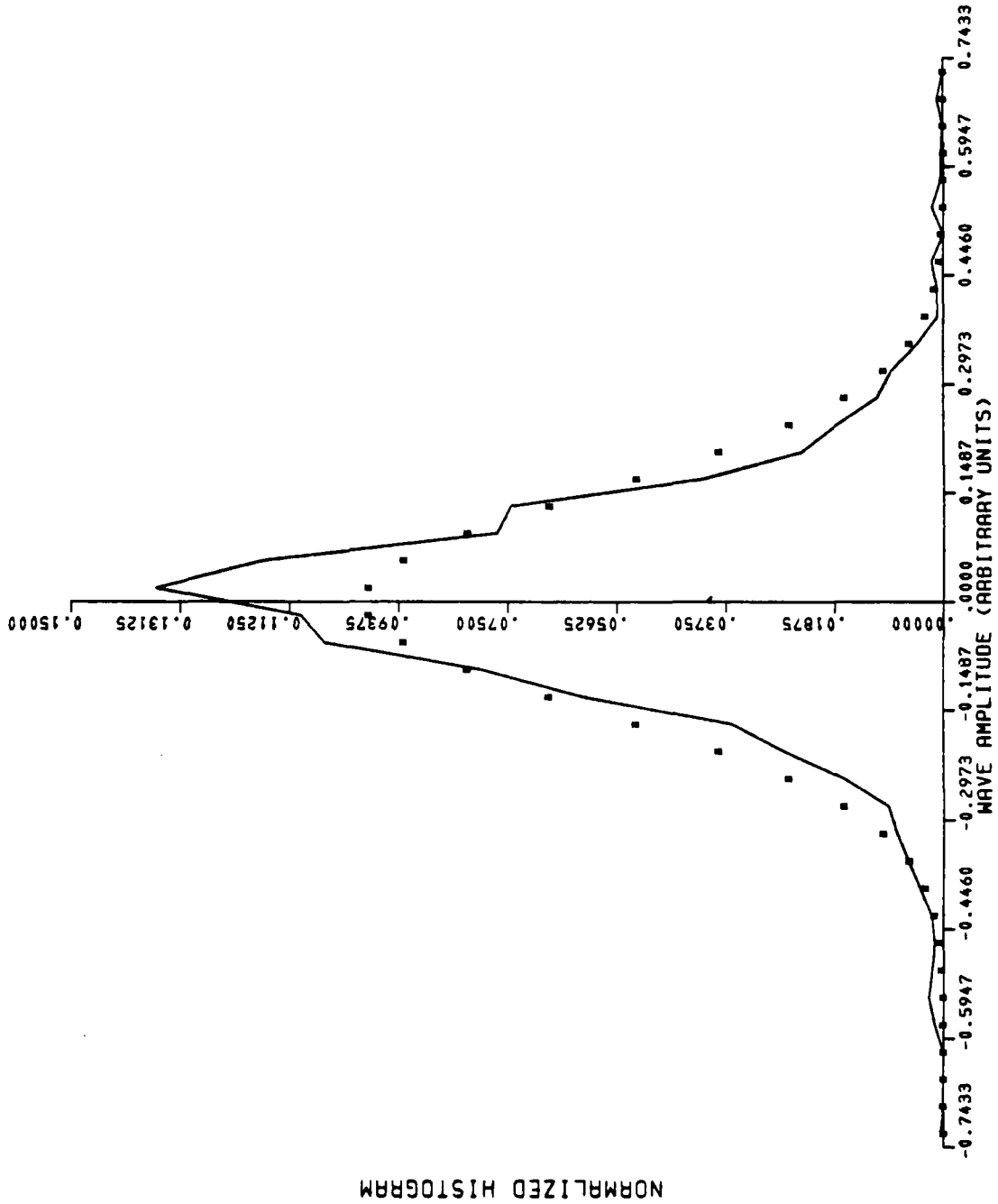


FIGURE 22C. NORMALIZED HISTOGRAM h(x) FOR DATA FILE A380T2

normalized histogram, or sample p.d.f., of the same record. The limits on the horizontal axis are determined by computing the r.m.s. value of $X(t)$ and multiplying it by +5 (for the right hand limit) and -5 (for the left). The dynamic range of the abscissa is then ten times the r.m.s. fluctuation. This range is subdivided into 100 "bins" of equal width, with 50 bins on each side of the vertical axis ($x = 0$). The two or three thousand sample values are sorted into the bins to obtain a histogram. The dotted curve shows the Gaussian p.d.f. with standard deviation equal to the r.m.s. fluctuation.

Table 1 summarizes the authors' observation on the 20 trios of charts contained in Figures 3 through 22. The first two columns in the table establish the correspondences between the figure numbers and the file I.D. numbers. The third column indicates the modality of the spectral density. A "1" in the third column means there is only one distinct center frequency. A "2" in the third column says the spectral density is Bimodal, as illustrated most clearly in Figure 9b, where the two modes appear to be at around 0.07 Hz and 0.17 Hz. If a "1*" appears in the third column, it refers to the fact that the spectral density is unimodal and asymmetric, declining more sharply to the left of the peak, more gradually to the right. The Bretschneider spectrum and most of the other theoretical ocean wave spectra predict this kind of unimodal asymmetry. The fourth column in the table comments on the proximity of the normalized histogram to the Gaussian p.d.f., with "1" indicating a reasonable fit, and "0" indicating a "poor fit." These entries are somewhat subjective and the reader may reach different conclusions.

Regarding the origins of the data, those files whose I.D. numbers begin with the prefix "P" were acquired in a sheltered, shallow, coastal location. The others, with prefixes "C" and "A", were acquired in the open ocean.

TABLE 1. OCEAN WAVE DATA

<u>Figure No.</u>	<u>File I.D.</u>	<u>Spectral Modality</u>	<u>Normality</u>
3	P577R6	1	1
4	P345R4	2	0
5	P340R3	1	1
6	P584R6	1*	1
7	P584R4	1	1
8	C506T4	1	1
9	C231T4	2	(0)
10	C540T4	(2)	(1)
11	C516T4	1*	1
12	C514T4	1	0
13	C237T4	(1*)	(0)
14	C211T4	(2)	1
15	C183T4	1	(1)
16	C558T4	1*	1
17	C518T4	1	0
18	A633T4	1	(1)
19	A455T4	1*	1
20	A515T2	1	0
21	A508T2	1*	0
22	A380T2	1	0

NON-GUASSIAN FLUCTUATIONS

A variety of techniques have been developed by statisticians for measuring the deviation of a sample distribution from the Gaussian "standard." Special graph papers are commonly employed. The analyst may compile the distribution of the squared sample values to perform a chi-squared goodness-of-fit test, since the squared Gaussian random variable has the chi-squared distribution. Another technique, which derives from communications-theoretic considerations, is to plot the function

$$Q(x) = - \frac{d}{dx} \log \hat{p}(x) \quad (14)$$

where $\hat{p}(x)$ is the best estimate of the p.d.f. of X , given the sampled values of X . For if $\hat{p}(x)$ is Gaussian, one has

$$- \frac{d}{dx} \log \left[\frac{1}{\sqrt{2\pi} \sigma} e^{-x^2/2\sigma^2} \right] = x/\sigma^2 ,$$

a straight line through the origin with slope of σ^{-2} . Thus the proximity of $Q(x)$ to a straight line with slope equal to the reciprocal mean square fluctuation, reflects the closeness of the distribution to the Gaussian.⁸

The determination of the "best estimate," $\hat{p}(x)$, from the normalized histogram, $h(x)$, is the subject of p.d.f. estimation theory. Perhaps the simplest procedure, which applies to cases in which the number of sample values far exceeds the number of "bins" used to compile the histogram, is distribution-independent linear smoothing.⁹ Let the bins be centered on the regular sequence of abscissas $X_1, X_2, \dots, X_j, \dots, X_{2J}$, spanning the full dynamic range, with $X_J + X_{J+1} = 0$. Let N_j be the number of sample values of $X(t)$ which fall into the j -th bin. Then if

$$N = \sum_{j=1}^{2J} N_j,$$

the normalized histogram is the sequence of numbers

$$H_j = N_j/N,$$

with H_j corresponding to $h(x_j)$. To symmetrize the sample p.d.f., let

$$P_j = 0.5 (H_j + H_{2J+1-j}),$$

so that

$$P_j = P_{2J+1-j}.$$

Now "smooth" the symmetric sample p.d.f. using

$$\hat{P}_j = 0.1P_{j-2} + 0.2P_{j-1} + 0.4P_j + 0.2P_{j+1} + 0.1P_{j+2}$$

or any similar rule that preserves the identity

$$\sum_{j=1}^{2J} \hat{P}_j = 1.$$

This procedure was applied to six of the normalized histograms shown previously; and the results are presented in Figures 23 through 28. These are the smoothed sample p.d.f.'s for data files A515T2, A508T2, A380T2, A455T4, C514T4, and P345R4, respectively.

The final step is to graph the six corresponding functions Q_j which represent $Q(x)$, defined in equation (14). Because

$$d(\log f)/dx = (1/f) df/dx,$$

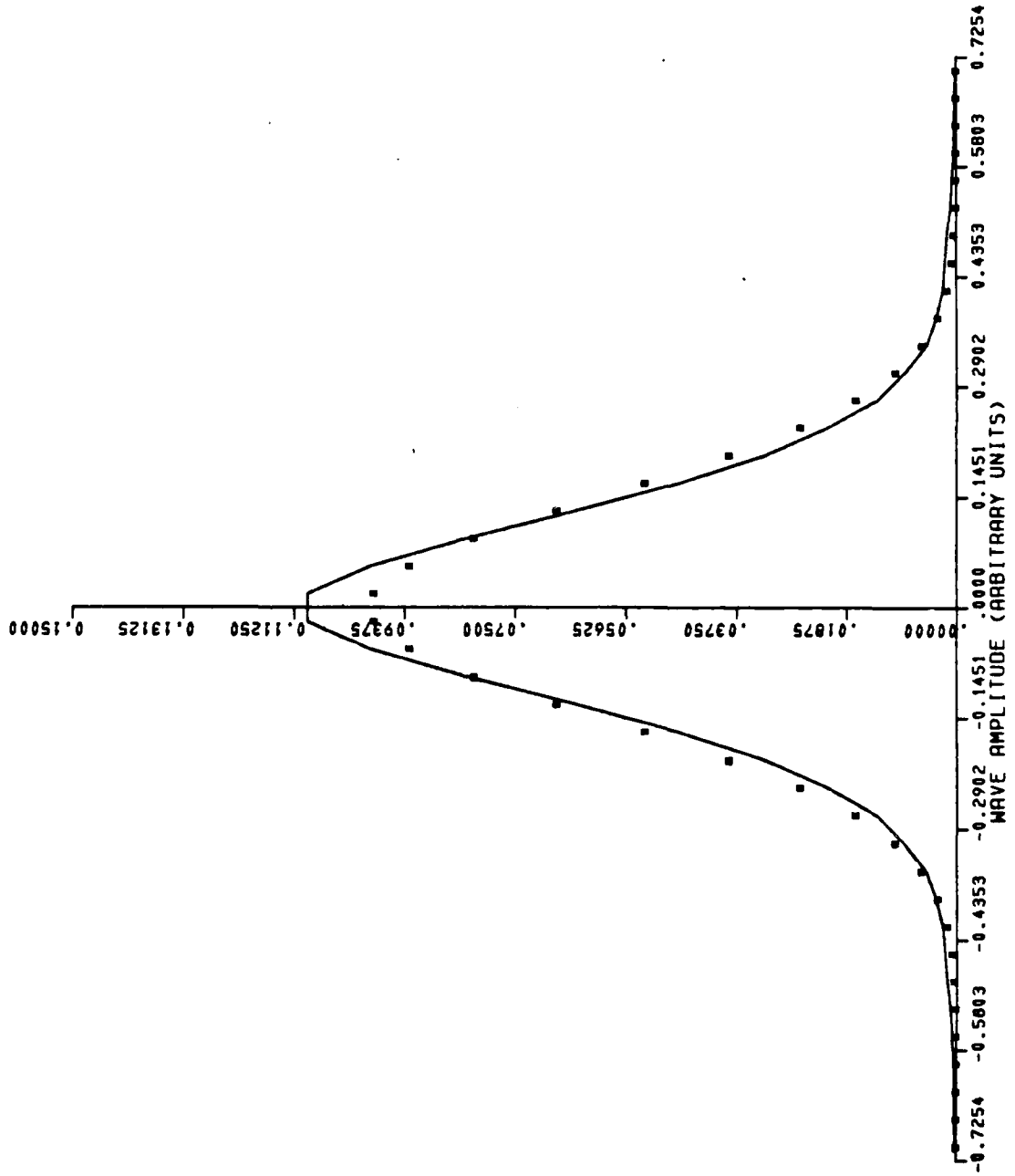


FIGURE 23. SMOOTH SAMPLE PDF FOR DATA FILE A515T2

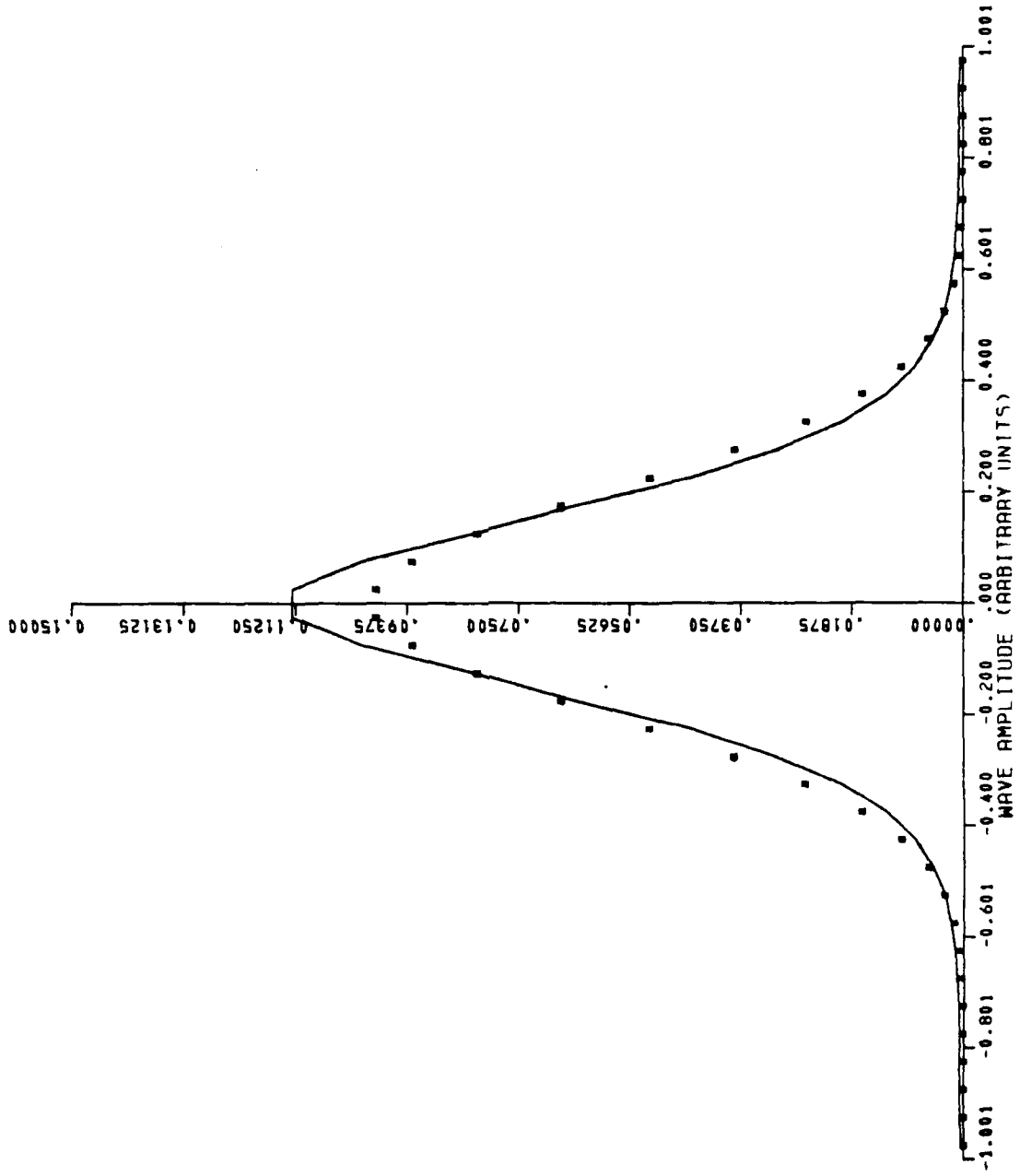


FIGURE 24. SMOOTH SAMPLE PDF FOR DATA FILE A508T2

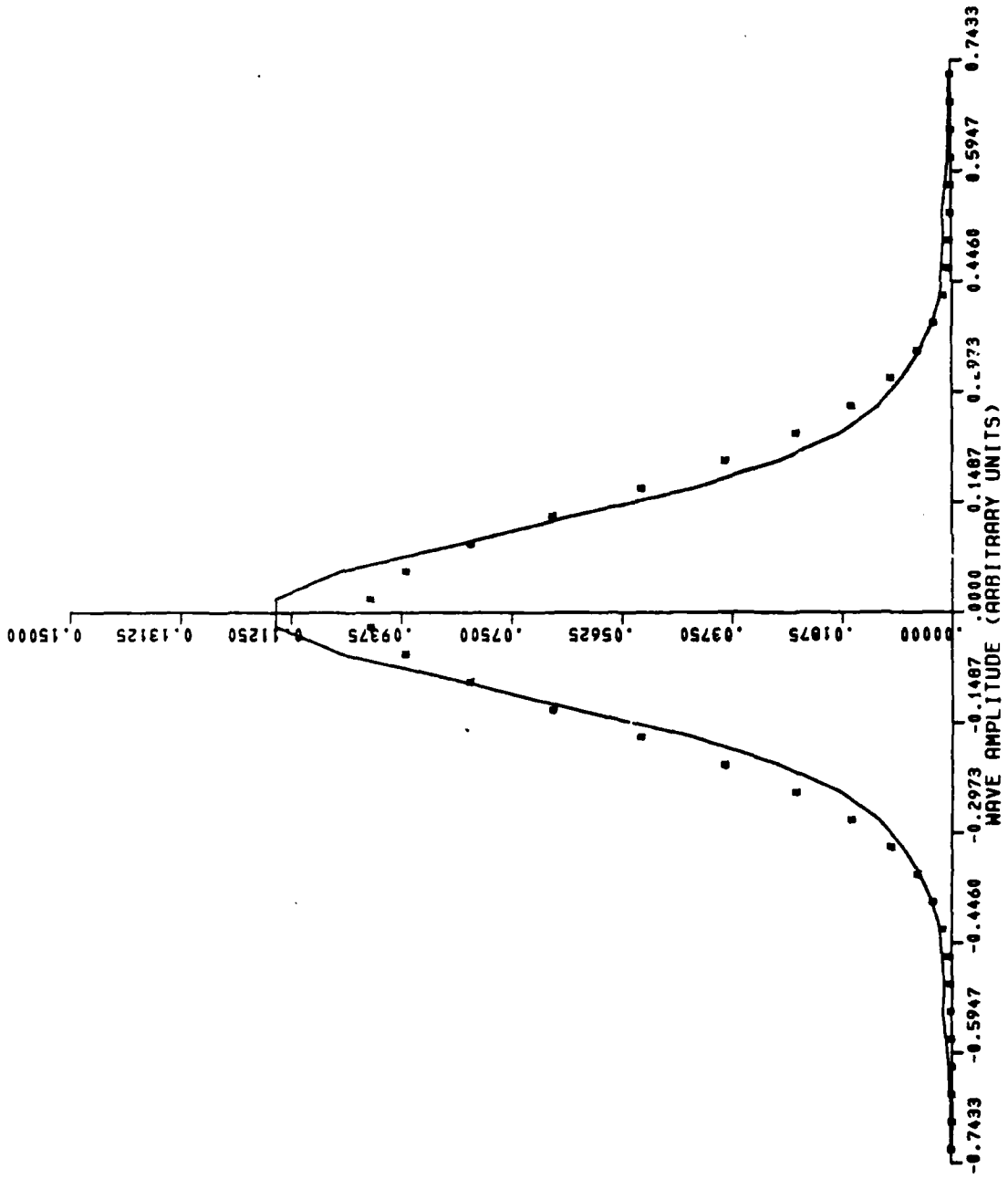


FIGURE 25. SMOOTH SAMPLE PDF FOR DATA FILE A380T2

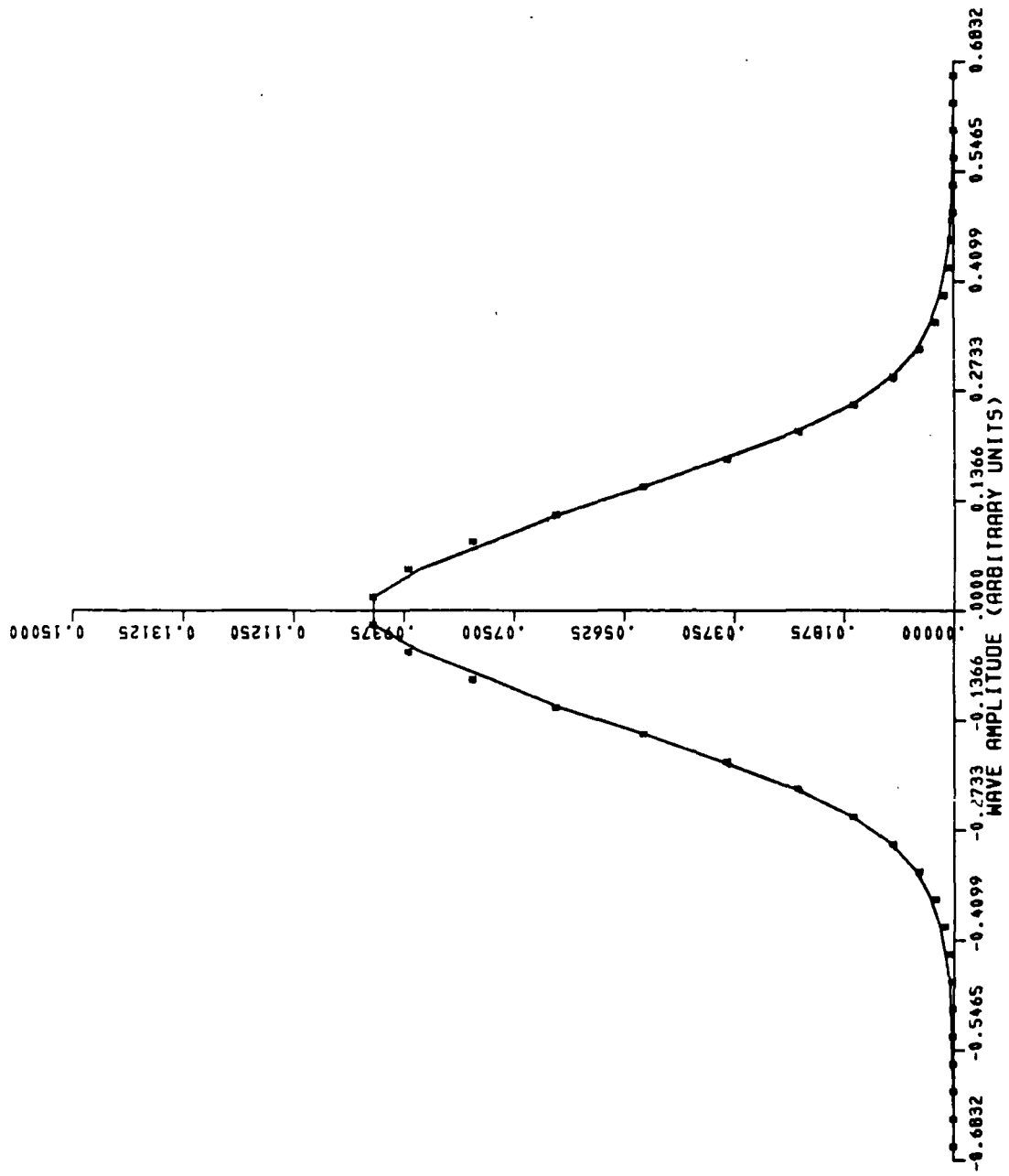


FIGURE 26. SMOOTH SAMPLE PDF FOR DATA FILE A455T4

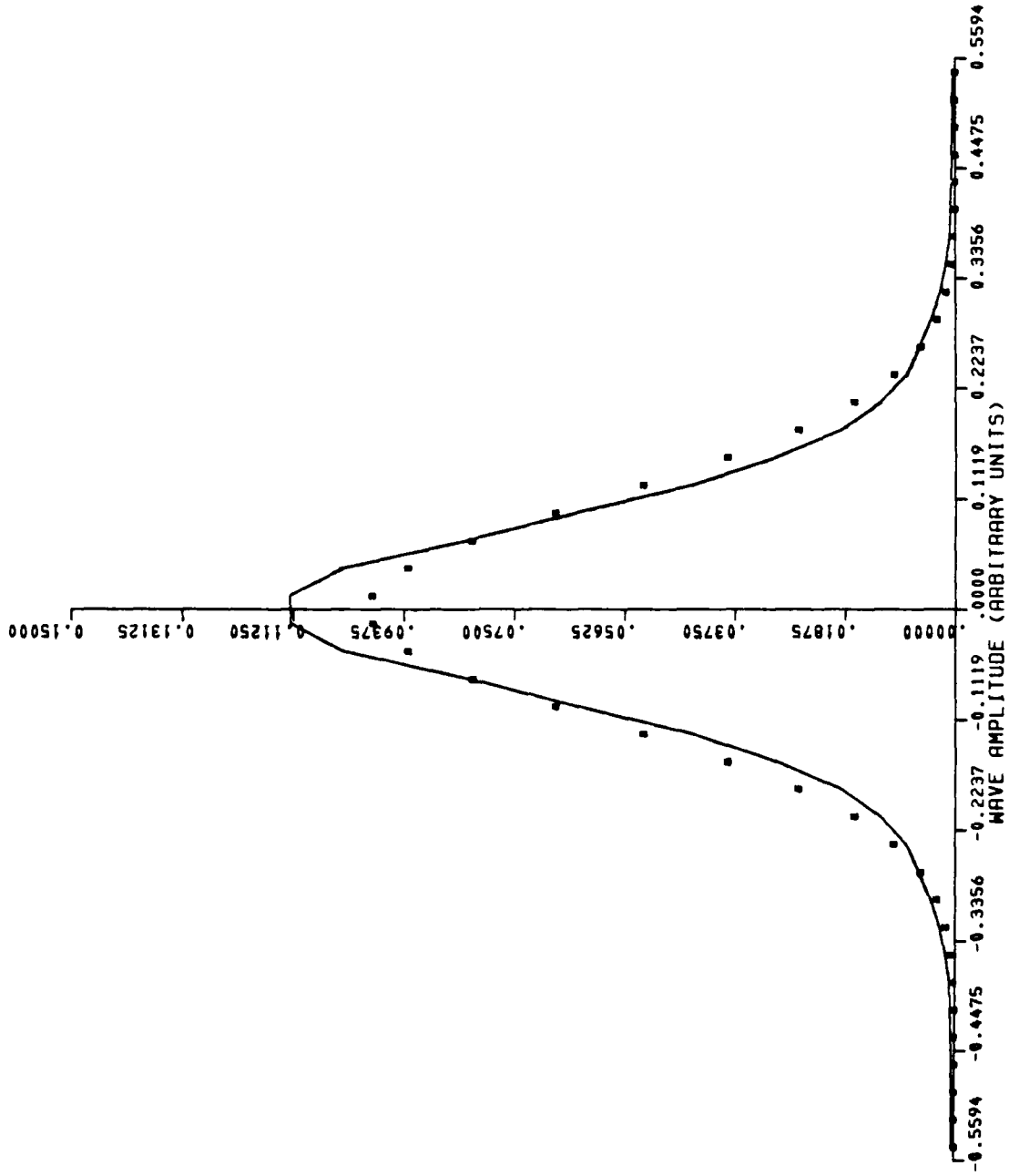


FIGURE 27. SMOOTH SAMPLE PDF FOR DATA FILE C514T4

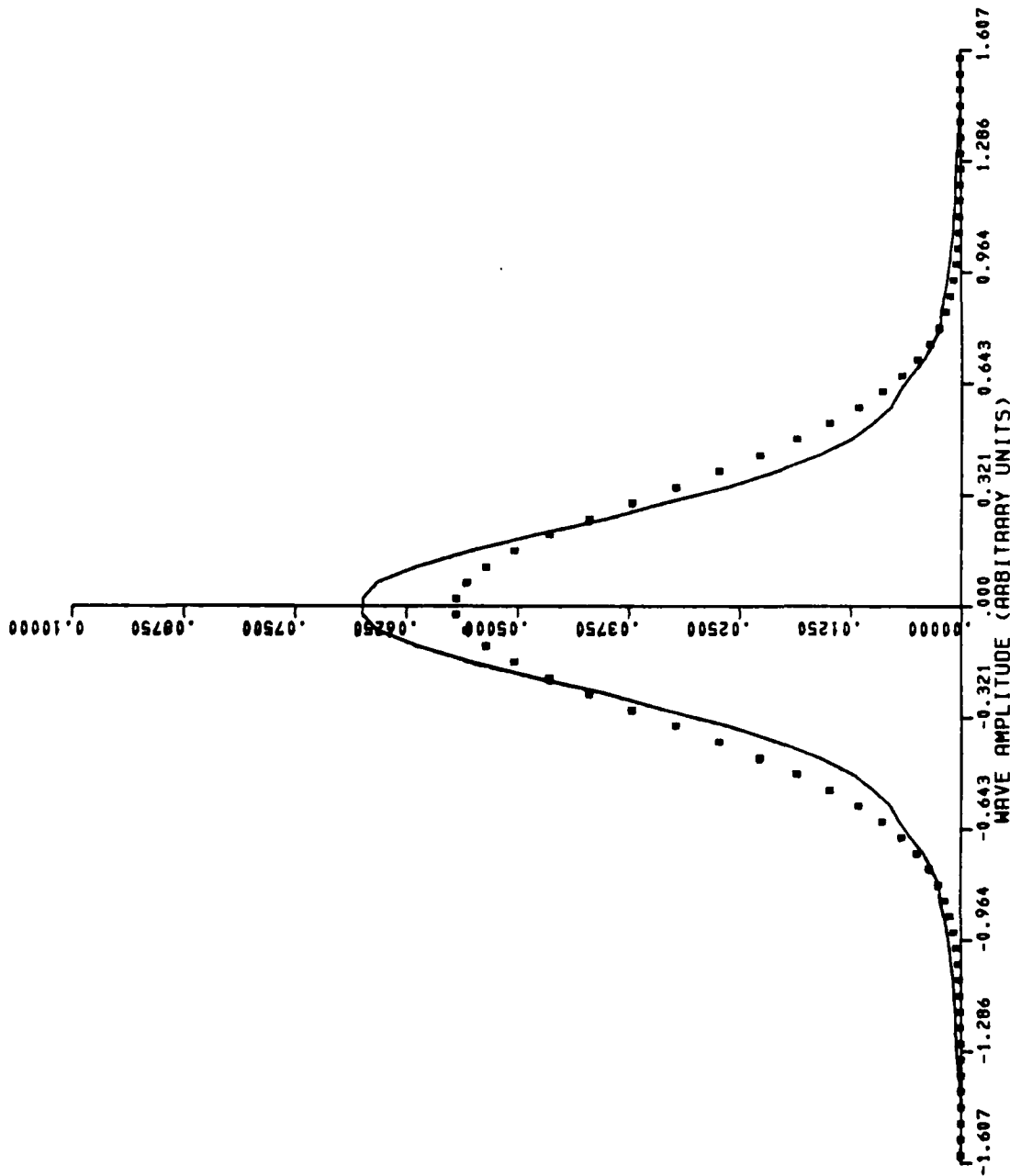


FIGURE 28. SMOOTH SAMPLE PDF FOR DATA FILE P345R4

one has

$$Q_j = (2/D) (\hat{P}_{j-1} - \hat{P}_j) / (\hat{P}_{j-1} + \hat{P}_j)$$

in the finite difference formalism, where D is the width of each bin in the original histogram. These results are shown in Figures 29 through 34, with Figure 29 corresponding to Figure 23, and so on. In each case, there is considerable "choppiness" in $Q(x)$ for x near the ends of the horizontal scale. The most nearly Gaussian of the smoothed sample p.d.f.'s appears to be that corresponding to data file A455T4 (Figure 26). It is not surprising that $Q(x)$ in Figure 32, corresponding to the same file, follows the straight line rather closely over the central portion of the range. Figure 23, corresponding to data file A515T2, appears more compressed in the center, and more persistent in the tails, than the Gaussian density (indicated by the discrete x-marks). Accordingly, the plot of $Q(x)$ in Figure 29 shows an S-curve in the central range and a clockwise curvature through the straight line outside the range. It can be shown that the clockwise bending of $Q(x)$ symptomizes "impulsiveness" in the underlying random process, while counter-clockwise bending means the fluctuations are more confined and that large fluctuations are less common than for a Gaussian process.

CONCLUSION

The data presented in this publication, which were not pre-selected or screened, provide limited support of ocean wave theories that predict a Gaussian distribution of fluctuations. On the other hand, those data which were subjected to a more detailed examination in the preceding section show a higher probability of large fluctuations (several times the r.m.s.) than predicted by a Gaussian model. The data files in this latter set were chosen to highlight the disparity.

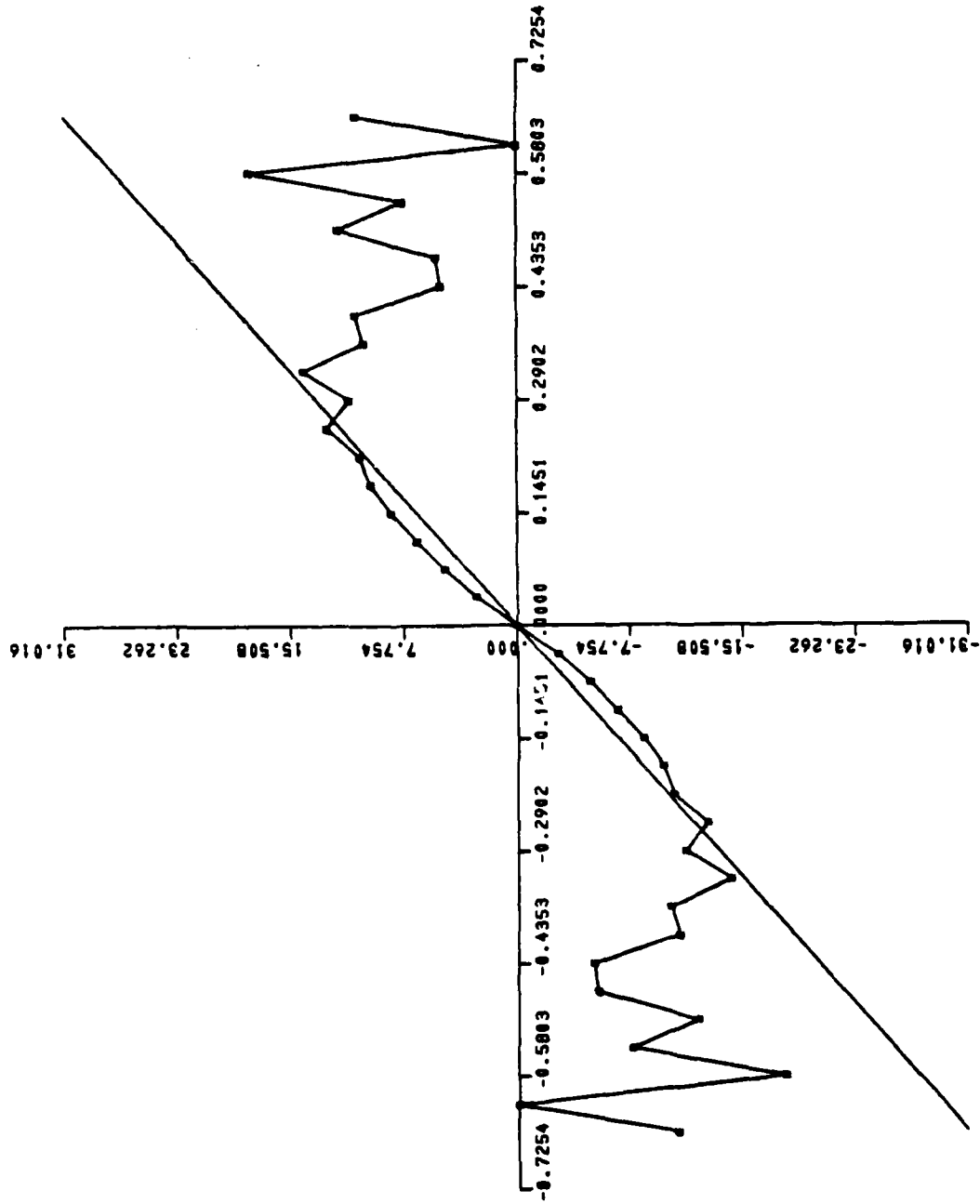


FIGURE 29. Q(x) FOR DATA FILE A515T2

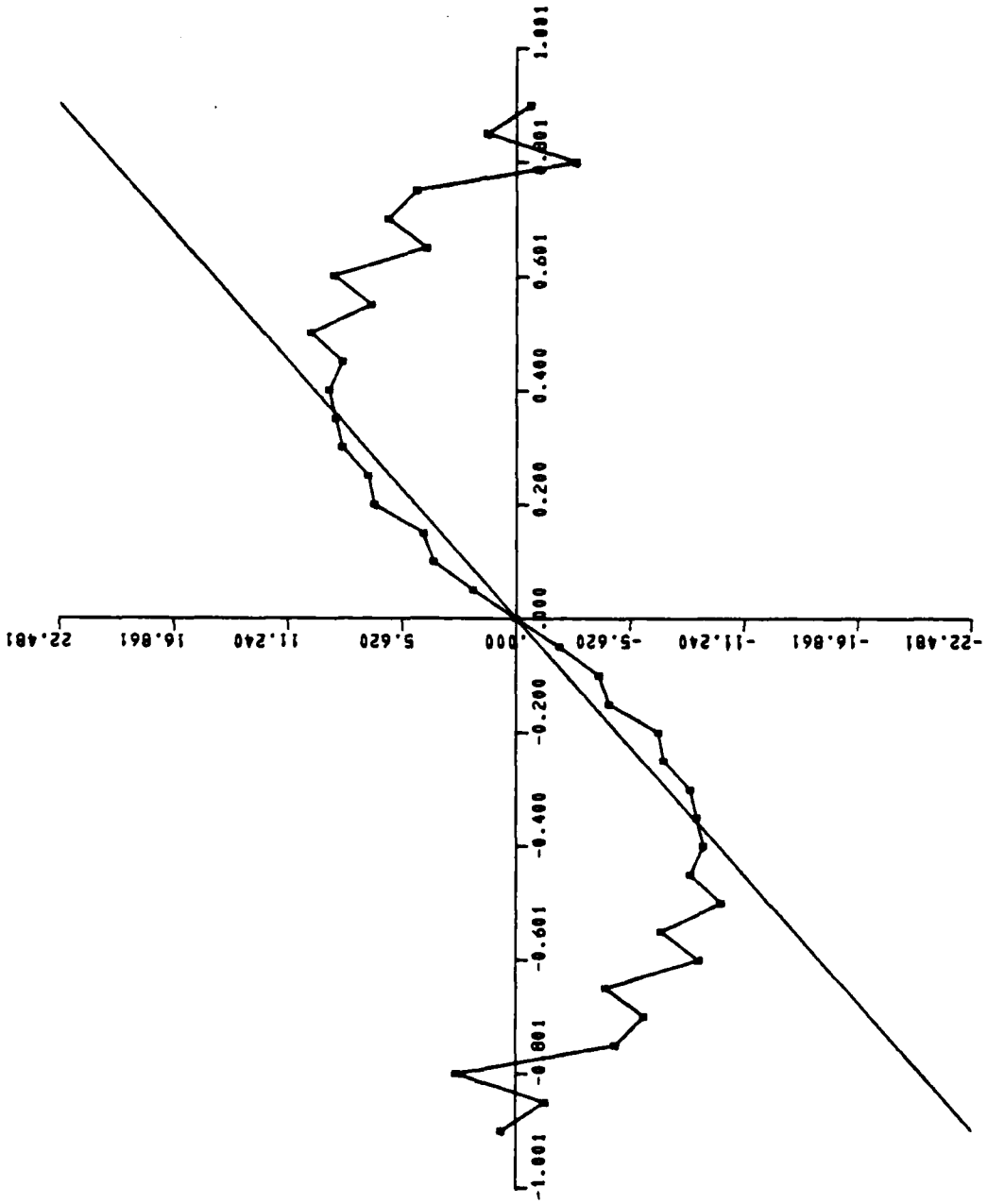


FIGURE 30. Q(x) FC~ DATA FILE A508T2

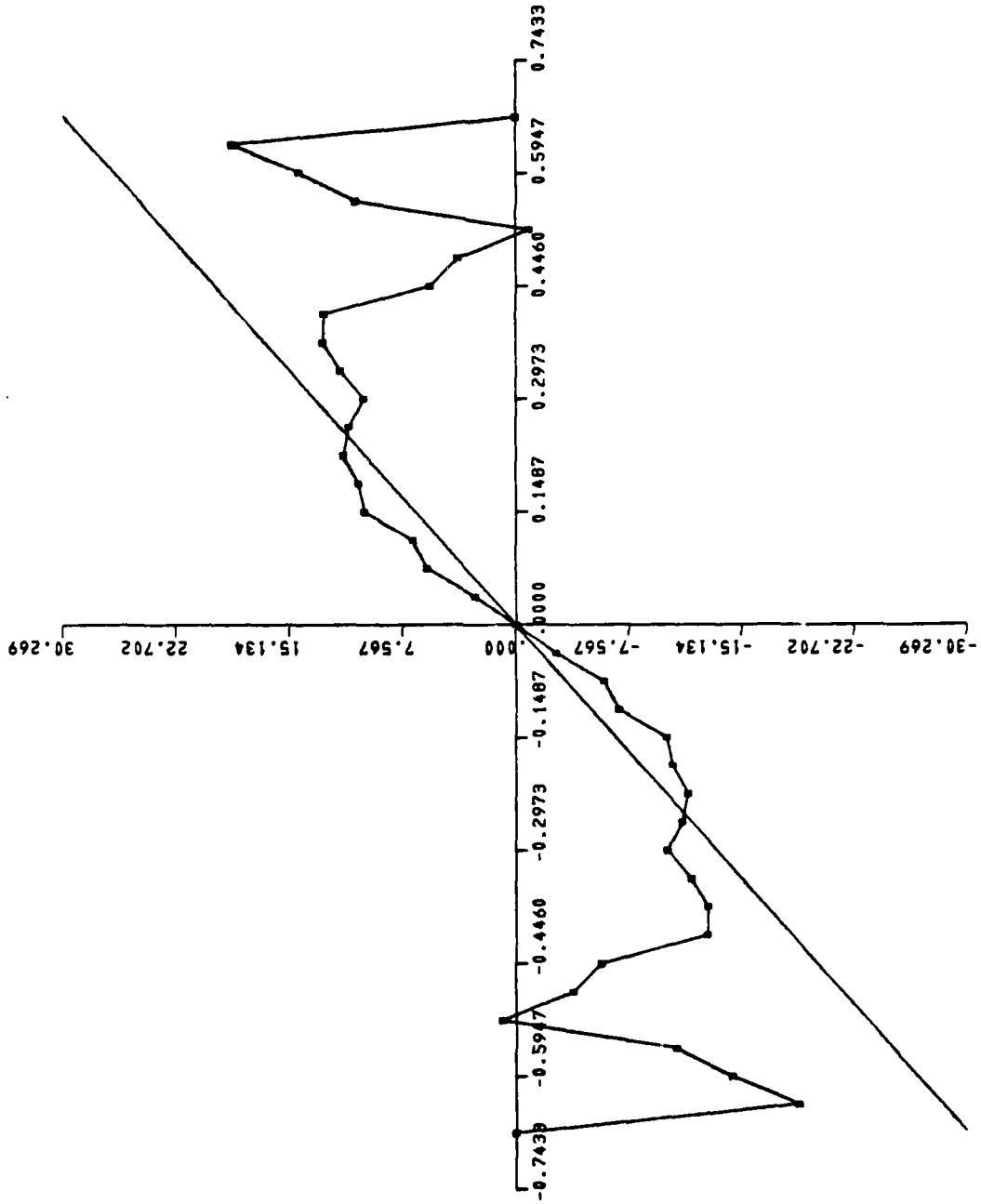


FIGURE 31. Q(x) FOR DATA FILE A380T2

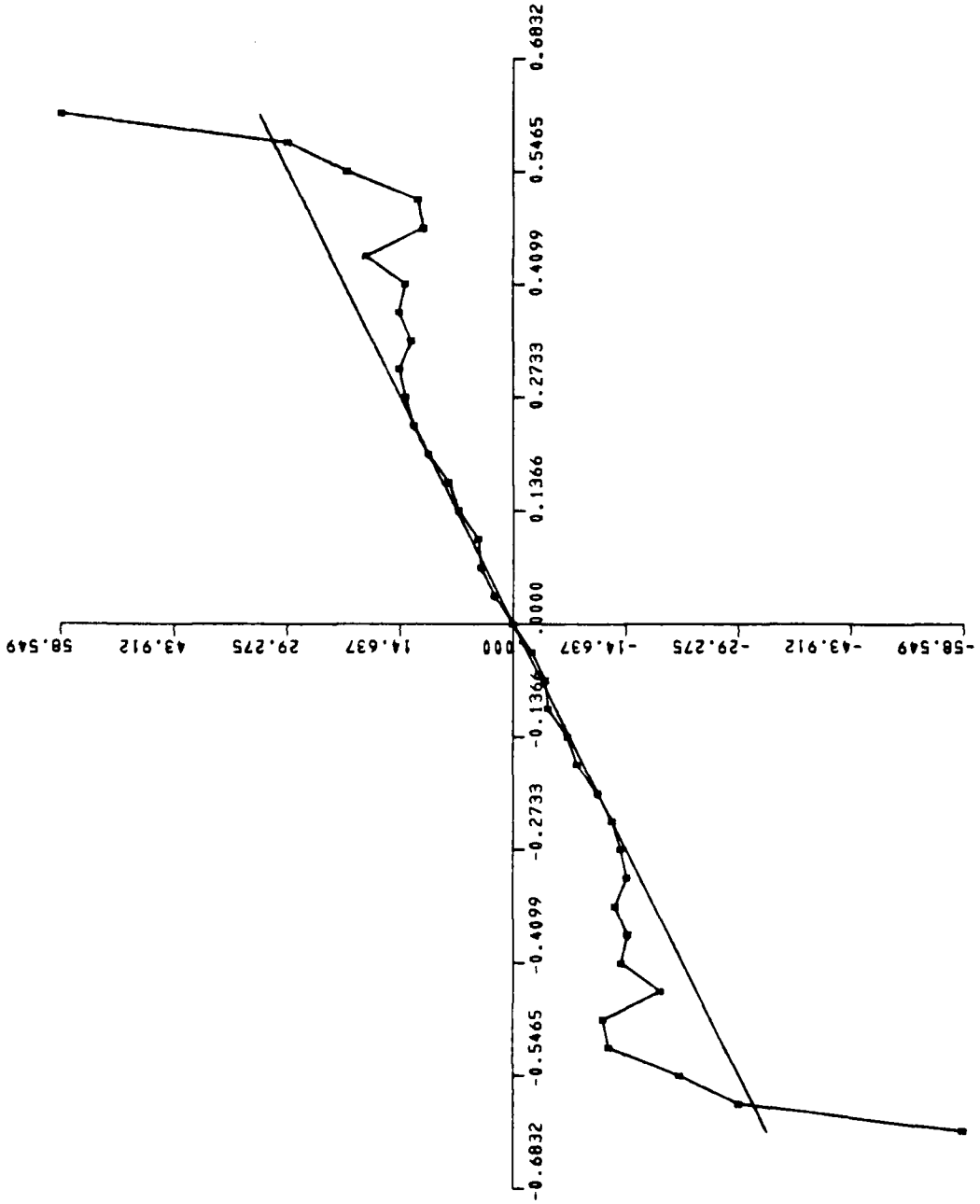


FIGURE 32. Q(x) FOR DATA FILE A455T4

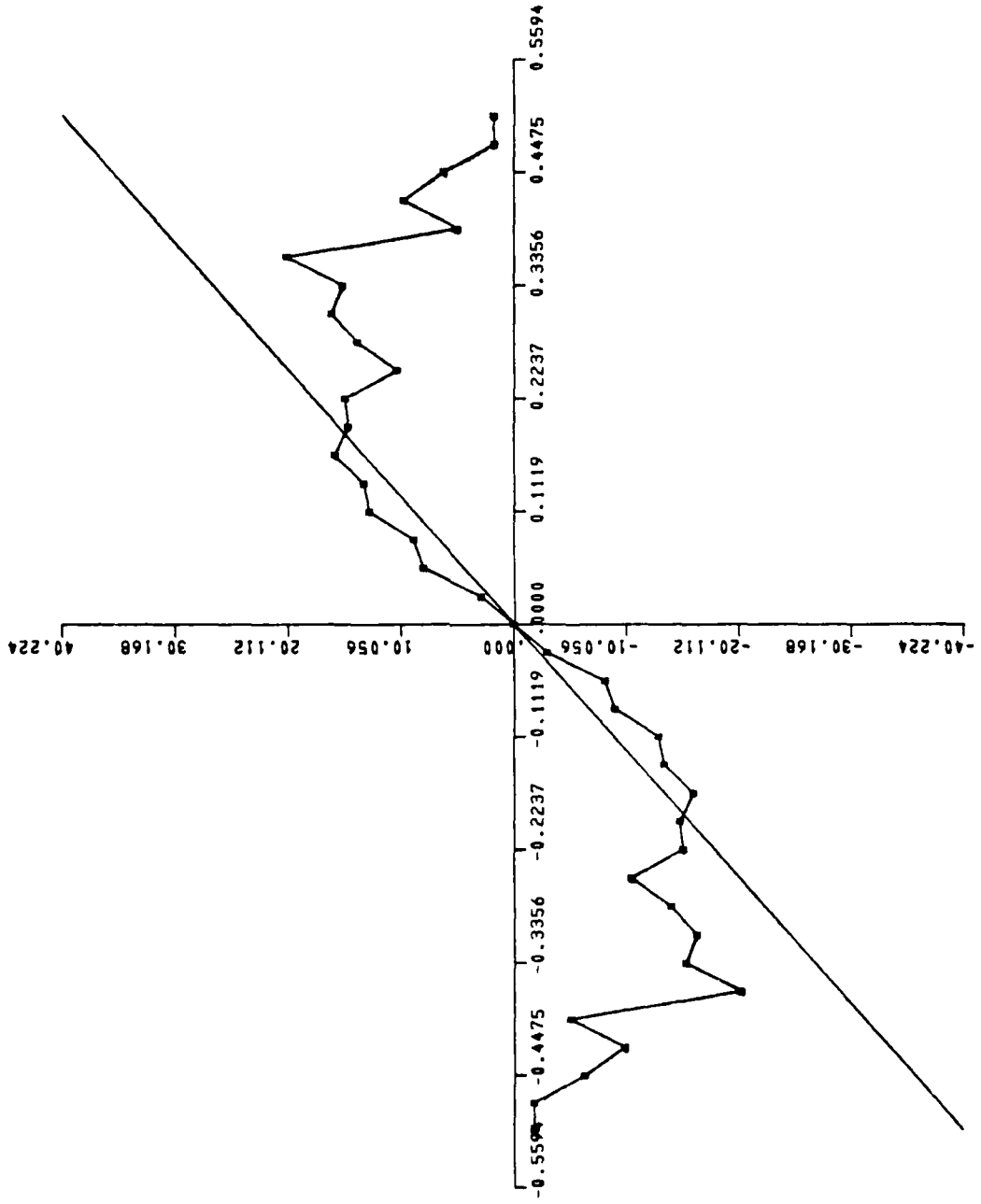


FIGURE 33. Q(x) FOR DATA FILE C514T4

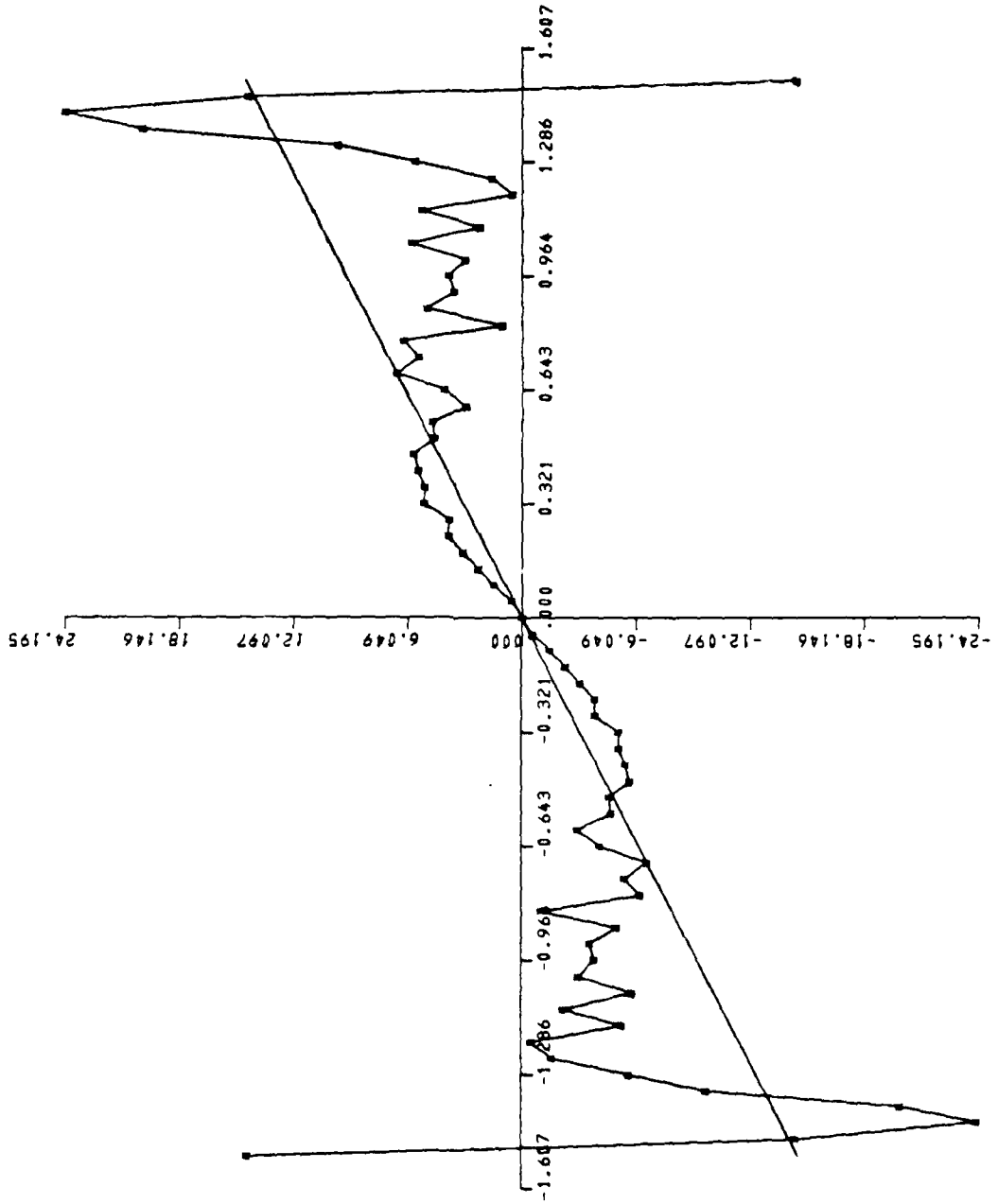


FIGURE 34. Q(x) FOR DATA FILE P345R4

AD-A148 706

AN ELEMENTARY ANALYSIS OF OCEAN WAVE STATISTICS(U)
NAVAL SURFACE WEAPONS CENTER SILVER SPRING MD
D LEE ET AL. AUG 83 NSWC/TR-83-350

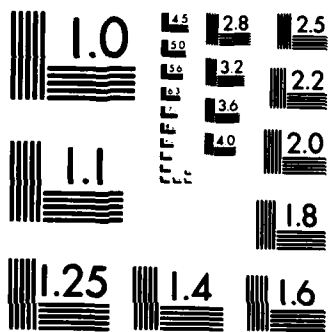
2/2

UNCLASSIFIED

F/G 8/3

NL

				END
				FILED
				DEC



MICROCOPY RESOLUTION TEST CHART
NATIONAL BUREAU OF STANDARDS-1963-A

Large fluctuations are most interesting to the engineer or analyst who is concerned with the design of an oceanic structure or system possessing a sensitivity to waves that is an increasing, nonlinear function of the amplitude. In such cases as these, one would rather have a p.d.f. that yields a good approximation to the extreme value distribution, even if the matchup is poor at low amplitudes. While the data presented here could be used to estimate the extreme value distribution, confidence in the result would be rather low owing to the insufficiency of the volume of data. Indeed, 19 records of 15 minutes each add up to 4.75 hours of observation; whereas the engineer may be concerned with systems that experience fluctuations for weeks or years consecutively.

REFERENCES

1. Neumann, G., and Pierson, W. J., Jr., "Known and Unknown Properties of the Frequency Spectrum of a Wind-Generated Sea," in Ocean Wave Spectra, Proc. of a Conference sponsored by U.S.N. Oceanographic Office, (New York: Prentice-Hall, 1963).
2. Taub, A. H., "Wave Propagation in Fluids," Part 3, Ch. 4, in The Handbook of Physics, Second Ed., (New York: McGraw-Hill, 1967).
3. Bretschneider, C. L., "A One-Dimensional Gravity Wave Spectrum," in Ocean Wave Spectra, (New York: Prentice-Hall, 1963).
4. Walden, H., "Comparison of One-Dimensional Wave Spectra Recorded in the German Bight with Various 'Theoretical' Spectra," in Ocean Wave Spectra, (New York: Prentice-Hall, 1963).
5. The Sea, (New York: Interscience Publishers Div. of John Wiley and Sons, 1962) Vol. 1, p. 570.
6. Deutsch, R., Nonlinear Transformations of Random Processes, (New York: Prentice-Hall, 1962).
7. Bracewell, R., The Fourier Transform and its Applications, (New York: McGraw-Hill, 1965), Chapter 16.
8. Baran, R. H., Adaptive Signal Detection for the Optimal Communications Receiver, NSWC TR 83-236, Jun 1983.
9. Evans, J. E., Probability Density Function Estimation, M.I.T. Lincoln Lab. Tech Note 1969-47, Aug 1969.

DISTRIBUTION

<u>Copies</u>	<u>Copies</u>
Office of Naval Research Attn: Technical Library Arlington, VA 22217	2
Commanding Officer Office of Naval Research Branch Office 495 Summer Street Boston, MA 02210	1
Commanding Officer Officer of Naval Research Branch Office 536 South Clark Street Chicago, IL 60605	1
Commander Naval Air Systems Command Attn: Technical Library Department of the Navy Washington, DC 20361	1
Commander Naval Sea Systems Command Attn: Technical Library (99612) Washington, DC 20362	2
Commander Naval Electronics Systems Command Attn: Technical Library Department of the Navy Washington, DC 20360	1
Commander Naval Ocean Systems Center Attn: Technical Library San Diego, CA 92152	1
	Commanding Officer Naval Underwater Systems Center Attn: Technical Library Newport, RI 02844
	1
	Commander Naval Weapons Center Attn: Technical Library China Lake, CA 93555
	1
	Commanding Officer Naval Research Laboratory Attn: Code 1000 Technical Library Washington, DC 20375
	1
	1
	Defense Technical Information Center Cameron Station, Building 5 Alexandria, VA 22314
	2
	Library of Congress Attn: Gift and Exchange Div. Washington, DC 20540
	4
	Internal Distribution: U12 (R. H. Baran)
	12
	R43 (D. G. Jablonski)
	1
	R43 (J. Coughlin)
	1
	U21 (P. D. Jackins)
	1
	R04 (D. L. Love)
	1
	U12 (J. D. Sherman)
	1
	E431
	9
	E432
	3
	E35
	1

END

FILMED

1-85

DTIC